Transcriptomic analyses of gastrulation-stage C57BL/6J and C57BL/6NHsd mouse embryos with differential susceptibility to alcohol

Karen E. Boschen[1], Travis S. Ptacek[2,3], Matthew E. Berginski[4], Jeremy M. Simon[2,3,5], Scott E. Parnell[1,6,7]*

[1]Bowles Center for Alcohol Studies, The University of North Carolina at Chapel Hill, Chapel Hill, NC, USA

[2]Carolina Institute for Developmental Disabilities, The University of North Carolina at Chapel Hill, Chapel Hill, NC, USA

[3]UNC Neuroscience Center, University of North Carolina at Chapel Hill, Chapel Hill, NC, USA

[4] Department of Pharmacology, The University of North Carolina at Chapel Hill, Chapel Hill, NC, USA

[5] Department of Genetics, The University of North Carolina at Chapel Hill, Chapel Hill, NC, USA

[6] Department of Cell Biology and Physiology, The University of North Carolina at Chapel Hill, Chapel Hill, NC, USA

[7] Carolina Institute for Developmental Disabilities, The University of North Carolina at Chapel Hill, Chapel Hill, NC, USA

*Address correspondence to: Scott E. Parnell, Ph.D.

Bowles Center for Alcohol Studies

University of North Carolina

104 Manning Drive

CB# 7178 Thurston Bowles

Chapel Hill, NC 27599

Phone: 919-966-8195, Fax: 919-966-5679

Email: sparnell@med.unc.edu, ORCID: 0000-0003-2038-6548

SUMMARY STATEMENT

RNA-seq in gastrulation-stage mouse embryos provides information about gene expression patterns during normal mouse development and evidence that pre-existing genetic variability mediates risk to prenatal alcohol-induced birth defects.

ABSTRACT

Fetal Alcohol Spectrum Disorders (FASD) are a serious public health concern, affecting approximately 5% of live births in the US. The more severe craniofacial and central nervous system malformations characteristic of FASD are caused by alcohol exposure during gastrulation (embryonic day 7 in mice; 3rd week of human pregnancy). Genetics are a known contributor to differences in alcohol sensitivity in humans and in animal models of FASD. Our study profiled gene expression in gastrulation-stage embryos from two commonly used, genetically similar mouse substrains, C57BL/6J and C57BL/6NHsd, that differ in alcohol sensitivity. First, we established normal gene expression patterns at three finely resolved timepoints during gastrulation and developed a web-based interactive tool. Baseline transcriptional differences across strains were associated with immune signaling, indicative of their molecular divergence. Second, we examined the gene networks impacted by alcohol in each strain. Alcohol was associated with a more pronounced transcriptional effect in the 6J's vs. 6N's, matching the 6J's increased susceptibility. The 6J strain exhibited down-regulation of cell proliferation and morphogenic signaling pathways and up-regulation of pathways related to cell death and craniofacial defects, while 6N's show enrichment of hypoxia (up) and cellular metabolism (down) pathways. Collectively, these datasets 1) provide insight into the changing transcriptional landscape across gastrulation in two commonly used mouse strains, 2) establish a valuable resource that enables the discovery of candidate genes that may modify susceptibility to prenatal alcohol exposure that can be validated in humans, and 3) identify novel pathogenic mechanisms potentially involved in alcohol's impact on development.

Keywords: Fetal Alcohol Spectrum Disorders, apoptosis, inflammation, embryo, brain development

INTRODUCTION

Alcohol exposure during the first weeks of pregnancy is associated with significant birth defects involving the craniofacial region and central nervous system (Cook et al., 1987). Specifically, prenatal alcohol exposure (PAE) during gastrulation (3rd week of human pregnancy, embryonic day [E] 7 in mice) results in the craniofacial malformations characteristic of Fetal Alcohol Syndrome (FAS), including a thin upper lip, smooth philtrum, reduced head circumference, and small eyes (Cook et al., 1987). In addition, gastrulation-stage PAE is associated with loss of midline brain tissue, including agenesis of the corpus callosum and holoprosencephaly (Higashiyama et al., 2007, Godin et al., 2010), disrupted morphogenic signaling (Zhang et al., 2014, Kietzman et al., 2014, Aoto et al., 2008), and widespread apoptosis (Dunty et al., 2001).

An ongoing question in the field of prenatal alcohol research is why some children exposed to alcohol *in utero* develop significant physical and cognitive deficits whereas others are relatively unaffected. While the dose and timing of alcohol exposure are certainly factors, it is known that environmental factors, such as stress or nutrition, and genetics can predispose an embryo to alcohol sensitivity or resistance. Studies using twins exposed to heavy prenatal alcohol revealed that dizygotic twins were less likely to both be diagnosed with FAS as compared to monozygotic twins (Streissguth and Dehaene, 1993, Abel, 1988). Of the monozygotic twins examined, if one twin was diagnosed with FAS then the other was also diagnosed in 100% of cases, compared with only 64% concordance in the dizygotic twin sets. In addition, experiments in animal models of FASD have demonstrated that strains of mice and chicken exhibit different degrees of incidence and severity of PAE-related birth defects (Downing et al., 2009, Su et al., 2001). These data clearly suggest that there is a genetic component to FAS. While the genetic differences that alter susceptibility to PAE between these strains are not yet clear, it is known that the deletion of certain genes can alter susceptibility to PAE (Eberhart and Parnell, 2016). For example, deleting one copy of either Sonic hedgehog (*Shh*) (Kietzman et al., 2014), the Shh co-receptor Cell adhesion associated Oncogene associated (*Cdon*) (Hong and Krauss, 2012, Hong and Krauss, 2013), and downstream transcriptional activator Gli Family Zinc Finger 2 (*Gli2*) (Fish et al., 2017) increases susceptibility to PAE in the brain, face, and limbs. Likewise, deletion of one or both copies of the ciliary-related gene *Mns1* exacerbates the effects of PAE on the brain and face in a gene dose-dependent manner (Boschen et al., 2018). However, the identification of further genes that may alter susceptibility to PAE remains elusive.

In order to identify candidate genes that may alter susceptibility to early developmental alcohol exposure, our current study identifies PAE-induced transcriptomic changes in the gastrulation-stage embryo using two closely related mouse strains, the C57BL/6J obtained from Jackson Laboratories and the C57BL/6NHsd obtained from Envigo (formerly Harlan, referred to henceforth as 6N). Previous work

has demonstrated that the 6J strain has a higher incidence of eye defects after prenatal alcohol compared to the 6N strain (Dou et al., 2013, Green et al., 2007b). These strains were both derived from the original C57BL/6J mice bred by Jackson Laboratories but were separated when the 6J strain was given to NIH in 1951 and given from NIH to Harlan in 1974. Now, over 200 generations separate the 6J and 6N strains. Notably, two known genetic mutations have emerged over the years. First, the 6J strain has a mutation in the *Nnt* gene, which encodes nicotinamide nucleotide transhydrogenase, an enzyme important for production of NADPH and removal of reactive oxygen species (ROS) from the mitochondria (Ronchi et al., 2013). The mutation in the 6J mice is comprised of two separate mutations: a missense (M35T) mutation in the mitochondrial leader sequence and a multi-exonic deletion of exons 7-11, resulting in a non-functional protein. 6J mice have been shown to have five- to seven-fold lower levels of Nnt in the islets and liver (Toye et al., 2005), impaired insulin secretion, and mitochondrial redox abnormalities (Ronchi et al., 2013). Mutations in this gene could cause reduced NADPH and glutathione stores and impaired oxidative stress responses in the 6J embryos, possibly priming these embryos to be more likely to undergo cell death following alcohol exposure. Second, the 6N strain carries a single nucleotide deletion in the *Crb1* gene, called the *Rd8* mutation (Mattapallil et al., 2012). This mutation is associated with retinal degeneration, lesions, and folding.

While the *Nnt* and *Rd8* mutation are two well-studied differences between the 6J and 6N strains, it is possible that other genetic variation is present during development that could modulate strain differences in risk and resilience to alcohol damage. In addition, it is unknown what effect these mutations have on gene expression during early embryonic development. The goals of this experiment were two-pronged. First, we used the gathered transcriptome data to provide information about gene expression across gastrulation during normal mouse development. To this end, a web-based tool was created to allow gene-by-gene exploration of expression patterns across the first 12 hr of gastrulation in both the 6J and 6N strains. Second, we examined PAE-induced gene expression changes 6 and 12 hr after exposure (E7.25 and 7.5, respectively), adding valuable information about the molecular targets of this mouse model of FASD.

RESULTS

Web-based tool as a resource for data visualization and exploration

We performed whole transcriptomic analyses of 6J and 6N mouse embryos at three time points (E7.0, E7.25, and E7.5) using RNA-seq (Fig 1A). We assembled a transcriptomic database of normal embryonic development, as well as characterized how strain differences and PAE treatment governs these processes. A web-based visualization tool (http://parnell-lab.med.unc.edu/Embryo-

Transcriptomics/) was created for a gene-by-gene query of the transcriptomic data from both strains and from both control and PAE-treated embryos at each timepoint. Strain and prenatal treatment options can be toggled on or off to compare relative expression of a gene of interest in a single strain across time points, or between the 6J and 6N across time. For example, expression of *Wdfy1* significantly differs between the strains across all time points but is not affected by PAE (Fig 1B). Conversely, *Shh* increases in expression in both strains over time, but PAE significantly reduces expression in the 6J (Fig 1C). The gene expression data generated in this study comprise a valuable resource for developmental biologists, toxicologists, mouse geneticists, and researchers interested in models of FASD.

Transcriptional differences at between 6J and 6N mouse embryos during gastrulation

Gene expression across the first 12 hr normal mouse gastrulation was compared between the 6J and 6N strains (representative image of gastrulation-stage mouse embryo in Fig 2A). Heatmaps showing hierarchical clustering of gene expression of all significant genes for all replicates are in Fig S1- S7 and VST-normalized values for all significant genes are in Dataset S1. We first focused on how 6J and 6N embryonic gene expression differs at E7.0 to establish a baseline and explore strain-dependent transcriptional differences prior to alcohol exposure. Eighty genes were identified as differentially expressed between the 6J and 6N strains at E7.0. Of these, 67 showed higher expression (83.8%) and 13 showed lower expression (16.2%) in the 6J relative to the 6N (Fig 2B). Functional profiling revealed up-regulation of pathways related to inflammation and cytokine production, cell migration, and intracellular signaling (Fig 2C; Table S1).

Multiple genes that encode cytokines/chemokines and immune signaling molecules had higher expression in the 6J, including *Ccl4*, *Il1r1*, *Il1rn*, and *Tntrsf9*. The most up-regulated gene (largest positive $\log_2$ fold-change [Log_2FC]), *Ide*, encodes an insulin-degrading enzyme that is known to degrade the B chain of insulin and amyloid beta (Bennett et al., 2000), suggesting a role in Alzheimer's disease. Expression of *Ide* has been found to be relatively low in embryonic *Drosophila* (Stoppelli et al., 1988) and neonatal rat (Kuo et al., 1993) compared to their adult counterparts, suggesting a more prevalent role of this protein during adulthood. There were no significantly over-enriched pathways among the down-regulated genes, however the *Nnt* gene was significantly down-regulated in the 6J strain, corroborating the well-known mutation in the 6J mouse strain (Ronchi et al., 2013). The gene most down-regulated in the 6J relative to 6N was *Wdfy1*, which encodes an adaptor protein involved in protein-protein and protein-DNA interactions. Wdfy1 also acts as an adaptor protein for Toll-like receptors 3 and 4 (Hu et al., 2015), implicating this protein in the immune signaling response. *Efcab7*

was also down-regulated in the 6J relative to 6N; this gene is associated with primary cilia function and, in particular, Shh signaling via Smoothened (Smo) (Pusapati et al., 2014).

Since the majority of pathways and genes were related to the cellular immune signaling response, we hypothesized that 6J mice have heightened immune signaling activity that influences the stress response to a stimulus such as alcohol. We therefore sought to more comprehensively characterize the disrupted *de novo* gene networks using the Ingenuity Pathway Analysis (IPA) database of known protein-protein interactions. IPA allows insight into the functional relationships between differentially expressed genes that are not captured in the canonical terms and pathways used in the gene set enrichment analysis above. Six networks were dysregulated in the 6J relative to 6N (Table 1, Table S2A) related to immune signaling (*Inflammatory Disease*, *Immune Cell Trafficking*, *Inflammatory Response*) and cell proliferation (*Cell Cycle*, *Cell Movement, Cellular Assembly and Organization*), supporting that baseline immune signaling differs between the strains. Differences in cell movement are likely linked to immune cell migration, though the source, type, and function of these immune cells and related signaling molecules in the gastrulation-stage embryo is not yet clear. Overall, these genetic differences set the stage for the disparate responses to PAE observed in these two strains both hours (Fig 4, Fig 6) and days (Dou et al., 2013, Green et al., 2007a) later in development.

We next compared the 6J and 6N strains either 6 or 12 hr after E7.0 following two injections of vehicle solution to investigate strain differences at later developmental time points in the absence of alcohol. Gastrulation is a critical time of embryonic development involving cell proliferation and fate decisions that establish the embryonic germ layers, with developmental events relying on temporally- and spatially-specific gene expression (Pijuan-Sala et al., 2019). At E7.25, 6 hr post-vehicle injection, 315 genes were differentially expressed between the two strains. Of these genes, 128 genes were up-regulated (40.6%) and 187 were down-regulated (59.4%) in the 6J relative to the 6N. Twelve hours after vehicle treatment, E7.5, there were 304 differentially expressed genes between 6J and 6N. Of these, similar to the E7.25 time point, 120 genes were up-regulated (39.5%) and 184 genes were downregulated (60.5%) in the 6J.

Functional profiling of genes from the E7.25 time point revealed only a small number of biological pathways that differed between the two strains, including altered hydrolase and endopeptidase activity and pathways related to cAMP signaling and apoptosis related to the down-regulated genes (Table S3). The top ten *de novo* networks were related to cell death, intercellular signaling, nutrient metabolism, and embryonic development (Table S2B). At E7.5, functional profiling of the up-regulated genes indicated increased prostaglandin signaling and GPCR signaling (Table S4). The down-regulated pathways were again related to hydrolase and endopeptidase activity, consistent

with the E7.25. *De novo* network analysis identified functions related to organ development, drug metabolism, protein processing, and the cell cycle (Table S2C).

Overall, there was little change in which genes were strongly up- or down-regulated across these 12 hours of development, consistent with other studies showing most genes expressed during gastrulation show relatively stable expression prior to the onset of organogenesis (Mitiku and Baker, 2007). *Wdfy1* showed the largest down-regulation by Log_2FC at both time points in the 6J relative to 6N (-3.94 and -3.67 Log_2FC, respectively), consistent with what was observed in these two strains at E7.0 prior to any injection. *Efcab7*, which had lower baseline expression in 6J, exhibited the same effect at E7.25 (-1.78 Log_2FC), but not at E7.5. The most up-regulated gene in the 6J relative to 6N at E7.25 was *Hist1h4m*, or histone cluster 1, H4m, a gene related to nucleosome assembly. This gene also showed a large up-regulation at E7.5 and a small but statistically significant up-regulation at E7.0. Interestingly, this gene was found to be down-regulated in the hippocampus of fetal 6J mice (purchased from Orient Bio Inc) following alcohol exposure from E8-12 (Mandal et al., 2015). The fact that expression of *Hist1h4m* differs between alcohol sensitive and resistant strains and expression is affected in certain models of PAE is strongly suggestive that this gene is a possible target of alcohol and mediator of alcohol sensitivity.

Strain-specific differences in transcriptional response to PAE are evident as early as 6 hours after exposure

We next compared the effect of PAE on embryonic gene expression in each strain at E7.25 to explore how strain differences modulate the initial transcriptional response to alcohol. At E7.25 (6 hr post-PAE), 810 genes were significantly differentially expressed between PAE and vehicle in the 6J strain, and 702 genes were differentially expressed between PAE and vehicle in the 6N strain. In the 6J, 355 genes were upregulated (43.8%) and 455 were down-regulated (56.2%) (Fig 3A). In the 6N, 372 genes were upregulated (52.9%) and 330 were down-regulated (47.1%) (Fig 3B). Of the differentially expressed genes, 228 were altered in both strains (Fig 3C). In most cases, the directionality (up- or down-regulated) was the same between strains, indicating that while there is a substantial subset of genes that are similarly affected in both the 6J and 6N, the majority of genes with significantly altered expression in each strain are unique.

Functional profiling of the genes up-regulated following PAE in the 6J at E7.25 revealed pathways related to catalytic activity (specifically, hydrolases and endopeptidases) were dysregulated (Fig 4A; Table S5). Interestingly, we identified “Activation, myristolyation of BID and translocation to mitochondria” as up-regulated by PAE. BID (BH3 interacting-domain death agonist) is a pro-apoptotic protein of the Bcl-2 family that is activated by the posttranslational modification N-myristoylation.

Activation of BID causes insertion of Bax into the mitochondrial membrane and release of Cytochrome C (Eskes et al., 2000). This pathway, in combination with others related to cytolysis and apoptotic signaling, indicate that cell death pathways have begun to be activated in the 6J strain as early as 6 hr post-PAE (E7.25). Analysis of down-regulated genes in the 6J found that cellular metabolism and binding activity were reduced. “Binding activity” included enzymatic, DNA, and protein binding, and likely indicates an overall reduction in cellular activity that coincides with decreased metabolism. Multiple terms related to cell cycle regulation were also identified in the down-regulated genes, suggesting that cell proliferation is slowed or paused while the embryo responds to the alcohol insult. *De novo* network analysis revealed multiple associations with organ health and development, cancer/cell cycle, drug metabolism, and cell death (Table 2A; Table S2D).

The top two genes down-regulated following PAE in the 6J at E7.25 were *Srsf2*, a protein that regulates constitutive and alternative splicing of pre-mRNA that has been linked to cell death through the p53 pathway (Comiskey et al., 2020), and *Alyref*, which encodes the molecular chaperone Aly/REF export factor which is involved in RNA processing and nuclear export. The most upregulated gene in 6J was *Chac1*, which encodes Glutathione-specific gamma-glutamylcyclotransferase-1 (Gamma-GCG 1), a protein involved in glutathione cleavage, induction of oxidative stress-related apoptosis, and a negative regulator of Notch signaling (Chi et al., 2012). *Trib3* was also significantly upregulated and encodes Tribbles pseudokinase 3 (Trb-3), which is induced by NF-κB signaling and creates a negative feedback loop controlling Atf4 activity in response to cellular stress and prevents apoptosis. Interestingly, Trb-3 has also been shown to block expression of Gamma-GCG 1 (encoded by *Chac1*) (Örd et al., 2016), thus limiting apoptosis through another pathway. Multiple types of cellular stress up-regulated Trb-3, including nutritional deprivation (Liu et al., 2012) and endoplasmic reticulum (ER) stress (Örd et al., 2014). In sum, alcohol-induced reductions in expression of cellular metabolism and gene transcription pathways, as well as up-regulation of genes related to oxidative stress and apoptosis, could lead to perturbed cell proliferation and embryonic growth in PAE 6J embryos.

We next compared gene expression patterns following PAE in 6N mice. Although 372 genes were upregulated, there were no significantly enriched pathways among them. However, analysis of the 330 down-regulated genes revealed a reduction in cellular metabolism and methyltransferase activity (Fig 4B; Table S6). Similar to the 6J, PAE seemingly caused a reduction in cellular activity in the 6N. Alteration of methylation could have effects on gene expression and protein function; some of the specific methyltransferases targeted by PAE included *Kdm1a*, *Kdm4b*, *Mettl3*, *Mettl4*, *Mettl16*, *Prdm5*, among others. Gene network analyses also revealed pathways related to organ and tissue disease, cell cycle/DNA replication and repair, and cell and tissue morphology (Table 2B; Table S2E). The two most down-regulated genes were *Rsrp1*, which encodes the relatively unknown protein Arginine/serine rich

protein 1, a target of Heat Shock Protein 1 under certain conditions (Korfanty et al., 2014), and *Alyref,* described above. *Tap2*, a transporter protein involved in multi-drug resistance and antigen presentation through localization of peptides to the ER where they are then transported to the cell surface, and *Sox15*, a member of the Sox family, were the two most up-regulated genes. The Sox family is comprised of transcription factors that play vital roles in embryonic development and specification of cell fate. Sox15 expression is highest in undifferentiated embryonic stem cells (Maruyama et al., 2005), suggesting that PAE may disrupt cell differentiation in 6N mice, resulting in increased expression of *Sox15*. Overall, while PAE causes a reduction in cellular activity that could disrupt proliferation and cell fate decisions, there is no evidence that cell death pathways are activated at this point in the 6N, a notable difference from the 6J.

Large-scale strain-specific differences in transcriptional response to PAE apparent 12 hours following exposure

To explore how strain differences continue to modulate the transcriptional landscape 12 hours after alcohol exposure, we next compared the effect of PAE on embryonic gene expression in each strain at E7.5. At E7.5 (12 hr post-PAE), the 6J strain continued to have more pronounced gene expression changes relative to the 6N; in fact, the number of differentially expressed genes increased over three-fold in the 6J while it remained relatively stable in the 6N. In the 6J, 2,987 genes were differentially expressed 12 hr after PAE. Of these, 1,641 were up-regulated (54.9%) and 1,346 were down-regulated (45.1%) (Fig 5A). Conversely, only 641 genes were altered by PAE in the 6N at this time point, with 366 up-regulated (57.1%) and 275 down-regulated (42.9%) (Fig 5B). The significant increase in the number of differentially expressed genes in the 6J but not the 6N provides further evidence that 6J mice are more sensitive to PAE; 291 genes in total overlapped between the two strains (Fig 5C). While most genes significantly altered by PAE in both strains showed the same direction of change, most of the overlapping genes were up-regulated at E7.5, as compared to most overlapping genes being down-regulated in both strains at E7.25.

Functional profiling of the genes up-regulated 12 hr following PAE in 6J mice revealed pathways related to intracellular signaling, protein transport and localization, and cell death (Fig 6A; Table S7). One of the upregulated pathways we identified in 6J mice was “Formation of xylulose-5-phosphate”. Xylulose-5-phosphate is a ketose sugar known to promote gene transcription through the ChREBP transcription factor (encoded by *Mlxipl*). This was interesting because *Mlxipl* was itself significantly upregulated in the 6J mice at this time point. ChREBP is part of the Myc superfamily and has been found to affect cell proliferation through regulation of transcription of cyclins in certain cell types (Filhoulaud et al., 2013, Tong et al., 2009), though its exact function in early gestational embryos is not

known. In addition, ChREBP has multiple isoforms and can be stored in an inactive form. The down-regulated genes in the 6J mice were enriched for embryonic organogenesis and skeletal development, including the head, palate, and circulatory system. Notably, holoprosencephaly, cleft palate, and abnormal lip, ear, and face shape were identified using the Human Phenotype Ontology (HPO) database as phenotypes associated with PAE. These craniofacial malformations have been associated with heavy alcohol exposure during early gestation in the human population (DeRoo et al., 2008, Romitti et al., 2007, Johnson and Rasmussen, 2010, Jones et al., 2010). Analysis of *de novo* gene networks found differences in pathways related to organismal injury and abnormalities, cell death, organ disease, embryonic development, and protein and RNA post-translational modifications of RNA and proteins (Table 3A; Table S2F).

The most down-regulated gene in the 6J at E7.5 was *Shh*. Multiple other members of the Shh pathway were also down-regulated by PAE in the 6J at this time point, including *Ptch1*, *Smo*, and *Gli3*. In contrast, *Gli3* was the only member of the pathway affected by alcohol in the 6N mice at either time point. Dysregulation of the Shh pathway is linked to craniofacial malformations such as holoprosencephaly in genetic ciliopathies (Brugmann et al., 2015, Chang et al., 2016) and PAE both down-regulates Shh expression (Higashiyama et al., 2007) and causes more severe craniofacial and limb defects in transgenic mice lacking genes in the Shh pathway (Fish et al., 2017, Kietzman et al., 2014). If alcohol is more likely to impact Shh signaling in the 6J than the 6N, this presents one way in which 6J may be more likely to develop craniofacial and eye defects. Whether there is an association between the higher baseline expression of immune genes in the 6J and differences in Shh signaling after alcohol exposure is not yet clear, but these findings warrant further exploration. *Efcab7*, a gene linked to Smo transduction in the primary cilia (Pusapati et al., 2014), was up-regulated by PAE at E7.5 (+0.81 Log_2FC). This gene had lower expression in the 6J relative to the 6N at E7.0 and E7.25, suggesting possible pre-existing differences between the strains, however, more work needs to be done to determine the exact role of Efcab7 during gastrulation and, in particular, in relation to Shh signaling. Another down-regulated gene, *Tcf21*, encodes transcription factor 21, a protein with varied and important functions during lung, kidney, heart, and gonadal development (Braitsch et al., 2012, Quaggin et al., 1999, Tamura et al., 2001). Down-regulation of the *Shh* pathway and *Tcf21* suggest serious and widespread defects in organogenesis within the 6J just 12 hours following PAE, an effect that does seem to occur in the 6N mice.

The top two up-regulated genes in the 6J were *Tap2* and *Fam46b*, the first of which was also one of the top up-regulated genes in the 6N at E7.25. Fam46b (also known as TENT5B in humans) has recently been shown to be highly expressed in undifferentiated embryonic stem cells, with a sharp drop in expression following cell differentiation (Hu et al., 2020). While its biological functions remain to be

fully elucidated, particularly in the embryo, Fam46b could play a role in cell cycle regulation as it inhibits cell proliferation in *in vitro* models of prostate cancer (Liang et al., 2018). Overall, these data indicate that PAE has a profoundly damaging effect in the 6J that is apparent within 12 hours following exposure. In addition to the down-regulation of Shh pathway genes, multiple genes regulating the p53 pathway were also dysregulated, including *Hif1a*, *Mdm2*, *Sirt1*, and *Sco2*, indicating that cell proliferation, DNA damage repair mechanisms, cell cycle regulation, and apoptosis are among the primary targets modulated by PAE in this strain. These data establish an association between baseline genetic variations between strains that lead to more deleterious outcomes in response to alcohol exposure.

Analysis of up-regulated genes in the 6N indicated that PAE caused an increased inflammatory signaling response in these embryos compared to controls, as well as catalytic activity and RAGE receptor binding (Fig 6B; Table S8). Increased IL-17 signaling was also identified as an up-regulated pathway in this data set, further supporting that PAE is causing immune signaling activation, which could have downstream effects on cell survival and tissue growth. Multiple phenotypes related to hypoxemia were found to be up-regulated in the 6N using the HPO database, indicating that PAE could be affecting cellular oxygen levels up to 12 hr later. Analysis of down-regulated genes in the 6N revealed pathways related to overall cellular activity, DNA binding, and skeletal and neuronal development. Network analysis revealed that pathways related to cell morphology, embryonic development, cell death, cellular metabolism, and inflammation were also altered by PAE in the 6N at E7.5 (Table 3B; Table S2G).

The top down-regulated genes in the 6N at E7.5 were *Mef2c* and *Nkx2-5*. *Mef2c* encodes the transcription factor myocyte enhancer factor 2C (Mef2c) important for skeletal muscle and central nervous system (CNS) development. Humans with mutations in this gene exhibit severe intellectual disabilities, loss of muscle tone, mild craniofacial dysmorphologies, and severe seizures. Transgenic mice with a knockout of *Mef2c* display disorganized vasculature and cardiovascular defects. *Nkx2-5* encodes NK2 homeobox 5, known to be involved in heart development and highly expressed in the cardiac crescent cells at E7.5. Knockdown of this gene is embryonically lethal at ~E9-10 and causes growth retardation and heart defects.

The top two up-regulated genes were *S100a9* and *Retnlg*. S100a9 is a damage-associated molecular pattern molecule (DAMP) that makes a heterodimer with S100a8 to create calprotectin, a protein complex that produces pro-inflammatory activity when secreted from neutrophils, though cells from a neutrophil lineage are not known to be present in the embryo during gastrulation (McGrath et al., 2014). Increased concentrations of extracellular S100a9 and S100a8 induce apoptosis and stimulate ROS production in certain cell types (Lim et al., 2010). S100a9 is also known to interact with the RAGE

receptor pathway, a part of the innate immune system and a primary receptor for Hmgb1, a protein previously shown to be part of the inflammatory response to alcohol in the adolescent and adult brain (Coleman Jr et al., 2018, Vetreno and Crews, 2012). The function of resistin-like gamma (*Retnlg*) is largely unexplored, though it shares some similarity with human resistin (RETN), a hormone released by adipose tissue.

In summary, while PAE affects pathways related to embryonic development in the 6N, these pathways do not seem to be as clearly linked to craniofacial development as those identified in the 6J, possibly contributing to the phenotypic differences observed between these strains following PAE.

Limited overlap in PAE-induced transcriptional differences between 6J and 6N strains 6–12 hours following exposure

Only seven genes were differentially expressed following PAE in both strains at both time points (Fig S8). Three of these genes, *Aven*, *Hist3h2a*, and *Tbx1* were strongly down-regulated in both strains at both time points. *Aven* encodes the Cell death regulator Aven protein, which inhibits apoptosis through suppression of pro-apoptotic Apaf1 and augmentation of anti-apoptotic BCL-X_L activity and regulates the G2/M DNA damage checkpoint during cell cycle progression (Gross, 2008). Interestingly, this gene was also down-regulated in the rostroventral neural tube of 6J mice 6 hr after neurulation-stage alcohol exposure in a previous study (Boschen et al., 2020), revealing this gene as a marker of prenatal alcohol exposure across multiple models of FASD. The next gene, *Hist3h2a* (also called *H2aw*), is translated into a core component of chromatin, histone H2A cluster 3. Chromatin dynamics regulate access of transcription factors to the DNA and control processes such as cell proliferation and differentiation. *Hist3h2a* was also found to be down-regulated by neurulation-stage alcohol in a whole embryo culture model derived from C57BL/6J mice (Zhou et al., 2011). The third down-regulated gene, *Tbx1*, encodes Tbox-1, a well-studied transcription factor important for cell proliferation during embryonic development. Loss of Tbx1 function is associated with 22q11 deletion/DiGeorge syndrome phenotypes, including heart defects, craniofacial abnormalities, and cleft palates (Jerome and Papaioannou, 2001, Verdelli et al., 2017, Yagi et al., 2003). One of the genes that was up-regulated in both strains at both time points was *Sdr39u1*, which encodes a short chain dehydrogenase with oxidoreductase activity localized to the mitochondria and is thought to have a binding site on NADP. While this protein has been identified as a possible biomarker candidate for neurodegenerative diseases such as Alzheimer's disease (Rahman et al., 2019), its exact function is still under scrutiny. While there is little evidence directly linking Sdr39u1 to the oxidative stress response, production of NADP is a key player in cellular antioxidation.

DISCUSSION

Understanding variables that modulate prenatal alcohol sensitivity has been an important area of research given the well-known variability of outcomes in both children exposed to alcohol *in utero* and in animal models of FASD. The wide range of signs and symptoms of prenatal alcohol exposure present problems not only for diagnosis and treatment of individuals with FASD, but for a complete understanding of the pathogenic mechanisms of alcohol. The current study adds valuable information regarding the contribution of genetics to prenatal alcohol susceptibility by demonstrating that baseline genetic differences between two closely related mouse sub-strains can result in significantly different molecular responses to a teratogen such as alcohol. While only 80 genes differed between the alcohol-sensitive 6J compared to the 6N at E7.0, the 6J had significantly more genes dysregulated by alcohol 6–12 hr later. Functional profiling also revealed that the biological functions affected by alcohol in the 6J differed from those identified in the 6N. Gene expression pathways related to cell proliferation, apoptosis, and those controlling craniofacial and brain development were affected in the 6J embryos. In contrast, cellular metabolism, hypoxemia, and inflammation pathways were altered in the 6N. Overall, these data indicate that gastrulation-stage alcohol exposure might alter cell proliferation in both strains, but apoptosis pathways are more strongly enriched in the 6J, likely contributing to the increased incidence of eye defects following PAE in the 6J fetuses compared to the 6N (Dou et al., 2013).

The most well-studied difference between the 6J and 6N strains is the *Nnt* mutation. Nnt is a component of the mitochondrial inner membrane that passes hydrogen atoms that are then used in the conversion of NADP+ to NADPH, an important co-enzyme that regulates metabolism along with NADH. A primary function of NADPH is removal of ROS from the mitochondria (Fig 7). NADH is the reduced form of NAD+, and these co-factors are important for redox metabolism, cellular respiration, and ATP production. In addition, NADPH converts glutathione from the oxidized (GSSG) to the reduced state (GSH) via glutathione reductase (GR). GSH neutralizes ROS and sequesters and eliminates H_2O_2. Reductions in Nnt disrupt the NADPH/NADH balance, causing smaller NADPH pools and lower GSSG/GSH conversion with less capacity for ROS removal, as well as increased NADH, leading to an overproduction of ATP and dysregulation of glycolysis and the TCA cycle. While little research has been done on the effect of the *Nnt* mutation on ROS levels in the 6J embryo, endothelial cells from 6J mice exhibit increased superoxide production after Angiotensin II stimulation and reduced glutathione peroxidase activity compared to 6N mice (both sub-strains obtained from Jackson Labs), indicating altered mitochondrial function as a result of the *Nnt* mutation. (Leskov et al., 2017). In addition, the *Nnt* mutation has been shown to be a modifier of other genetic mutations, such as *Bcl2l2* (Navarro et al., 2012) and mitochondrial superoxide dismutase (Huang et al., 2006). Increased DNA damage and altered immune signaling have been observed in the 6J strain compared to others in response to other

chemical and environmental stressors, including in the lung after exposure to 1,3-Butadiene, a carcinogenic inhalant (Chappell et al., 2017), and in the brain following postnatal hypoxic ischemia (Wolf et al., 2016), though the specific effects seem to be exposure, organ, and age-dependent. Aberrant Nnt function has also been implicated in cancer, indicating a possible role in cell growth (Ho et al., 2017). A buildup of ROS as a result of the *Nnt* mutation could predispose the embryo to be sensitive to external stressors such as alcohol exposure, which produces oxidative stress on its own (Brocardo et al., 2011, Henderson et al., 1995, Henderson et al., 1999).

Oxidative stress can induce inflammation and expression of pro-apoptotic molecules NF-κB and p53 and oxidative stress proteins HIF-1α and PPAR-γ (Reuter et al., 2010). The *Nnt* mutation has also been directly linked to increased expression of HIF-1α in the mouse liver. This molecule is critical for cellular response to hypoxia and can protect against oxidative stress. While *Hif1a* expression did not differ between the strains at baseline, it was down-regulated by PAE in the 6J strain at the E7.5 time point. The current study found that the 6J strain had increased expression of genes related to inflammation at baseline. The 6N mice showed an upregulation of inflammation-related genes at E7.5, while the 6J did not show many alcohol-induced changes in inflammatory pathways at either time point, possibly due to the fact that immune signaling genes were already comparatively activated in the 6J at baseline. Interpretation of the up-regulation of inflammatory signaling in the 6J relative to 6N at E7.0 is limited since the exact function of immune molecules during gastrulation remains under investigation. Early macrophages are detected in the yolk sac during neurulation (~E9 in mice) (Naito, 2008), while cells from a neutrophil lineage do not emerge in the embryo until E11.5 (McGrath et al., 2014), far after the time points under observation here. However, cytokines and chemokines have been suggested to play a role in cell migration (Nair and Schilling, 2008, Katsumoto and Kume, 2011), cell adhesion, and tissue remodeling during gastrulation (Aller et al., 2014). In addition, it is possible that some of the pro-inflammatory signals are due to transfer from maternal circulation or the placenta. A direct link between the timing of immune signaling activity (higher at baseline in the 6J's vs. PAE-induced activation in 6N's) and differences in alcohol sensitivity between the strains remains to be determined.

Motile and immotile cilia play important roles throughout embryonic development. Previous work from our lab has demonstrated that alcohol administered during neurulation alters over 100 cilia genes in the neural tube within the first 6 hr after exposure (Boschen et al., 2020). During gastrulation, motile cilia in the primitive node beat to create a morphogenic gradient that regulates left-right asymmetry. Previously, we have shown that knockdown of the cilia gene *Mns1* results in increased incidence and severity of ocular and craniofacial defects following gastrulation-stage alcohol exposure (Boschen et al., 2018), indicating a possible role for cilia dysfunction in the development of prenatal alcohol-related birth defects. Cilia-related genes in the current data set were identified through comparison of each gene list

with the CiliaCarta compendium (Van Dam et al., 2019). Gastrulation-stage alcohol exposure altered cilia-related genes in both strains but to a greater degree in the 6J (25 cilia genes in the 6J vs. 21 genes in the 6N at E7.25; 101 cilia genes in the 6J vs. 24 genes in the 6N at E7.5; Table S9). Immotile cilia, called primary cilia, are responsible for transduction of the Shh pathway as Smo is trafficked into the cilia following binding of Shh to Ptch1, and the Gli transcription factors are processed within the cilia axoneme. In the 6J mice, multiple genes within the Shh pathway (*Shh, Ptch1, Smo, Gli3*) were down-regulated 12 hr after alcohol. This time point also coincided with a relatively large increase in the number of cilia genes dysregulated by alcohol in this strain compared to the 6N. Further investigation is needed to determine if the cilia genes altered by alcohol exposure in the 6J are directly related to the down-regulation of Shh pathway genes or are indicative of any significant motile or immotile cilia dysfunction.

The 6J and 6N strains are widely used to study the effects of prenatal drug exposure. Factors such as timing of alcohol exposure (gastrulation vs. neurulation), time elapsed between alcohol administration and tissue collection (e.g. 3 hr in Green and colleagues (Green et al., 2007a), 6 – 12 hr in our study), and specific tissue type assessed (head fold tissue vs. whole embryo) contribute to the differences between previously published gene expression profiles and those reported here. Our previous work (Boschen et al., 2020) sequenced RNA collected from rostroventral neural tube tissue 12 or 24 hr after alcohol the 6J strain only. Despite methodological differences between these experiments, common targets of alcohol are apparent when the studies are compared. Mitochondrial function and ribosome biogenesis have been reported to be disrupted in multiple models of FASD (Green et al., 2007a, Garic et al., 2014, Boschen et al., 2020, Berres et al., 2017) and identified as down-regulated pathways in the 6J PAE-treated embryos at E7.5 in the current study. Compromised ribosome biogenesis and mitochondrial function could be indicative of impaired cell growth as synthesis of ribosomes is necessary for cell cycle progression. Cell motility and adhesion have also been determined to be targets of alcohol during early gestation (Dou et al., 2013, Boschen et al., 2020, Green et al., 2007a). While cell motility was up-regulated in the 6J's vs. 6N's at E7.0 in the current study, pathways related to cell movement were not enriched by PAE at either time point. Finally, competition between alcohol and retinoic acid (RA) as a mechanism of prenatal alcohol pathogenesis has been a long-standing hypothesis in the field (Deltour et al., 1996, Johnson et al., 2007). While the current study did not find statistical enrichment of any RA pathways, three genes related to RA signaling were dysregulated after PAE: *Lrat* (Lecithin retinol acyltransferase, +0.42 Log2FC in 6J's at E7.25), *Rara* (Retinoic acid receptor-α, +0.46 Log2FC in 6N's at E7.25), and *Crabp2* (Cellular retinoic acid binding protein 2, -1.04 and -0.87 Log2FC in 6J's and 6N's, respectively, at E7.5). However, interpretation of these single genes is difficult in the absence of other changes to the pathway. RA has

been shown to be a regulator of Shh signaling (Ribes et al., 2006, Helms et al., 1997), which was significantly down-regulated in the 6J strain 12 hr after PAE, though it is beyond the scope of this study to determine if this change was related to RA signaling.

These data provide information about gene expression patterns in two widely used strains of mice across normal gastrulation and in response to a teratogen. The web tool created to allow for exploration of the dataset visually demonstrates the dynamic nature of certain genes across gastrulation (e.g. *Shh* increases expression over time, *Fgf5* shows reduced expression). The tool will also provide a valuable resource during experimental design, as there are significant differences in gene expression between the two strains that might support the use of one over the other for certain paradigms. The future directions of this study will explore the nuances of gene expression profiles in these two strains, including whether biological sex contributes to prenatal alcohol sensitivity. While all time points used in this study occur prior to gonadal sexual differentiation, differences in gene expression and growth rates have been reported between male and female pre-implantation embryos (Deegan et al., 2019, Werner et al., 2017). Though no sex differences were apparent in the differentially expressed genes in this study, as determined by the consistency between samples (Fig S1-S7), this question needs to be fully explored. In addition, our study used whole embryo tissue, whereas newer sequencing technologies such as single-cell and spatial transcriptomics will allow for investigation of localized mRNA expression patterns, spatiotemporal cell-cell interactions, and a direct link between gene expression and tissue morphology in the gastrulating embryo.

In conclusion, our study demonstrates that a pre-existing genetic susceptibility can mediate sensitivity to teratogens such as alcohol in mice. Not only did the sensitive 6J mice show a larger response to PAE in sheer number of genes/biological pathways affected, but pathways regulating cell death, proliferation, and craniofacial and CNS development were altered to a greater degree in this strain. We hypothesize that the known mutation in *Nnt* in the 6J strain predisposes these embryos to have increased expression of inflammatory signaling genes than make them more sensitive to the addition of an external stressor such as PAE (Fig 7). Understanding how genetic variability can mediate risk and resiliency to PAE can help elucidate how alcohol acts on the embryo at the cellular level and, ultimately, assist in identifying candidate genes as biomarkers of prenatal alcohol exposure in the human population.

MATERIALS AND METHODS

Animals

Male and female adult C57BL/6J (Jackson Labs, Bar Harbor, ME; Stock #: 000664) and C57BL/6NHsd (Envigo, Indianapolis, IN) mice (*mus musculus*) were obtained. Males were housed singly and females were housed in groups up to five in standard polycarbonate cages with cob bedding, shelter, and nesting material. Mice had *ad libitum* access to food (Prolab Isopro RMH 3000, LabDiet, St. Louis, MO) and water and were maintained on a 12:12 hr light/dark cycle. Up to two female mice were placed into the cage of a male for each 2 hr mating session. Upon discovery of a vaginal plug, E0 was defined as the beginning of the mating session (Fig 1). All experimental procedures were approved by the Animal Care and Use Committee at UNC-Chapel Hill in accordance with NIH Guidelines (Approval #18-203). On E7.0, dams were weighed and pregnant dams were either dissected immediately or assigned to one of the experimental treatment groups.

Alcohol Exposure Paradigm (PAE)

On E7.0, dams were administered two doses of 2.9 g/kg ethanol (25% vol/vol; Pharmaco-Aaper, Brookfield, CT) in Lactated Ringer's solution 4 hr apart via i.p. injection (Fig 1). This dose and pattern of alcohol exposure results in maternal blood alcohol concentrations of ~400 mg/dl (O'Leary-Moore et al., 2010). Control mice were administered an equal volume of Lactated Ringer's solution (1.5 ml/100 g body weight).

RNA Isolation

RNA was collected from embryos either before alcohol administration (E7.0) or 6 or 12 hr after the first alcohol injection (E7.25 or E7.5) (Fig 1). Dams were sacrificed via CO_2 followed by cervical dislocation and embryos were dissected from the placenta. All extraembryonic tissue was removed and embryos were stage-matched based on morphological assessment (Theiler Stages 10-11; representative image in Fig 2A).. A total of 6 embryos per group were used, with no more than two embryos collected per litter to minimize litter effects. Sex was not considered as a biological variable as all time points occur prior to gonadal sexual differentiation. RNA was isolated using the RNeasy Plus Micro Kit (Qiagen, Germantown, MD) and RNA concentrations and purity were assessed using a NanoDrop 2000 and Qubit 3.0 Fluorimeter (Thermofisher Scientific, Waltham, MA). A separate group of samples was collected at the E7.0 time point and isolated for validation of gene expression using qRT-PCR. Expression of *Wdfy1*, *Entpd4,* and *Efcab7* was analyzed in each strain and found to validate the RNA-seq results from this time point (Fig S9). All samples were run in triplicate (n = 6/strain).

RNA-seq

A total of 6 samples per group were submitted for sequencing. Libraries for RNA sequencing (RNA-seq) were prepared using the SMARTr Ultra Low Input RNA (Clontech, Mountainview, CA) and Nextera XT DNA (Illumina, San Diego, CA) kits by the UNC High Throughput Sequencing Facility. Samples were pooled only for sequencing, after RNA extraction and library preparation. For E7.0 samples (12 embryos total), there were 4 samples per pool (2/group), 3 pools total, 1 pool per lane. For E7.25 and E7.5 samples (24 samples/time point), there were 4 samples per poll (1/group), 6 pool total, 1 pool per lane. Paired-end (50bp) sequencing was performed (Illumina HiSeq 4000).

RNA-seq and qRT-PCR data analysis and display

Reads were filtered and aligned as described previously (Boschen et al., 2020). Transcript abundance was measured using Salmon (Patro et al., 2017), and differential expression tests were performed using *DESeq2* 1.22.2 (Anders and Huber, 2010). Gene expression differences were considered significant at an adjusted *p*-value threshold of 0.05. At the E7.5 time point, 3 outliers were detected and removed from the analysis: one from the 6J vehicle-treated group and two from the 6N PAE group. Final sample sizes are noted in the figure captions. We used gProfiler 0.1.6 (Raudvere et al., 2019) to detect significantly enriched pathways among differentially expressed genes, primarily using Gene Ontology (GO) (Ashburner et al., 2000, The Gene Ontology Consortium, 2018), the Kyoto Encyclopedia of Genes and Genomes (KEGG) (Kanehisa et al., 2019, Kanehisa and Goto, 2000), Reactome (Jassal et al., 2020, Fabregat et al., 2018), and Human Phenotype Ontology (HPO) (Kohler et al., 2019). In addition, differentially expressed genes were assayed in a *de novo* network analysis using Ingenuity Software (Qiagen, Germantown, MD). For the E7.0 time point, network analysis was limited to 35 molecules (genes/proteins/protein complexes) per network due to the small number of input genes. For the E7.25 and 7.5 time points, analysis was limited to 70 focus molecules per network. Networks were ranked by the negative $\log_{10}$ Fisher's exact *p*-value testing the likelihood of a similar network being formed by the same number (35 or 70) random molecules. Gene lists were also compared to the CiliaCarta compendium (Van Dam et al., 2019) to analyze number of cilia-related genes disrupted by alcohol at each time point and in each strain.

qRT-PCR data was analyzed with unpaired *t*-tests corrected for multiple comparisons and a *p*-value of < 0.05 designated as statistically significant.

The gene expression data browser web-tool was developed using the R shiny framework is hosted through the Apache HTTP webserver. Several packages are used to process and display the gene expression data including, the tidyverse, here, ggplot2, reactable, dqshiny and shinylogs packages. The computer code for the data browser is available through github (https://github.com/mbergins/Embryo-Genes).

DATA AVAILABILITY

RNA-seq data have been deposited in GEO under accession GSE163796. The accession is currently private, but reviewers can access with the following password: uhydcsyknzyxhmv.

ACKNOWLEDGEMENTS AND FUNDING SOURCES

The authors would like to thank Haley N. Mendoza-Romero and Casey E. Hunter for technical support on this project and Charlotte A. Love for the image of the E7 embryo. The visualization tool was created in collaboration with UNC's Bioinformatics and Analytics Research Collaborative (BARC) and is hosted by the UNC School of Medicine. Fig 1 and 8 created with Biorender.com.

Funding for this research was provided by the National Institutes of Health/National Institute of Alcohol and Alcoholism (NIH/NIAAA) grants: U01AA021651 and R01AA026068 to S.E.P., F32AA026479 and K99AA028273 to K.E.B. All or part of this work was done in conjunction with the Collaborative Initiative on Fetal Alcohol Spectrum Disorders (CIFASD), which is funded by grants from NIAAA. Additional information about CIFASD can be found at www.cifasd.org. J.M.S. and T.S.P. were supported by The Eunice Kennedy Shriver National Institute of Child Health and Human Development (U54HD079124) and NINDS (P30NS045892).

COMPETING INTERESTS

The authors have no conflicts of interest to disclose.

AUTHOR CONTRIBUTIONS

S.E.P and K.E.B. conceptualized and designed the experiment. K.E.B. performed the investigation and validation studies. T.S.P. and J.M.S. performed the formal analysis. T.S.P., M.E.B., and J.M.S. performed data curation and visualized the findings along with K.E.B. All authors were involved in provision of resources for their specific contributions to the manuscript. K.E.B. wrote the original draft, M.E.B., J.M.S. and S.E.P. reviewed and edited the manuscript. S.E.P. supervised and acted as project administrator. Financial support was acquired by K.E.B., T.S.P., J.M.S., and S.E.P.

REFERENCES

ABEL, E. L. 1988. Fetal alcohol syndrome in families. *Neurotoxicology and Teratology,* 10**,** 1-2.

ALLER, M.-A., ARIAS, J.-I., ARRAEZ-AYBAR, L.-A., GILSANZ, C. & ARIAS, J. 2014. Wound healing reaction: A switch from gestation to senescence. *World Journal of Experimental Medicine,* 4**,** 16.

ANDERS, S. & HUBER, W. 2010. Differential expression analysis for sequence count data. *Genome biology,* 11**,** 1.

AOTO, K., SHIKATA, Y., HIGASHIYAMA, D., SHIOTA, K. & MOTOYAMA, J. 2008. Fetal ethanol exposure activates protein kinase A and impairs Shh expression in prechordal mesendoderm cells in the pathogenesis of holoprosencephaly. *Birth Defects Research Part A: Clinical and Molecular Teratology,* 82**,** 224-231.

ASHBURNER, M., BALL, C. A., BLAKE, J. A., BOTSTEIN, D., BUTLER, H., CHERRY, J. M., DAVIS, A. P., DOLINSKI, K., DWIGHT, S. S., EPPIG, J. T., HARRIS, M. A., HILL, D. P., ISSEL-TARVER, L., KASARSKIS, A., LEWIS, S., MATESE, J. C., RICHARDSON, J. E., RINGWALD, M., RUBIN, G. M. & SHERLOCK, G. 2000. Gene ontology: tool for the unification of biology. The Gene Ontology Consortium. *Nature genetics,* 25**,** 25-29.

BENNETT, R. G., DUCKWORTH, W. C. & HAMEL, F. G. 2000. Degradation of amylin by insulin-degrading enzyme. *Journal of biological chemistry,* 275**,** 36621-36625.

BERRES, M. E., GARIC, A., FLENTKE, G. R. & SMITH, S. M. 2017. Transcriptome profiling identifies ribosome biogenesis as a target of alcohol teratogenicity and vulnerability during early embryogenesis. *PLoS One,* 12**,** e0169351.

BOSCHEN, K. E., GONG, H., MURDAUGH, L. B. & PARNELL, S. E. 2018. Knockdown of Mns1 Increases Susceptibility to Craniofacial Defects Following Gastrulation-Stage Alcohol Exposure in Mice. *Alcoholism: Clinical and Experimental Research,* 42**,** 2136-2143.

BOSCHEN, K. E., PTACEK, T. S., SIMON, J. M. & PARNELL, S. E. 2020. Transcriptome-wide Regulation of Key Developmental Pathways in the Mouse Neural Tube by Prenatal Alcohol Exposure. *Alcoholism: Clinical and Experimental Research*.

BRAITSCH, C. M., COMBS, M. D., QUAGGIN, S. E. & YUTZEY, K. E. 2012. Pod1/Tcf21 is regulated by retinoic acid signaling and inhibits differentiation of epicardium-derived cells into smooth muscle in the developing heart. *Developmental biology,* 368**,** 345-357.

BROCARDO, P. S., GIL-MOHAPEL, J. & CHRISTIE, B. R. 2011. The role of oxidative stress in fetal alcohol spectrum disorders. *Brain research reviews,* 67**,** 209-225.

BRUGMANN, S., CHANG, C.-F. & MILLINGTON, G. 2015. GLI-dependent Etiology of Craniofacial Ciliopathies. *The FASEB Journal,* 29**,** 86.2.

CHANG, C.-F., CHANG, Y.-T., MILLINGTON, G. & BRUGMANN, S. A. 2016. Craniofacial ciliopathies reveal specific requirements for GLI proteins during development of the facial midline. *PLoS genetics,* 12**,** e1006351.
CHAPPELL, G. A., ISRAEL, J. W., SIMON, J. M., POTT, S., SAFI, A., EKLUND, K., SEXTON, K. G., BODNAR, W., LIEB, J. D., CRAWFORD, G. E., RUSYN, I. & FUREY, T. S. 2017. Variation in DNA-Damage Responses to an Inhalational Carcinogen (1,3-Butadiene) in Relation to Strain-Specific Differences in Chromatin Accessibility and Gene Transcription Profiles in C57BL/6J and CAST/EiJ Mice. *Environ Health Perspect,* 125**,** 107006.
CHI, Z., ZHANG, J., TOKUNAGA, A., HARRAZ, M. M., BYRNE, S. T., DOLINKO, A., XU, J., BLACKSHAW, S., GAIANO, N., DAWSON, T. M. & DAWSON, V. L. 2012. Botch promotes neurogenesis by antagonizing Notch. *Dev Cell,* 22**,** 707-20.
COLEMAN JR, L. G., ZOU, J., QIN, L. & CREWS, F. T. 2018. HMGB1/IL-1β complexes regulate neuroimmune responses in alcoholism. *Brain, behavior, and immunity,* 72**,** 61-77.
COMISKEY, D. F., MONTES, M., KHURSHID, S., SINGH, R. K. & CHANDLER, D. S. 2020. SRSF2 regulation of MDM2 reveals splicing as a therapeutic vulnerability of the p53 pathway. *Molecular Cancer Research,* 18**,** 194-203.
COOK, C. S., NOWOTNY, A. Z. & SULIK, K. K. 1987. Fetal alcohol syndrome: eye malformations in a mouse model. *Archives of Ophthalmology,* 105**,** 1576-1581.
DEEGAN, D. F., KARBALAEI, R., MADZO, J., KULATHINAL, R. J. & ENGEL, N. 2019. The developmental origins of sex-biased expression in cardiac development. *Biol Sex Differ,* 10**,** 46.
DELTOUR, L., ANG, H. L. & DUESTER, G. 1996. Ethanol inhibition of retinoic acid synthesis as a potential mechanism for fetal alcohol syndrome. *The FASEB journal,* 10**,** 1050-1057.
DEROO, L. A., WILCOX, A. J., DREVON, C. A. & LIE, R. T. 2008. First-trimester maternal alcohol consumption and the risk of infant oral clefts in Norway: a population-based case-control study. *American journal of epidemiology,* 168**,** 638-646.
DOU, X., WILKEMEYER, M. F., MENKARI, C. E., PARNELL, S. E., SULIK, K. K. & CHARNESS, M. E. 2013. Mitogen-activated protein kinase modulates ethanol inhibition of cell adhesion mediated by the L1 neural cell adhesion molecule. *Proceedings of the National Academy of Sciences,* 110**,** 5683-5688.
DOWNING, C., BALDERRAMA-DURBIN, C., BRONCUCIA, H., GILLIAM, D. & JOHNSON, T. E. 2009. Ethanol teratogenesis in five inbred strains of mice. *Alcoholism: Clinical and Experimental Research,* 33**,** 1238-1245.
DUNTY, W. C., CHEN, S. Y., ZUCKER, R. M., DEHART, D. B. & SULIK, K. K. 2001. Selective Vulnerability of Embryonic Cell Populations to Ethanol-Induced Apoptosis: Implications for Alcohol-Related Birth Defects and Neurodevelopmental Disorder. *Alcoholism: Clinical and Experimental Research,* 25**,** 1523-1535.
EBERHART, J. K. & PARNELL, S. E. 2016. The genetics of fetal alcohol spectrum disorders. *Alcoholism: Clinical and Experimental Research,* 40**,** 1154-1165.
ESKES, R., DESAGHER, S., ANTONSSON, B. & MARTINOU, J. C. 2000. Bid induces the oligomerization and insertion of Bax into the outer mitochondrial membrane. *Mol Cell Biol,* 20**,** 929-35.
FABREGAT, A., JUPE, S., MATTHEWS, L., SIDIROPOULOS, K., GILLESPIE, M., GARAPATI, P., HAW, R., JASSAL, B., KORNINGER, F., MAY, B., MILACIC, M., ROCA, C. D., ROTHFELS, K., SEVILLA, C., SHAMOVSKY, V., SHORSER, S., VARUSAI, T., VITERI, G., WEISER, J., WU, G., STEIN, L., HERMJAKOB, H. & D'EUSTACHIO, P. 2018. The Reactome Pathway Knowledgebase. *Nucleic Acids Res,* 46**,** D649-d655.
FILHOULAUD, G., GUILMEAU, S., DENTIN, R., GIRARD, J. & POSTIC, C. 2013. Novel insights into ChREBP regulation and function. *Trends in Endocrinology & Metabolism,* 24**,** 257-268.
FISH, E. W., MURDAUGH, L. B., SULIK, K. K., WILLIAMS, K. P. & PARNELL, S. E. 2017. Genetic Vulnerabilities to Prenatal Alcohol Exposure: Limb Defects in Sonic Hedgehog and GLI2 Heterozygous Mice. *Birth Defects Research Part A: Clinical and Molecular Teratology*.

GARIC, A., BERRES, M. E. & SMITH, S. M. 2014. High-Throughput Transcriptome Sequencing Identifies Candidate Genetic Modifiers of Vulnerability to Fetal Alcohol Spectrum Disorders. *Alcoholism: Clinical and Experimental Research,* 38**,** 1874-1882.

GODIN, E. A., O'LEARY-MOORE, S. K., KHAN, A. A., PARNELL, S. E., AMENT, J. J., DEHART, D. B., JOHNSON, B. W., ALLAN JOHNSON, G., STYNER, M. A. & SULIK, K. K. 2010. Magnetic Resonance Microscopy Defines Ethanol-Induced Brain Abnormalities in Prenatal Mice: Effects of Acute Insult on Gestational Day 7. *Alcoholism: Clinical and Experimental Research,* 34**,** 98-111.

GREEN, M. L., SINGH, A. V., ZHANG, Y., NEMETH, K. A., SULIK, K. K. & KNUDSEN, T. B. 2007a. Reprogramming of genetic networks during initiation of the Fetal Alcohol Syndrome. *Developmental Dynamics,* 236**,** 613-631.

GREEN, M. L., SINGH, A. V., ZHANG, Y., NEMETH, K. A., SULIK, K. K. & KNUDSEN, T. B. 2007b. Reprogramming of genetic networks during initiation of the Fetal Alcohol Syndrome. *Dev Dyn,* 236**,** 613-31.

GROSS, A. 2008. A new Aven-ue to DNA-damage checkpoints. *Trends in Biochemical Sciences,* 33**,** 514-516.

HELMS, J., KIM, C., HU, D., MINKOFF, R., THALLER, C. & EICHELE, G. 1997. Sonic hedgehogParticipates in Craniofacial Morphogenesis and Is Down-regulated by Teratogenic Doses of Retinoic Acid. *Developmental biology,* 187**,** 25-35.

HENDERSON, G., DEVI, B., PEREZ, A. & SCHENKER, S. 1995. In utero ethanol exposure elicits oxidative stress in the rat fetus. *Alcoholism: Clinical and Experimental Research,* 19**,** 714-720.

HENDERSON, G. I., CHEN, J. & SCHENKER, S. 1999. Ethanol, oxidative stress, reactive aldehydes, and the fetus. *Front Biosci,* 4**,** 541-550.

HIGASHIYAMA, D., SAITSU, H., KOMADA, M., TAKIGAWA, T., ISHIBASHI, M. & SHIOTA, K. 2007. Sequential developmental changes in holoprosencephalic mouse embryos exposed to ethanol during the gastrulation period. *Birth Defects Res A Clin Mol Teratol,* 79**,** 513-23.

HO, H.-Y., LIN, Y.-T., LIN, G., WU, P.-R. & CHENG, M.-L. 2017. Nicotinamide nucleotide transhydrogenase (NNT) deficiency dysregulates mitochondrial retrograde signaling and impedes proliferation. *Redox Biology,* 12**,** 916-928.

HONG, M. & KRAUSS, R. S. 2012. Cdon mutation and fetal ethanol exposure synergize to produce midline signaling defects and holoprosencephaly spectrum disorders in mice. *PLoS genetics,* 8**,** e1002999.

HONG, M. & KRAUSS, R. S. 2013. Rescue of Holoprosencephaly in Fetal Alcohol-Exposed Cdon Mutant Mice by Reduced Gene Dosage of Ptch1. *PLOS ONE,* 8**,** e79269.

HU, J.-L., LIANG, H., ZHANG, H., YANG, M.-Z., SUN, W., ZHANG, P., LUO, L., FENG, J.-X., BAI, H. & LIU, F. 2020. FAM46B is a prokaryotic-like cytoplasmic poly (A) polymerase essential in human embryonic stem cells. *Nucleic acids research,* 48**,** 2733-2748.

HU, Y. H., ZHANG, Y., JIANG, L. Q., WANG, S., LEI, C. Q., SUN, M. S., SHU, H. B. & LIU, Y. 2015. WDFY1 mediates TLR3/4 signaling by recruiting TRIF. *EMBO Rep,* 16**,** 447-55.

HUANG, T. T., NAEEMUDDIN, M., ELCHURI, S., YAMAGUCHI, M., KOZY, H. M., CARLSON, E. J. & EPSTEIN, C. J. 2006. Genetic modifiers of the phenotype of mice deficient in mitochondrial superoxide dismutase. *Hum Mol Genet,* 15**,** 1187-94.

JASSAL, B., MATTHEWS, L., VITERI, G., GONG, C., LORENTE, P., FABREGAT, A., SIDIROPOULOS, K., COOK, J., GILLESPIE, M., HAW, R., LONEY, F., MAY, B., MILACIC, M., ROTHFELS, K., SEVILLA, C., SHAMOVSKY, V., SHORSER, S., VARUSAI, T., WEISER, J., WU, G., STEIN, L., HERMJAKOB, H. & D'EUSTACHIO, P. 2020. The reactome pathway knowledgebase. *Nucleic Acids Res,* 48**,** D498-d503.

JEROME, L. A. & PAPAIOANNOU, V. E. 2001. DiGeorge syndrome phenotype in mice mutant for the T-box gene, Tbx1. *Nature Genetics,* 27**,** 286-291.

JOHNSON, C. S., ZUCKER, R. M., HUNTER, E. S. & SULIK, K. K. 2007. Perturbation of retinoic acid (RA)-mediated limb development suggests a role for diminished RA signaling in the teratogenesis of ethanol. *Birth Defects Research Part A: Clinical and Molecular Teratology,* 79**,** 631-641.

JOHNSON, C. Y. & RASMUSSEN, S. A. 2010. Non-genetic risk factors for holoprosencephaly. *American Journal of Medical Genetics Part C: Seminars in Medical Genetics,* 154C**,** 73-85.

JONES, K. L., HOYME, H. E., ROBINSON, L. K., DEL CAMPO, M., MANNING, M. A., PREWITT, L. M. & CHAMBERS, C. D. 2010. Fetal alcohol spectrum disorders: Extending the range of structural defects. *Am J Med Genet A,* 152a**,** 2731-5.

KANEHISA, M. & GOTO, S. 2000. KEGG: kyoto encyclopedia of genes and genomes. *Nucleic Acids Res,* 28**,** 27-30.

KANEHISA, M., SATO, Y., FURUMICHI, M., MORISHIMA, K. & TANABE, M. 2019. New approach for understanding genome variations in KEGG. *Nucleic Acids Res,* 47**,** D590-d595.

KATSUMOTO, K. & KUME, S. 2011. Endoderm and mesoderm reciprocal signaling mediated by CXCL12 and CXCR4 regulates the migration of angioblasts and establishes the pancreatic fate. *Development,* 138**,** 1947-1955.

KIETZMAN, H. W., EVERSON, J. L., SULIK, K. K. & LIPINSKI, R. J. 2014. The teratogenic effects of prenatal ethanol exposure are exacerbated by Sonic Hedgehog or GLI2 haploinsufficiency in the mouse. *PloS one,* 9**,** e89448.

KOHLER, S., CARMODY, L., VASILEVSKY, N., JACOBSEN, J. O. B., DANIS, D., GOURDINE, J. P., GARGANO, M., HARRIS, N. L., MATENTZOGLU, N., MCMURRY, J. A., OSUMI-SUTHERLAND, D., CIPRIANI, V., BALHOFF, J. P., CONLIN, T., BLAU, H., BAYNAM, G., PALMER, R., GRATIAN, D., DAWKINS, H., SEGAL, M., JANSEN, A. C., MUAZ, A., CHANG, W. H., BERGERSON, J., LAULEDERKIND, S. J. F., YUKSEL, Z., BELTRAN, S., FREEMAN, A. F., SERGOUNIOTIS, P. I., DURKIN, D., STORM, A. L., HANAUER, M., BRUDNO, M., BELLO, S. M., SINCAN, M., RAGETH, K., WHEELER, M. T., OEGEMA, R., LOURGHI, H., DELLA ROCCA, M. G., THOMPSON, R., CASTELLANOS, F., PRIEST, J., CUNNINGHAM-RUNDLES, C., HEGDE, A., LOVERING, R. C., HAJEK, C., OLRY, A., NOTARANGELO, L., SIMILUK, M., ZHANG, X. A., GOMEZ-ANDRES, D., LOCHMULLER, H., DOLLFUS, H., ROSENZWEIG, S., MARWAHA, S., RATH, A., SULLIVAN, K., SMITH, C., MILNER, J. D., LEROUX, D., BOERKOEL, C. F., KLION, A., CARTER, M. C., GROZA, T., SMEDLEY, D., HAENDEL, M. A., MUNGALL, C. & ROBINSON, P. N. 2019. Expansion of the Human Phenotype Ontology (HPO) knowledge base and resources. *Nucleic Acids Res,* 47**,** D1018-d1027.

KORFANTY, J., STOKOWY, T., WIDLAK, P., GOGLER-PIGLOWSKA, A., HANDSCHUH, L., PODKOWIŃSKI, J., VYDRA, N., NAUMOWICZ, A., TOMA-JONIK, A. & WIDLAK, W. 2014. Crosstalk between HSF1 and HSF2 during the heat shock response in mouse testes. *The international journal of biochemistry & cell biology,* 57**,** 76-83.

KUO, W., MONTAG, A. G. & ROSNER, M. R. 1993. Insulin-degrading enzyme is differentially expressed and developmentally regulated in various rat tissues. *Endocrinology,* 132**,** 604-611.

LESKOV, I., NEVILLE, A., SHEN, X., PARDUE, S., KEVIL, C. G., GRANGER, D. N. & KRZYWANSKI, D. M. 2017. Nicotinamide nucleotide transhydrogenase activity impacts mitochondrial redox balance and the development of hypertension in mice. *Journal of the American Society of Hypertension,* 11**,** 110-121.

LIANG, T., YE, X., LIU, Y., QIU, X., LI, Z., TIAN, B. & YAN, D. 2018. FAM46B inhibits cell proliferation and cell cycle progression in prostate cancer through ubiquitination of β-catenin. *Experimental & molecular medicine,* 50**,** 1-12.

LIM, S. Y., RAFTERY, M. J. & GECZY, C. L. 2010. Oxidative Modifications of DAMPs Suppress Inflammation: The Case for S100A8 and S100A9. *Antioxidants & Redox Signaling,* 15**,** 2235-2248.

LIU, J., ZHANG, W., CHUANG, G. C., HILL, H. S., TIAN, L., FU, Y., MOELLERING, D. R. & GARVEY, W. T. 2012. Role of TRIB3 in regulation of insulin sensitivity and nutrient metabolism during short-term fasting and nutrient excess. *American Journal of Physiology-Endocrinology and Metabolism,* 303**,** E908-E916.

MANDAL, C., PARK, J. H., LEE, H. T., SEO, H., CHUNG, I. Y., CHOI, I. G., JUNG, K. H. & CHAI, Y. G. 2015. Reduction of Nfia gene expression and subsequent target genes by binge alcohol in the fetal brain. *Neuroscience letters,* 598**,** 73-78.

MARUYAMA, M., ICHISAKA, T., NAKAGAWA, M. & YAMANAKA, S. 2005. Differential roles for Sox15 and Sox2 in transcriptional control in mouse embryonic stem cells. *Journal of Biological Chemistry,* 280**,** 24371-24379.

MATTAPALLIL, M. J., WAWROUSEK, E. F., CHAN, C.-C., ZHAO, H., ROYCHOUDHURY, J., FERGUSON, T. A. & CASPI, R. R. 2012. The Rd8 Mutation of the Crb1 Gene Is Present in Vendor Lines of C57BL/6N Mice and Embryonic Stem Cells, and Confounds Ocular Induced Mutant Phenotypes. *Investigative Ophthalmology & Visual Science,* 53**,** 2921-2927.

MCGRATH, K. E., FEGAN, K., CATHERMAN, S. & PALIS, J. 2014. Emergence of the neutrophil lineage in the mammalian embryo. *Experimental Hematology,* 42**,** S13.

MITIKU, N. & BAKER, J. C. 2007. Genomic analysis of gastrulation and organogenesis in the mouse. *Developmental cell,* 13**,** 897-907.

NAIR, S. & SCHILLING, T. F. 2008. Chemokine signaling controls endodermal migration during zebrafish gastrulation. *Science,* 322**,** 89-92.

NAITO, M. 2008. Macrophage differentiation and function in health and disease. *Pathology international,* 58**,** 143-155.

NAVARRO, S. J., TRINH, T., LUCAS, C. A., ROSS, A. J., WAYMIRE, K. G. & MACGREGOR, G. R. 2012. The C57BL/6J Mouse Strain Background Modifies the Effect of a Mutation in Bcl2l2. *G3 (Bethesda, Md.),* 2**,** 99-102.

O'LEARY-MOORE, S. K., PARNELL, S. E., GODIN, E. A., DEHART, D. B., AMENT, J. J., KHAN, A. A., JOHNSON, G. A., STYNER, M. A. & SULIK, K. K. 2010. Magnetic resonance microscopy-based analyses of the brains of normal and ethanol-exposed fetal mice. *Birth Defects Research Part A: Clinical and Molecular Teratology,* 88**,** 953-964.

ÖRD, D., ÖRD, T., BIENE, T. & ÖRD, T. 2016. TRIB3 increases cell resistance to arsenite toxicity by limiting the expression of the glutathione-degrading enzyme CHAC1. *Biochimica et Biophysica Acta (BBA) - Molecular Cell Research,* 1863**,** 2668-2680.

ÖRD, T., INNOS, J., LILLEVÄLI, K., TEKKO, T., SÜTT, S., ÖRD, D., KÕKS, S., VASAR, E. & ÖRD, T. 2014. Trib3 is developmentally and nutritionally regulated in the brain but is dispensable for spatial memory, fear conditioning and sensing of amino acid-imbalanced diet. *PloS one,* 9.

PATRO, R., DUGGAL, G., LOVE, M. I., IRIZARRY, R. A. & KINGSFORD, C. 2017. Salmon provides fast and bias-aware quantification of transcript expression. *Nat Methods,* 14**,** 417-419.

PIJUAN-SALA, B., GRIFFITHS, J. A., GUIBENTIF, C., HISCOCK, T. W., JAWAID, W., CALERO-NIETO, F. J., MULAS, C., IBARRA-SORIA, X., TYSER, R. C. & HO, D. L. L. 2019. A single-cell molecular map of mouse gastrulation and early organogenesis. *Nature,* 566**,** 490-495.

PUSAPATI, G. V., HUGHES, C. E., DORN, K. V., ZHANG, D., SUGIANTO, P., ARAVIND, L. & ROHATGI, R. 2014. EFCAB7 and IQCE regulate hedgehog signaling by tethering the EVC-EVC2 complex to the base of primary cilia. *Developmental cell,* 28**,** 483-496.

QUAGGIN, S. E., SCHWARTZ, L., CUI, S., IGARASHI, P., DEIMLING, J., POST, M. & ROSSANT, J. 1999. The basic-helix-loop-helix protein pod1 is critically important for kidney and lung organogenesis. *Development,* 126**,** 5771-5783.

RAHMAN, M. R., ISLAM, T., SHAHJAMAN, M., QUINN, J. M. W., HOLSINGER, R. M. D. & MONI, M. A. 2019. Identification of common molecular biomarker signatures in blood and brain of Alzheimer's disease. *bioRxiv***,** 482828.

RAUDVERE, U., KOLBERG, L., KUZMIN, I., ARAK, T., ADLER, P., PETERSON, H. & VILO, J. 2019. g:Profiler: a web server for functional enrichment analysis and conversions of gene lists (2019 update). *Nucleic Acids Research,* 47**,** W191-W198.
REUTER, S., GUPTA, S. C., CHATURVEDI, M. M. & AGGARWAL, B. B. 2010. Oxidative stress, inflammation, and cancer: How are they linked? *Free Radical Biology and Medicine,* 49**,** 1603-1616.
RIBES, V., WANG, Z., DOLLÉ, P. & NIEDERREITHER, K. 2006. Retinaldehyde dehydrogenase 2 (RALDH2)-mediated retinoic acid synthesis regulates early mouse embryonic forebrain development by controlling FGF and sonic hedgehog signaling. *Development,* 133**,** 351-361.
ROMITTI, P. A., SUN, L., HONEIN, M. A., REEFHUIS, J., CORREA, A. & RASMUSSEN, S. A. 2007. Maternal periconceptional alcohol consumption and risk of orofacial clefts. *Am J Epidemiol,* 166**,** 775-85.
RONCHI, J. A., FIGUEIRA, T. R., RAVAGNANI, F. G., OLIVEIRA, H. C., VERCESI, A. E. & CASTILHO, R. F. 2013. A spontaneous mutation in the nicotinamide nucleotide transhydrogenase gene of C57BL/6J mice results in mitochondrial redox abnormalities. *Free Radical Biology and Medicine,* 63**,** 446-456.
STOPPELLI, M. P., GARCIA, J. V., DECKER, S. J. & ROSNER, M. R. 1988. Developmental regulation of an insulin-degrading enzyme from Drosophila melanogaster. *Proc Natl Acad Sci U S A,* 85**,** 3469-73.
STREISSGUTH, A. P. & DEHAENE, P. 1993. Fetal alcohol syndrome in twins of alcoholic mothers: concordance of diagnosis and IQ. *American Journal of Medical Genetics Part A,* 47**,** 857-861.
SU, B., DEBELAK, K. A., TESSMER, L. L., CARTWRIGHT, M. M. & SMITH, S. M. 2001. Genetic influences on craniofacial outcome in an avian model of prenatal alcohol exposure. *Alcoholism: Clinical and Experimental Research,* 25**,** 60-69.
TAMURA, M., KANNO, Y., CHUMA, S., SAITO, T. & NAKATSUJI, N. 2001. Pod-1/Capsulin shows a sex-and stage-dependent expression pattern in the mouse gonad development and represses expression of Ad4BP/SF-1. *Mechanisms of development,* 102**,** 135-144.
THE GENE ONTOLOGY CONSORTIUM 2018. The Gene Ontology Resource: 20 years and still GOing strong. *Nucleic Acids Research,* 47**,** D330-D338.
TONG, X., ZHAO, F., MANCUSO, A., GRUBER, J. J. & THOMPSON, C. B. 2009. The glucose-responsive transcription factor ChREBP contributes to glucose-dependent anabolic synthesis and cell proliferation. *Proceedings of the National Academy of Sciences,* 106**,** 21660-21665.
TOYE, A. A., LIPPIAT, J. D., PROKS, P., SHIMOMURA, K., BENTLEY, L., HUGILL, A., MIJAT, V., GOLDSWORTHY, M., MOIR, L., HAYNES, A., QUARTERMAN, J., FREEMAN, H. C., ASHCROFT, F. M. & COX, R. D. 2005. A genetic and physiological study of impaired glucose homeostasis control in C57BL/6J mice. *Diabetologia,* 48**,** 675-686.
VAN DAM, T. J., KENNEDY, J., VAN DER LEE, R., DE VRIEZE, E., WUNDERLICH, K. A., RIX, S., DOUGHERTY, G. W., LAMBACHER, N. J., LI, C. & JENSEN, V. L. 2019. CiliaCarta: An integrated and validated compendium of ciliary genes. *PloS one,* 14**,** e0216705.
VERDELLI, C., AVAGLIANO, L., GUARNIERI, V., CETANI, F., FERRERO, S., VICENTINI, L., BERETTA, E., SCILLITANI, A., CREO, P., BULFAMANTE, G. P., VAIRA, V. & CORBETTA, S. 2017. Expression, function, and regulation of the embryonic transcription factor TBX1 in parathyroid tumors. *Laboratory Investigation,* 97**,** 1488-1499.
VETRENO, R. P. & CREWS, F. T. 2012. Adolescent binge drinking increases expression of the danger signal receptor agonist HMGB1 and Toll-like receptors in the adult prefrontal cortex. *Neuroscience,* 226**,** 475-488.
WERNER, R. J., SCHULTZ, B. M., HUHN, J. M., JELINEK, J., MADZO, J. & ENGEL, N. 2017. Sex chromosomes drive gene expression and regulatory dimorphisms in mouse embryonic stem cells. *Biol Sex Differ,* 8**,** 28.

WOLF, S., HAINZ, N., BECKMANN, A., MAACK, C., MENGER, M. D., TSCHERNIG, T. & MEIER, C. 2016. Brain damage resulting from postnatal hypoxic-ischemic brain injury is reduced in C57BL/6J mice as compared to C57BL/6N mice. *Brain Res,* 1650**,** 224-231.

YAGI, H., FURUTANI, Y., HAMADA, H., SASAKI, T., ASAKAWA, S., MINOSHIMA, S., ICHIDA, F., JOO, K., KIMURA, M., IMAMURA, S., KAMATANI, N., MOMMA, K., TAKAO, A., NAKAZAWA, M., SHIMIZU, N. & MATSUOKA, R. 2003. Role of TBX1 in human del22q11.2 syndrome. *Lancet,* 362**,** 1366-73.

ZHANG, C., FRAZIER, J. M., CHEN, H., LIU, Y., LEE, J. A. & COLE, G. J. 2014. Molecular and morphological changes in zebrafish following transient ethanol exposure during defined developmental stages. *Neurotoxicol Teratol,* 44**,** 70-80.

ZHOU, F. C., ZHAO, Q., LIU, Y., GOODLETT, C. R., LIANG, T., MCCLINTICK, J. N., EDENBERG, H. J. & LI, L. 2011. Alteration of gene expression by alcohol exposure at early neurulation. *BMC genomics,* 12**,** 124.

FIGURES

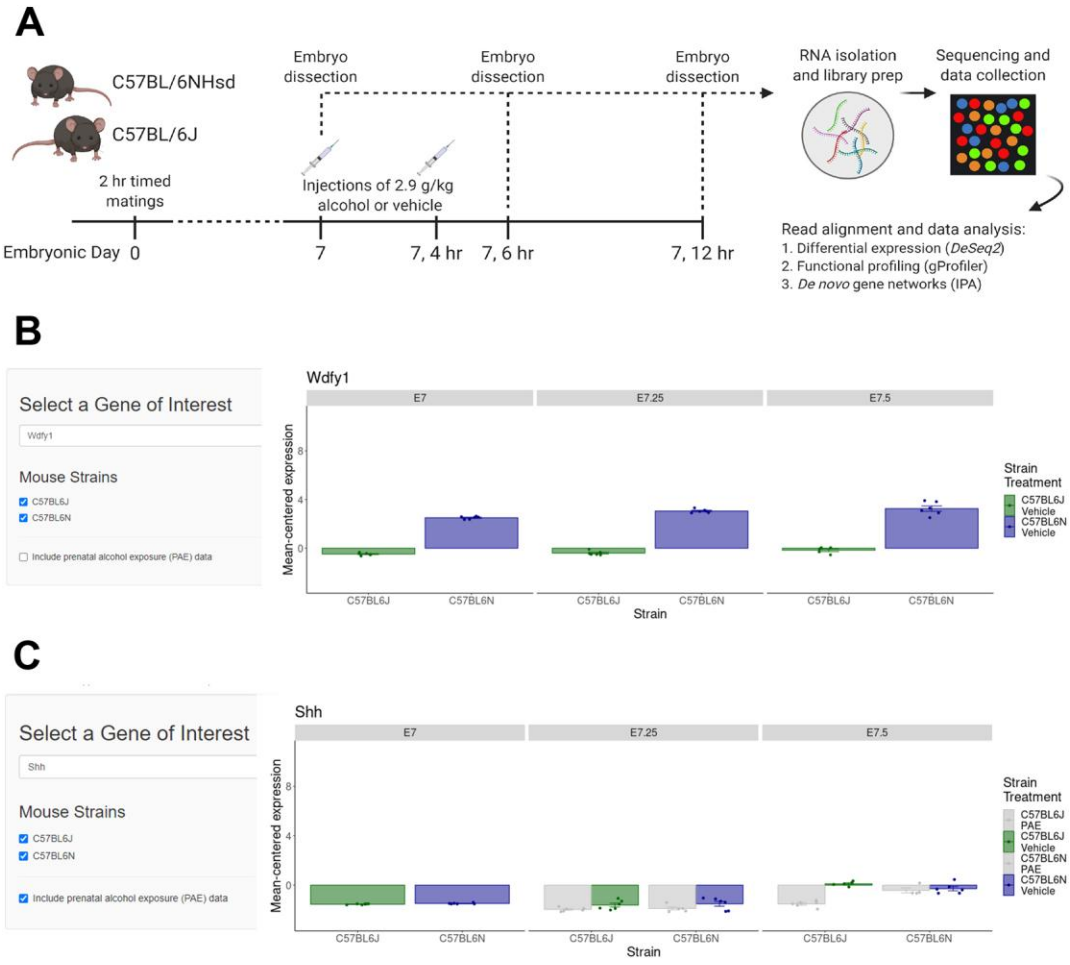

Figure 1. Experimental timeline (A) and example of web-based visualization tool. A web tool was created as a resource to allow gene-by-gene exploration of expression patterns across the first 12 hr of normal mouse gastrulation in the 6J and 6N strains. B) Comparison of expression of *Wdfy1*, a gene that significantly differed between the 6J and 6N strains, across time. Single strains can be selected for viewing using the toggles on the left. C) PAE data can be toggled on and off using the options. *Shh* expression was impacted by PAE in the 6J, but not 6N mice.

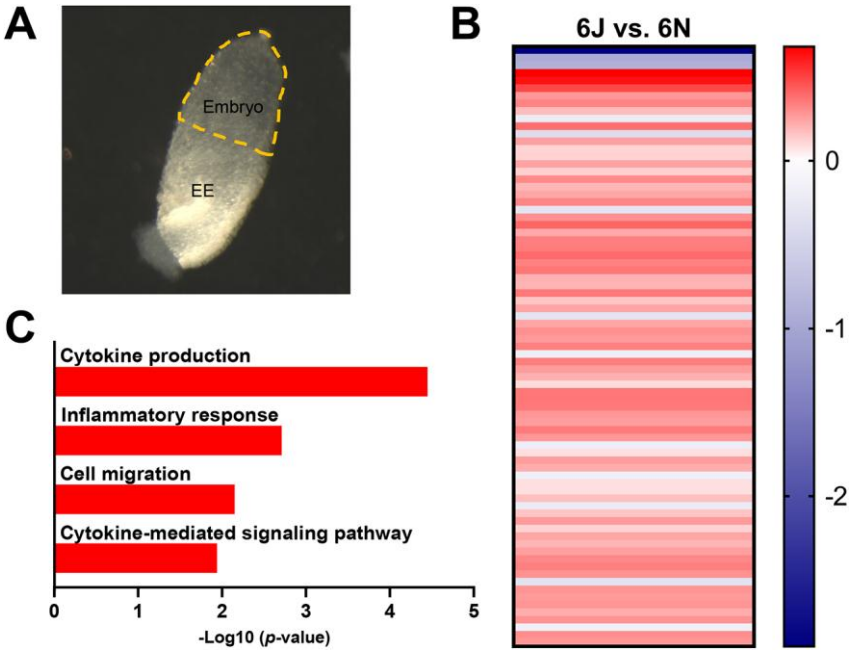

Figure 2. Immune signaling gene pathways are up-regulated in the 6J compared to the 6N strain. A) Representative image of E7.0 mouse embryo. Embryo highlighted in yellow was dissected from the extraembryonic tissue (EE) for sequencing. B) Heat map of genes altered in the 6J vs. 6N at baseline (prior to alcohol administration) on E7.0. Data are expressed as Log_2 fold change (Log_2FC). Blue = down-regulated genes, red = up-regulated genes. n = 6/group. C) Functional profiling of genes differentially expressed in the 6J vs. 6N at E7.0. n = 6/group.

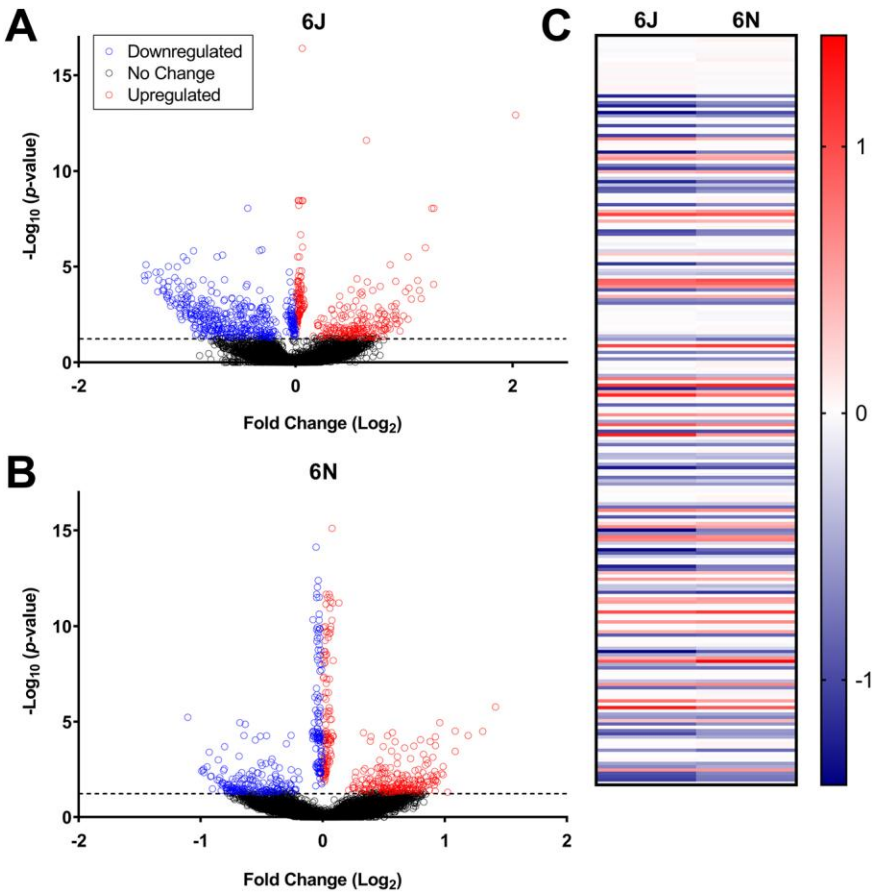

Figure 3. Gastrulation-stage alcohol dysregulated more genes in the 6J strain than the 6N strain 6 hr after exposure. A) Volcano plot of genes significantly dysregulated by alcohol in the 6J mice 6 hr after the first dose of alcohol (E7.25). B) Genes significantly dysregulated by alcohol in the 6N mice 6 hr after the first dose of alcohol (E7.25). C) Heat map comparing 228 genes altered by alcohol in both the 6J and 6N at the E7.25 time point. Data are expressed as Log_2FC. Blue = down-regulated genes, red = up-regulated genes. n = 6/group.

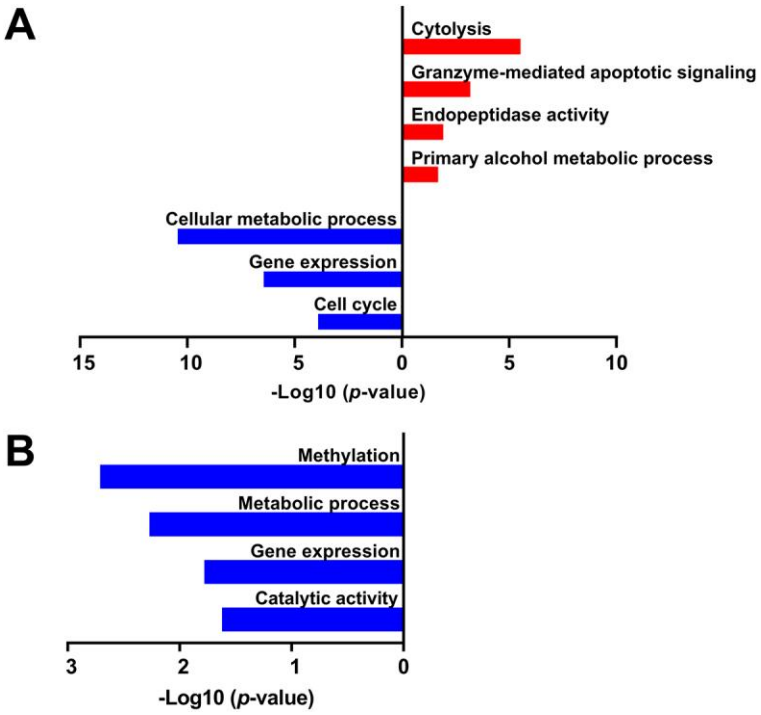

Figure 4. Functional profiling of biological pathways enriched in the (A) 6J and (B) 6N strains 6 hr after alcohol exposure (E7.25). n = 6/group.

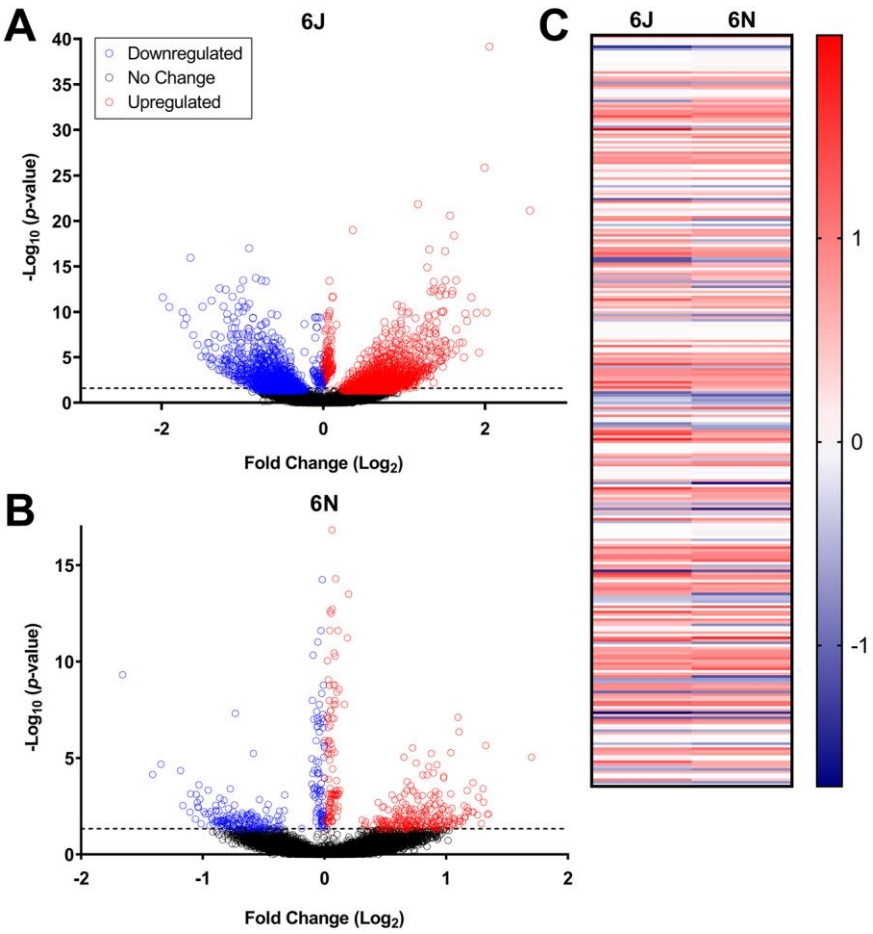

Figure 5. Gastrulation-stage alcohol dysregulated more genes in the 6J strain than the 6N strain 12 hr after exposure. A) Volcano plot of genes significantly dysregulated by alcohol in the 6J mice 12 hr after the first dose of alcohol (E7.5). n = 5 vehicle-treated, 6 PAE. B) Genes significantly dysregulated by alcohol in the 6N mice 12 hr after the first dose of alcohol (E7.5). n = 6 vehicle-treated, 4 PAE. C) Heat map comparing 228 genes altered by alcohol in both the 6J and 6N at the E7.5 time point. Data are expressed as Log_2FC. Blue = down-regulated genes, red = up-regulated genes. n = 6/group.

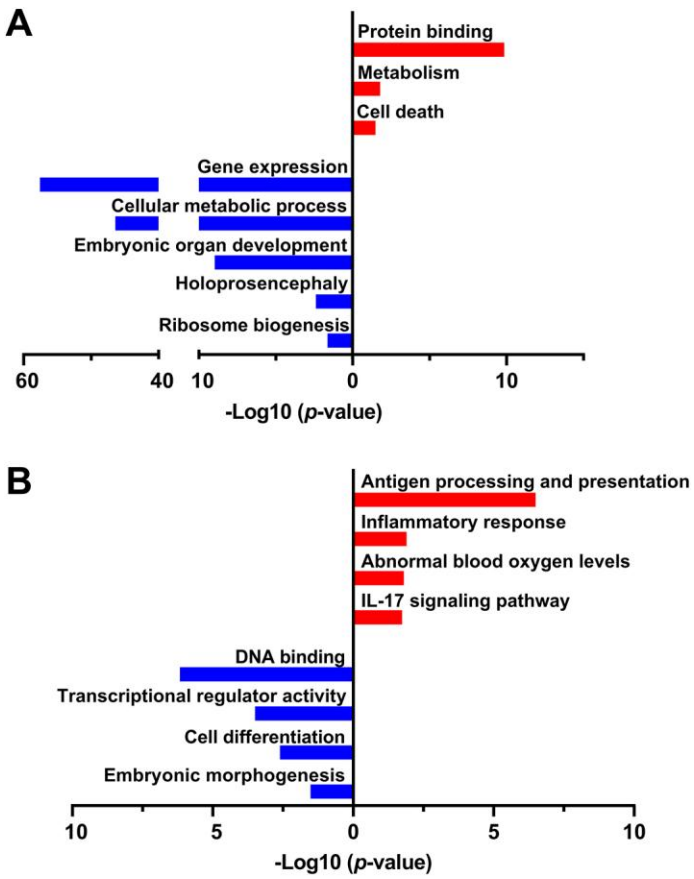

Figure 6. Functional profiling of biological pathways enriched in the (A) 6J and (B) 6N strains 12 hr after alcohol exposure (E7.5). n = 6/group.

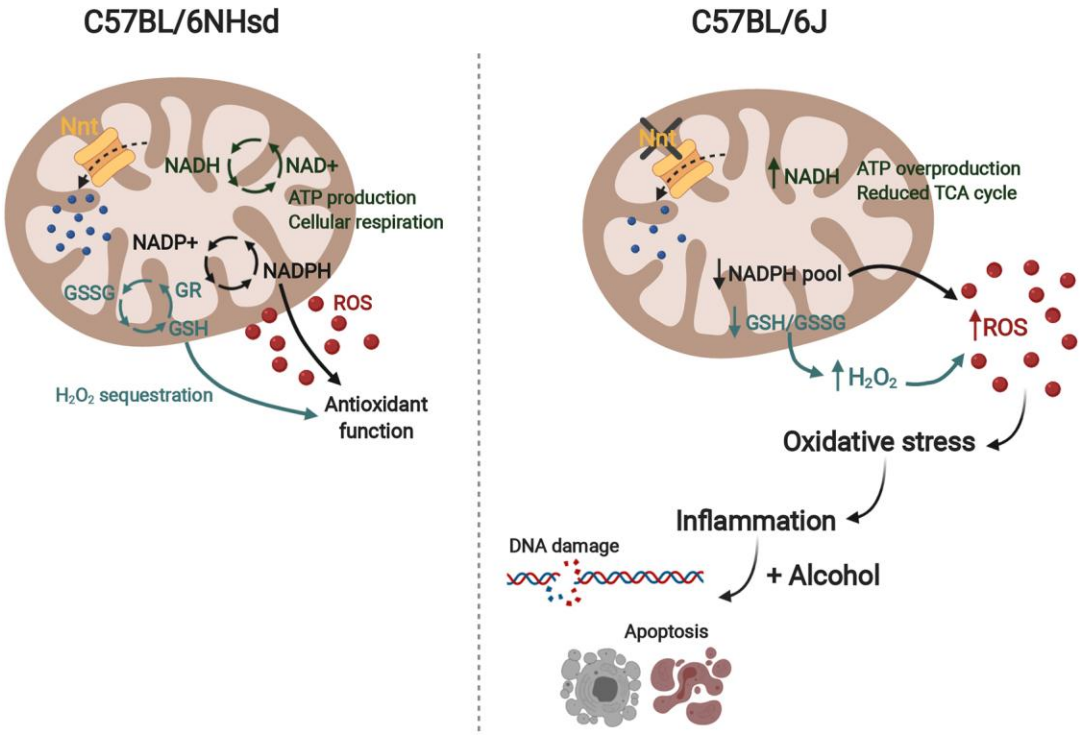

Figure 7. Schematic representing a hypothetical mechanism contributing to the difference in alcohol sensitivity between the 6J and 6N strains. The *Nnt* mutation in the 6J could affect reactive oxygen species (ROS) breakdown in the mitochondria, leading to higher baseline oxidative stress and inflammation. In the presence of alcohol, 6J would undergo increased apoptosis and DNA damage, ultimately resulting in more severe craniofacial and CNS anomalies. Nnt: Nicotinamide nucleotide transhydrogenase, NAD+/NADH: nicotinamide adenine dinucleotide (+ hydrogen), NADP+/NADPH: nicotinamide adenine dinucleotide phosphate, GR: glutathione reductase, GSSG: glutathione disulfide, GSH: glutathione.

Table 1. *De novo* gene networks altered in the sensitive 6J mice compared to the resistant 6N mice at baseline (E 7.0) (A), 6 hr after alcohol in 6J (B) and 6N (C) strains, or 12 hr after alcohol in 6J (D) and 6N (E) mice.

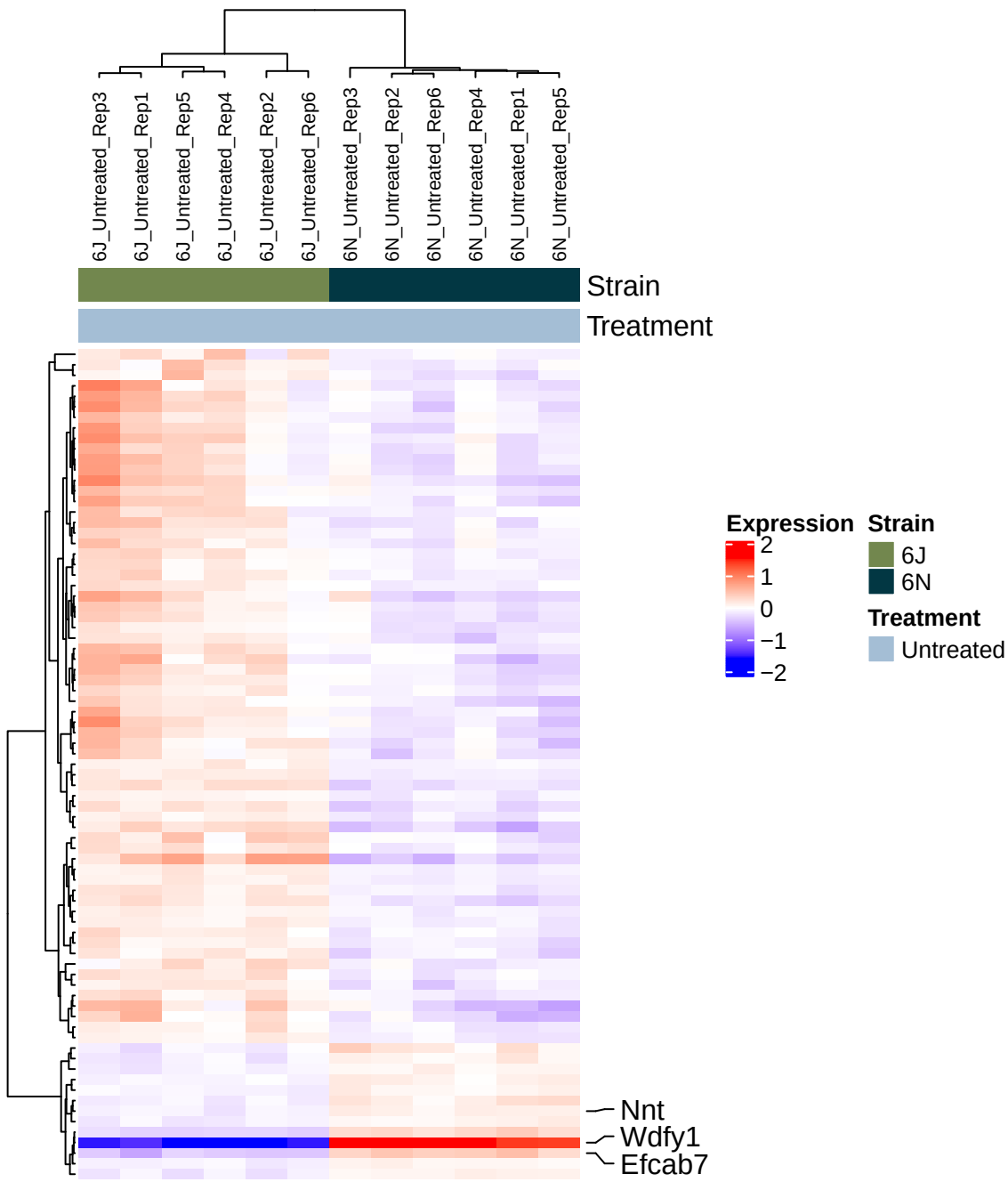

Figure S1.

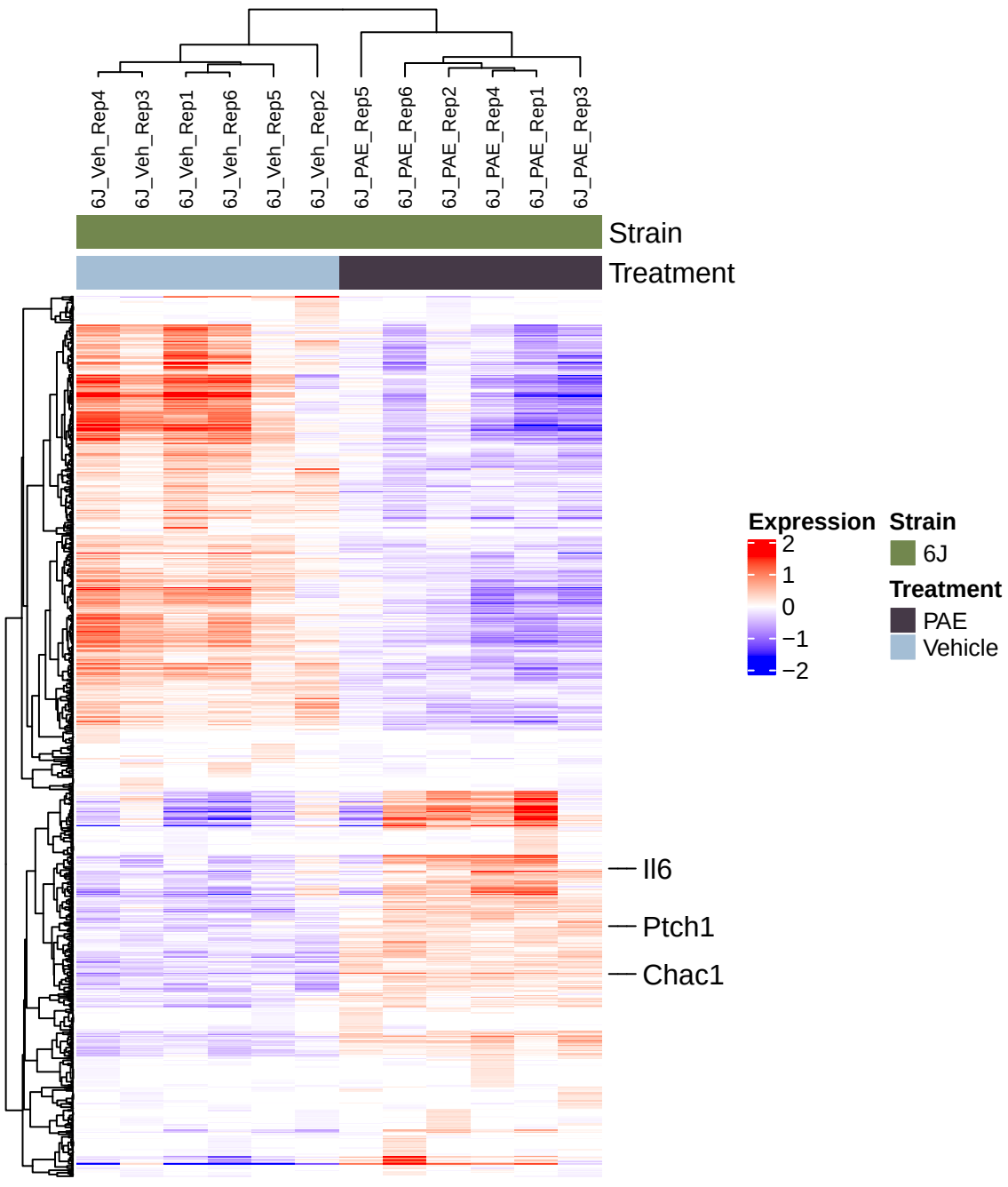
6J_Veh_Rep4
6J_Veh_Rep3
6J_Veh_Rep1
6J_Veh_Rep6
6J_Veh_Rep5
6J_Veh_Rep2
6J_PAE_Rep5
6J_PAE_Rep6
6J_PAE_Rep2
6J_PAE_Rep4
6J_PAE_Rep1
6J_PAE_Rep3
Strain
Treatment
Il6
Ptch1
Chac1
Expression
2
1
0
−1
−2
Strain
6J
Treatment
PAE
Vehicle

Figure S2.

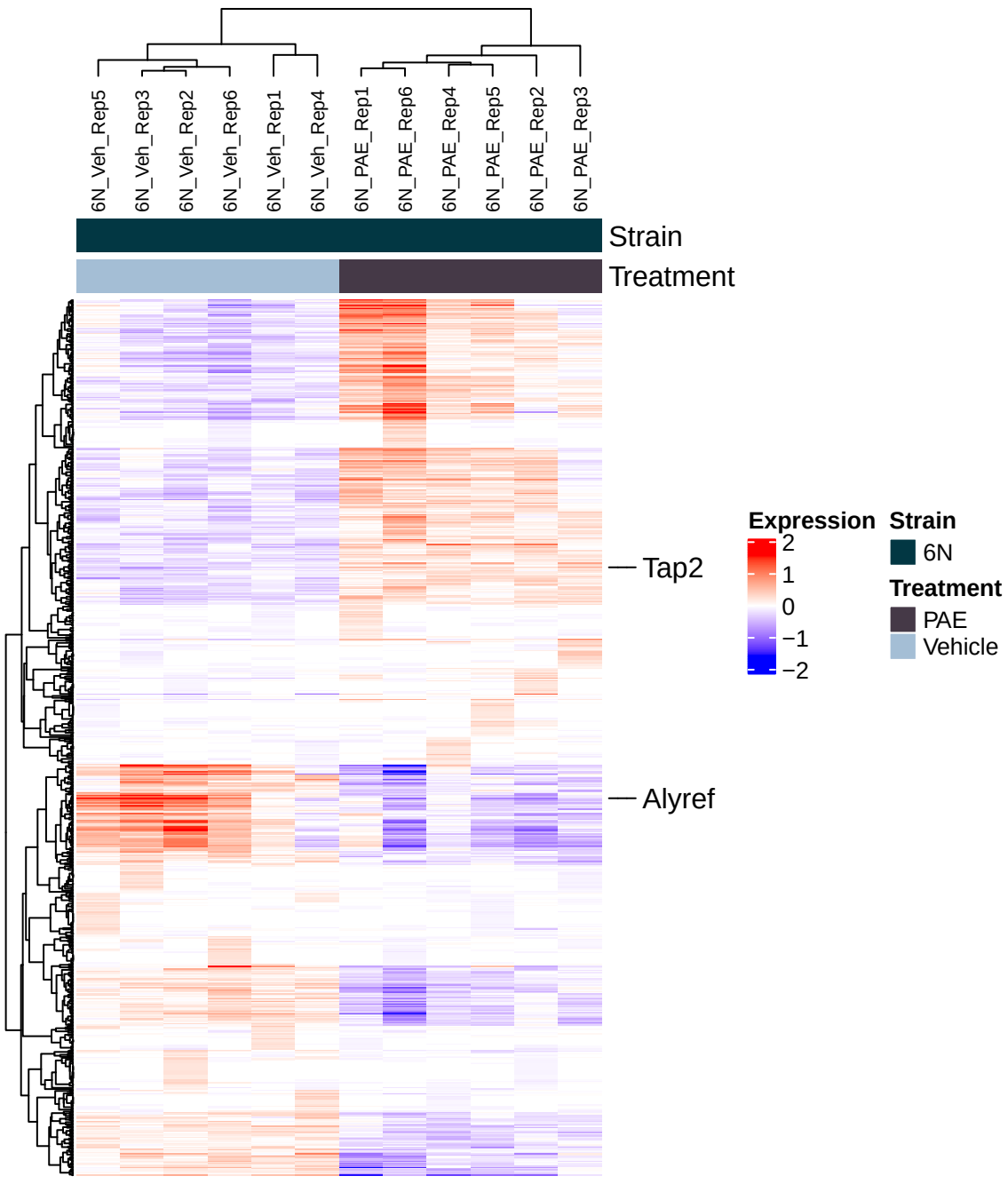
6N_Veh_Rep5
6N_Veh_Rep3
6N_Veh_Rep2
6N_Veh_Rep6
6N_Veh_Rep1
6N_Veh_Rep4
6N_PAE_Rep1
6N_PAE_Rep6
6N_PAE_Rep4
6N_PAE_Rep5
6N_PAE_Rep2
6N_PAE_Rep3
Strain
Treatment
Tap2
Alyref
Expression
2
1
0
−1
−2
Strain
6N
Treatment
PAE
Vehicle

Figure S3.

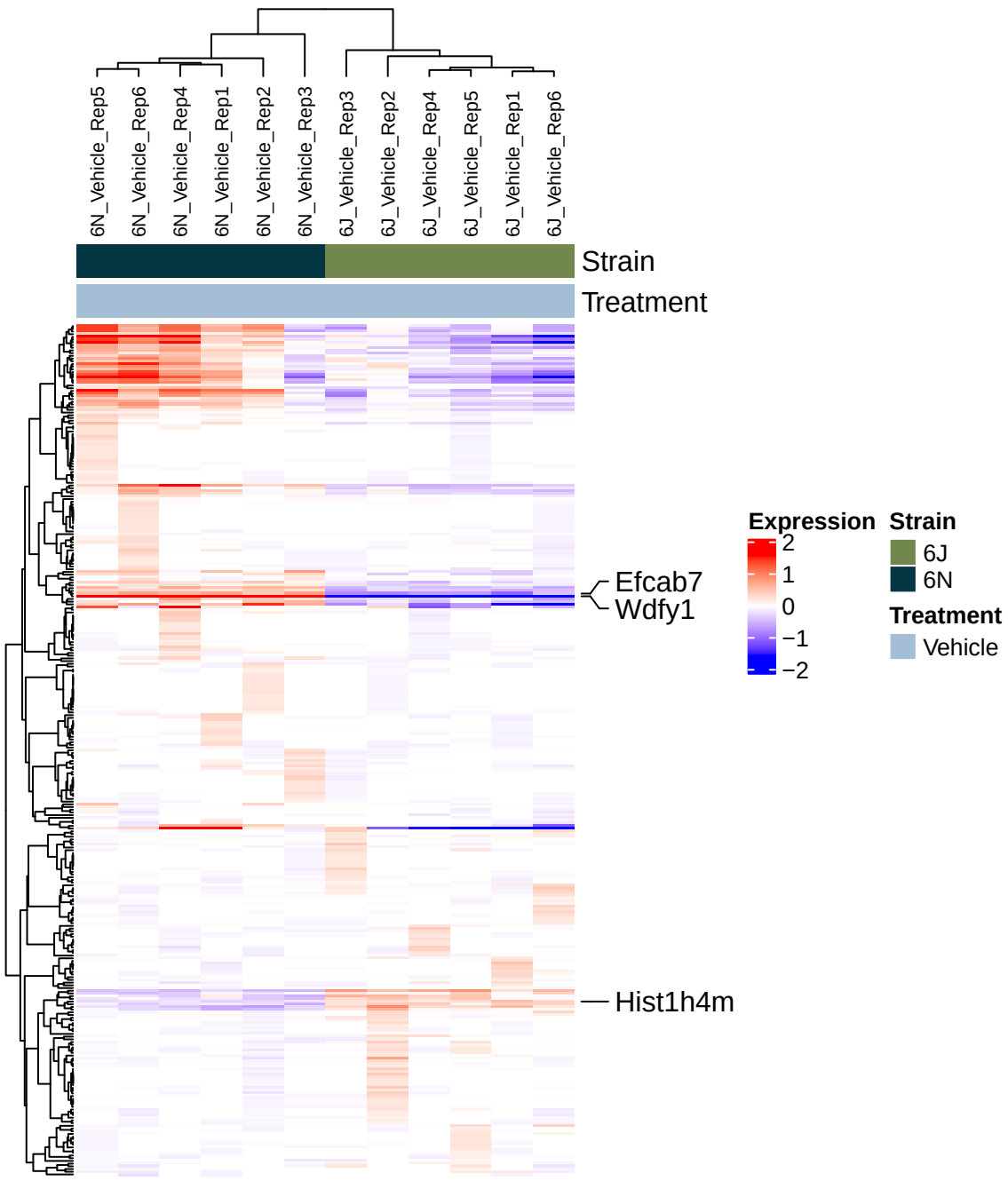
6N_Vehicle_Rep5
6N_Vehicle_Rep6
6N_Vehicle_Rep4
6N_Vehicle_Rep1
6N_Vehicle_Rep2
6N_Vehicle_Rep3
6J_Vehicle_Rep3
6J_Vehicle_Rep2
6J_Vehicle_Rep4
6J_Vehicle_Rep5
6J_Vehicle_Rep1
6J_Vehicle_Rep6
Strain
Treatment
Efcab7
Wdfy1
Hist1h4m
Expression
2
1
0
−1
−2
Strain
6J
6N
Treatment
Vehicle

Figure S4.

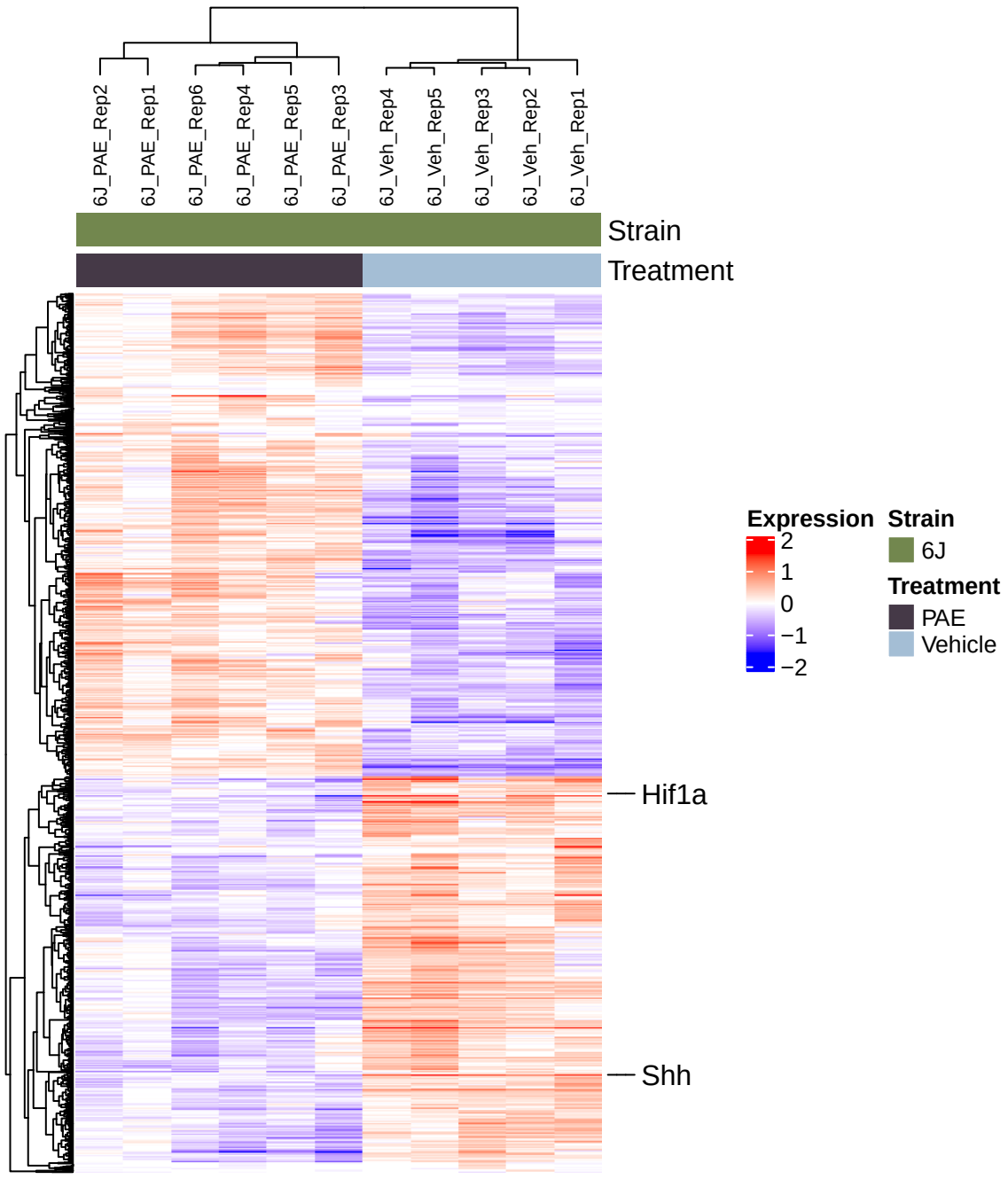
6J_PAE_Rep2
6J_PAE_Rep1
6J_PAE_Rep6
6J_PAE_Rep4
6J_PAE_Rep5
6J_PAE_Rep3
6J_Veh_Rep4
6J_Veh_Rep5
6J_Veh_Rep3
6J_Veh_Rep2
6J_Veh_Rep1
Strain
Treatment
Hif1a
Shh
Expression
2
1
0
−1
−2
Strain
6J
Treatment
PAE
Vehicle

Figure S5.

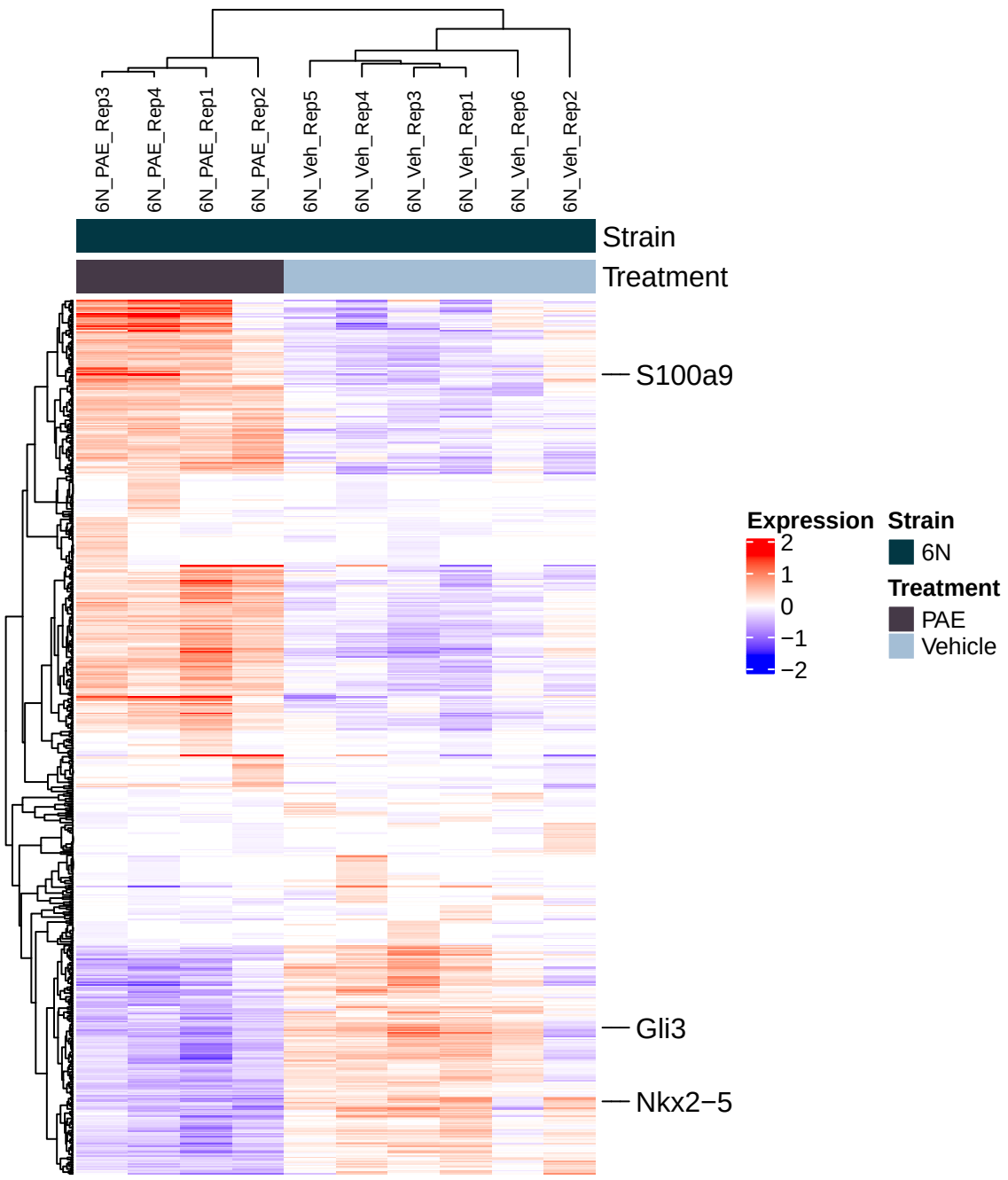
6N_PAE_Rep3
6N_PAE_Rep4
6N_PAE_Rep1
6N_PAE_Rep2
6N_Veh_Rep5
6N_Veh_Rep4
6N_Veh_Rep3
6N_Veh_Rep1
6N_Veh_Rep6
6N_Veh_Rep2
Strain
Treatment
S100a9
Gli3
Nkx2−5
Expression
2
1
0
−1
−2
Strain
6N
Treatment
PAE
Vehicle

Figure S6.

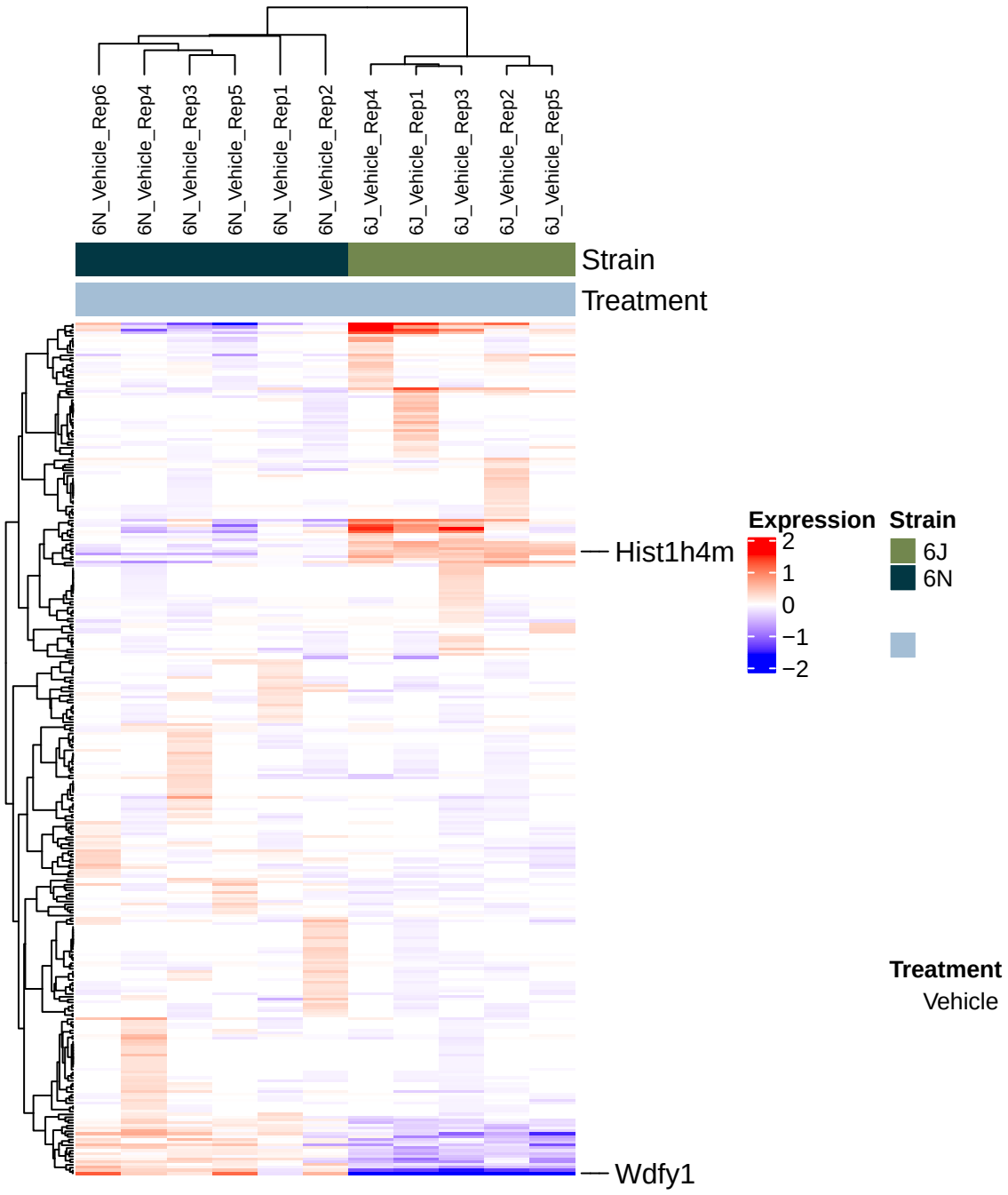
6N_Vehicle_Rep6
6N_Vehicle_Rep4
6N_Vehicle_Rep3
6N_Vehicle_Rep5
6N_Vehicle_Rep1
6N_Vehicle_Rep2
6J_Vehicle_Rep4
6J_Vehicle_Rep1
6J_Vehicle_Rep3
6J_Vehicle_Rep2
6J_Vehicle_Rep5
Strain
Treatment
Hist1h4m
Wdfy1
Expression
2
1
0
−1
−2
Strain
6J
6N
Treatment
Vehicle

Figure S7.

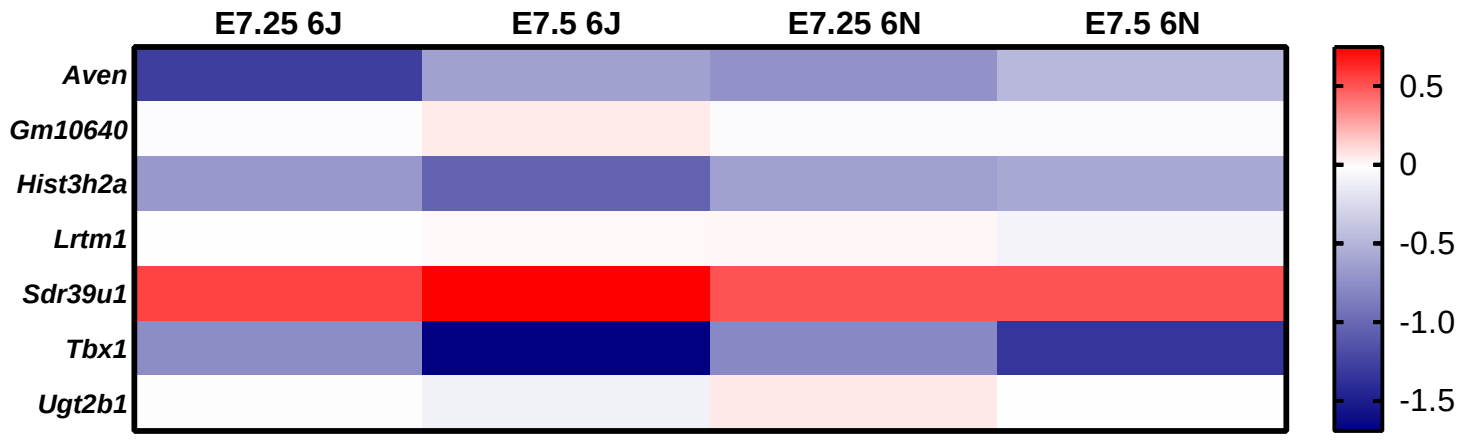

Figure S8.

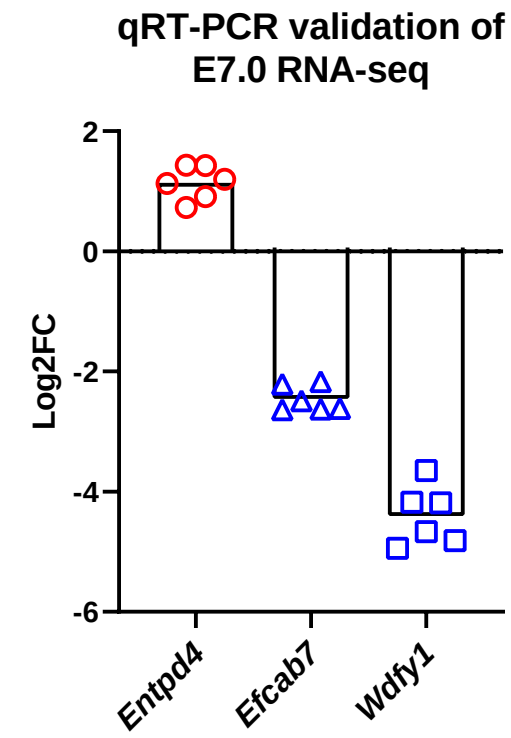

Figure S9.

Table S1.

Up-regulated Genes

Gene Ontology: Biological Process

Term name	Term ID	# of genes	Log10 *p*-value
Myeloid leukocyte migration	GO:0097529	8	3.68
Cytokine production	GO:0001816	12	2.71
Defense response	GO:0006952	17	2.58
Response to external stimulus	GO:0009605	22	2.22
Inflammatory response	GO:0006954	11	2.15
Cell migration	GO:0016477	15	1.94
Regulation of immune system process	GO:0002682	15	1.94
Cytokine-mediated signaling pathway	GO:0019221	8	1.49
Cell motility	GO:0048870	15	1.44
Localization of cell	GO:0051674	15.00	1.44

Gene Ontology: Molecular Function

Term name	Term ID	# of genes	Log10 *p*-value
Cytokine binding	GO:0019955	7.00	4.45
ATPase activity, coupled	GO:0042623	6.00	1.32

KEGG: Biological Process

Term name	Term ID	# of genes	Log10 *p*-value
Cytokine-cytokine receptor interaction	KEGG:04060	7.00	2.05

A E 7.0 6J vs. 6N

	Diseases and Functions	-log(Fisher's exact *p*-value)	Molecules in Network	Molecules
1	– Cell Cycle – Drug Metabolism – Molecular Transport	31	15	Aak1, Acad11, Adck2, Ahnak, App, Arfgap3, Arglu1, Atp8b1, Ccdc88c, Clpb, Dnah14, Dnajc28, Dynlrb2, Dynlt1, Hspa9, Hspb9, Igsf6, Klf12, Lilra5, Mbnl3, Mmp3, Myc, Myo1d, Neat1, Nnt, Nr1h4, Rxr, Sez6l, Sirt5, Tex2, Tktl2, Tmem267, Tnf, Tretinoin, Vgll3
2	– Cancer – Immunological Disease – Inflammatory Disease	28	14	26s Proteasome, Anxa11, Btaf1, Cd3, Creb, Cx3cr1, Efcab7, Entpd4, Erk, Fsh, Fxyd5, Gpcr, Histone H3, Hsp70, Htr2b, Ide, Insulin, Mapk, Nfkb (Complex), Pdgf Bb, Pi3k (Complex), Pka, Pkc(S), Plc, Proinsulin, Ras Homolog, Sct, Slc25a12, Src (Family), Tiam1, Tpm4, Ubiquitin, Uqcc2, Vegf, Wt1
3	– Cellular Movement – Immune Cell Trafficking – Inflammatory Response	25	13	Ap1, Ccl4, Collagen Alpha1, Collagen Type I (Complex), Collagen Type Ii, Collagen Type Iv, Collagen(S), Csf3r, Ddx58, Erk1/2, Fcer1, Fibrinogen, Hsd11b1, Ifn, Ifn Beta, Il-1r, Il1r1, Il1rn, Ldl, Litaf, Mmp, Mmp7, Mmp8, Olr1, Pkc Alpha/Beta, Pro-Inflammatory Cytokine, Rhob, Saa, Sftpd, Sod, Tgf Beta, Tlr, Tnf (Family), Tnfrsf9, Trypsin
4	– Cancer – Endocrine System Disorders – Organismal Injury and Abnormalities	25	13	Akt, Ampk, C1qtnf5, Chemokine, Cytokine, Hp1bp3, Ifi16, Ifn Alpha/Beta, Ifn Type 1, Ifnar, Ige, Igg, Igg1, Igm, Il1, Il12 (Complex), Il12 (Family), Immunoglobulin, Interferon Alpha, Irf7, Kit, Lh, Map2k1/2, Mtdh, N-Cor, Nfkbiz, Nos, Osbpl5, P70 S6k, P85 (Pik3r), Pglyrp1, Pthlh, S100a9, Top2b, Wdfy1
5	– Cellular Movement – Hematological System Development and Function – Immune Cell Trafficking	18	10	Adm2, Atp11b, Ccr1, Cd200, Cdx2, Cx3cr1, D1pas1, Defa1 (Includes Others), Defb104a/Defb104b, Gjb4, Gpr132, Gstp1, Hsh2d, Jnk, Lgals8, Mannan, Mip1, Mir-127, Mrc1, Mrc2, Nipal1, P38 Mapk, Pla2g7, Prr9, Rara, Retnlg, S1pr2, Sparc, Stra6, Tcr, Tlr10, Tmcc3, Tmem184a, Tnfrsf18, Traf5
6	– Cell Morphology – Cellular Assembly and Organization – Post-Translational Modification	16	9	1, 3, 4-Ip3, B4galt4, Brd8, Ceacam10, Ck2, Defb8, E2f8, Egf, Ep400, Epc1, H2az1, H4c4, Hdac2, Hoxc9, Ing2, Ing3, Irs1, Itpkc, Mier2, Mis18a, Nes, Oip5-As1, Papss1, Pcgf2, Pold2, Rbbp4, Rffl, Sap130, Sp3, Sprr2h, St5, Tcf21, Tip60, Tp53, Ube2q2

B E 7.25 6J vs. 6N Vehicle-treated

	Diseases and Functions	-log(Fisher's exact *p*-value)	Molecules in Network	Molecules
1	– Antimicrobial Response – Cell Death and Survival – DNA Replication, Recombination, and Repair	39	22	Asb9, Bglap, Casp12, Caspase, Cd200r1, Ces, Ces1b/Ces1c, Ces4a, Cngb3, Cytochrome C, Ecm, Fap, Granzyme, Gzma, Gzmb, Gzmc, Gzmh, Hsp27, Hsp70, Il12 (Family), Il6, Jun/Junb/Jund, Mir124a-1hg, Mt3, Nfkb (Complex), Padi2, Rxr, Serine Protease, Serpinb12, Spink5, Tcr, Tmprss11b, Tmprss7, Trim69, Usp17la (Includes Others)

2	– Cell-To-Cell Signaling and Interaction – Drug Metabolism – Nervous System Development and Function	34	20	Alpha Catenin, Ampk, Atp1b4, Calpain, Capn11, Cd3, Cd4, Cg, Cpa3, Creb, Efcab7, Fmo3, Fsh, Gabrg2, Glucuronosyltransferase, Hbg2, Histone H3, Hla-A, Hoxd10, Il1, Il1bos, Kcnj1, Mek, Nr2e1, P38 Mapk, Pi3k (Complex), Pkc(S), Ppp1r1b, Psca, Slco2b1, Tm4sf1, Ugt2a3, Ugt2b17, Ugt2b28, Vegf
3	– Cell Signaling – Molecular Transport – Vitamin and Mineral Metabolism	32	19	Amylase, Ccl1, Col28a1, Collagen, Collagen Type Ii, Cxcl13, Elastase, Erk1/2, Fcna, Fgf7, Fibrin, Gp6, Hcrt, Hla-Dr, Ifn Alpha/Beta, Il36b, Irak3, Klra7 (Includes Others), Lum, Mhc Class I (Complex), Mhc Ii, Mmp, Ppp1r3a, Pro-Inflammatory Cytokine, Reg3g, Rgs13, Serpina1, Syk/Zap, Tlr, Tnf (Family), Tnfsf15, Trem1, Trypsin, Ucn2, Xcl1
4	– Hematological System Development and Function – Hematopoiesis – Humoral Immune Response	30	18	Aim2, Akt, Bcr (Complex), Cd180, Cd36, Ctnna3, Dbh, Fcamr, Gcsam, Gm9573, Gpnmb, Hemoglobin, Ifn Beta, Ifnar, Iga, Igg, Igg1, Igg2a, Igg2b, Igg3, Igm, Il12 (Complex), Insrr, Ly9, Lyg2, Medag, Mhc Class Ii (Complex), Pax5, Plc Gamma, Stat5a/B, Tfap2b, Tnfrsf17, Trim29, Vav, Wap
5	– Cell Signaling – Molecular Transport – Vitamin and Mineral Metabolism	25	16	Adcy, Adgrf1, Bdkrb1, Calcrl, Calmodulin, Ccr6, Chemokine, Chemokine Receptor, Collagen Type I (Complex), Cxcr1, Cyp2c9, Dynlt1, Ffar2, Fshr, G Protein, G Protein Alphai, Ghrhr, Gpcr, Grm1, Growth Hormone, Gsk3, Jnk, Lh, Mapk, Myoc, Npy, Pka, Plc, Rac, Ras, Serpina3g (Includes Others), Tacr1, Tsh, Tshr, Voltage-Gated Calcium Channel
6	– Cell-To-Cell Signaling and Interaction – Skeletal and Muscular System Development and Function – Visual System Development and Function	23	15	Akr1c3, Aldh1a2, Aldose Reductase, Alp, Ap1, Calml5, Ces1, Collagen(S), Erk, Fcer1, Fgf, Fgf6, Ghrl, Gk, Hdl, Ige, Il23, Krt75, Ldl, Lilrb3, Myh4, Mylk2, Myosin, Nadph Oxidase, Nr1h, Pdgf Bb, Pi3k P85, Prkaa, Prl2c2 (Includes Others), Rap1gds1, Rock, Slfn12l, Src (Family), Tgf Beta, Txk
7	– Cardiovascular System Development and Function – Cellular Function and Maintenance – Tissue Morphology	23	15	60s Ribosomal Subunit, Abca13, Adamtsl3, Add1, Alas2, Aldh3b1, Arnt2, Bbox1, Cldn13, Clk1, Ddx54, Ess2, Fbxl18, Gata2, Gdf2, Grm6, Gypa, Hemgn, Krt40, Ly6a (Includes Others), Mrgprx3, Myc, Nat3, Ncaph, Noc2l, Nsfl1c, Prrg4, Rad21l1, Rffl, Rhag, Rpl39l, Tmem200c, Tsga10ip, Vcp, Wapl
8	– Cell Morphology – Cellular Function and Maintenance – Developmental Disorder	21	14	26s Proteasome, 4930417o13rik, Acyl-Coenzyme A, Aim2 Inflammasome, Alas2, Cd209d, Ceacam20, Ctcfl, Cyp1a2, Cytokine, Defb8, Ep400, H4c4, Histone, Histone H4, Hsp90, Ide, Immunoglobulin, Insulin, Interferon Alpha, Klhl38, Midn, Mylip, Paf1, Phosphatidylinositol 3, 4-Diphosphate, Phosphatidylinositol-3-Phosphate, Pla2g2a, Pold2, Ppm1k, Prap1, Proinsulin, Rna Polymerase Ii, Tip60, Tssk1b, Wdfy1
9	– Cell-To-Cell Signaling and Interaction – Nervous System Development and Function – Organismal Injury and Abnormalities	21	14	Acot5, Bdnf, Cntnap5, Ctcf, Drd1, Endocannabinoid, Fabp2, Foxa1, Ftsj3, Gpx4, Grb2, H1-1, Kri1, Ly6g6f, Nkx2-5, Olfr503, Or4n2, Pcdhb3, Pcdhb7, Pcdhb8, Plod1, Ppara, Ppp1r1b, Rp1l1, Rps27, S100a10, Scn10a, Scn11a, Sec14l5, Set, Set Complex, Slc17a8, Tespa1, Vgf, Xrn2

10	– Cell-To-Cell Signaling and Interaction – Cellular Function and Maintenance – Nervous System Development and Function	21	14	9-Cis-Retinal, Akap5, Apol11b (Includes Others), Apol9a/Apol9b, App, Arglu1, Asic1, Asic2, Asic3, Cdr1, Chrnb3, Crx, Dhx33, Dlg4, Dmrt1, Dmrtc2, Dopamine, Endocannabinoid, Etd, Girk, Gpr37, Gpr78, Hcrtr1, Ifn, Ifnar1, Irak, Myot, Opn5, Rho, Rnu12, Sectm1, Snrnp, Spata16, Tlr7, Trpv3

C **E 7.5 6J vs. 6N Vehicle-treated**

	Diseases and Functions	-log(Fisher's exact *p*-value)	Molecules in Network	Molecules
1	– Drug Metabolism – Lipid Metabolism – Small Molecule Biochemistry	50	26	Aim2, Amy2a, Amylase, Anxa13, Bglap, Cd200r1, Cdh16, Cebpe, Ces, Ces1, Ces3, Ces4a, Collagen Type Ii, Ctrb2, Cyp7a1, Erk1/2, Fgf7, Growth Hormone, Hcrt, Il36g, Klrc1, Magea3 (Includes Others), Mug1/Mug2, Mycs, Nxph2, Prex1, Proinsulin, Pxr Ligand-Pxr-Retinoic Acid-Rxrα, Rxr, Slco1b3, Syt2, T3-Tr-Rxr, Tph2, Ubash3a, Ucn3
2	– Connective Tissue Development and Function – Digestive System Development and Function – Skeletal and Muscular System Development and Function	42	23	Ackr2, Afm, Akt, C3ar1, Cd207, Cd55, Collagen Type I (Complex), Collagen Type Iv, Collagen(S), Csta, Ctsk, F9, Fhit, Fmod, Gm9573, Hephl1, Iga, Igg2a, Igg2b, Il23, Itga11, Ldl, Lyg2, Mucin, Myoc, Or51e2, Pdgf Bb, Prg3, Reg3a, Scgb3a1, Serpinb7, Siglec15, Slc13a1, Tcl1a, Tgf Beta
3	– Post-Translational Modification – Protein Degradation – Protein Synthesis	42	23	Ano3, Ccl1, Ccl24, Ccl7, Cd209c, Cd8b, Cnga3, Fcer1, Gngt1, Ifn Alpha/Beta, Ifn Beta, Ifnar, Ifnz (Includes Others), Interferon Alpha, Klk12, Klk5, Klra7 (Includes Others), Mhc Class I (Complex), Mhc Class I (Family), Mhc Class Ii (Complex), Mx2, Nfkb (Complex), Pmaip1, Prss42p, Serine Protease, Serpinb10, Slc46a2, Tap2, Tmprss11e, Tmprss15, Tmprss7, Tnf (Family), Tnfrsf17, Trypsin, Usp17la (Includes Others)
4	– Cancer – Dermatological Diseases and Conditions – Organismal Injury and Abnormalities	35	20	Adamtsl4, Alb, Atp6v1g3, Bcr (Complex), Chst4, Col8a1, Cox6a2, Creb, Ctnna3, Cxcl3, Cyclin A, Erk, Fhl5, Gabrg2, Gcsam, Gm10408 (Includes Others), Ige, Igg, Igg1, Il1, Il12 (Complex), Il13ra2, Immunoglobulin, Keratin, Krt16, Krt20, Krt73, Lh, Map2k1/2, Pax8, Pck2, Pou2af1, Ppy, Pro-Inflammatory Cytokine, Sos
5	– Developmental Disorder – Endocrine System Disorders – Hematological Disease	28	17	26s Proteasome, Asb9, Calmodulin, Cd3, Chemokine, Cxcr6, Cytokine, Efcab7, Gpcr, Gpr119, Gpr22, Gpr37, Histone H3, Histone H4, Hsp70, Hsp90, Itgad, Jnk, Kcnj1, Kcnj16, Micb, Pi3k (Complex), Pka, Pkc(S), Rb, Rho, Slc12a1, Tcr, Tesk2, Tnn, Tp63, Ube2d4, Ubiquitin, Vegf, Wdfy1

6	– Cancer – Endocrine System Disorders – Gastrointestinal Disease	26	16	Abr, Ahctf1, Alms1, Alpk2, Atxn7, Bbox1, Ccdc27, Ccdc88c, Cnnm2, Cntnap3, Ctcf, Ctnnb1, Cyb5b, Fhit, Gabrq, Gjd4, Hepacam, Itprid2, Lhx6, Lmna, Lnx1, Lvrn, Mastl, Nes, Pcdhb8, Pcdhb8, Plec, Rasl11b, Rnf133, Ropn1, Sall1, Spag11b, Ube2i, Ube2q1, Virma
7	– Cancer – Organismal Injury and Abnormalities – Tissue Morphology	23	15	Abcb8, Adam30, Ankrd34c, Atf3, Bpifc, Cpn2, Creb1, Cst9l, Dio2, Dmrt1, Dnm3os, Fbxw21 (Includes Others), Glra1, Hmmr, Ifi202b, Kcnb1, Mapk1, Metalloprotease, Myl6b, Nr1h5, Pdcl2, Prkar2a, Prl3c1, Rest, Rhox3a (Includes Others), Robo1, S6k1, Scn10a, Scn3b, Tp53, Traf6, Trank1, Triiodothyronine, Reverse, Vnn1, Vsig1
8	– Nutritional Disease – Psychological Disorders – Small Molecule Biochemistry	21	14	14, 15-Epoxyeicosatrienoic Acid, Adamdec1, Ar, Beta-Estradiol, Cilp, Cldn18, Cldn6, Drd4, Ear2 (Includes Others), Elovl2, Endothelin, Eppin, Gata2, Gchfr, Gp2, Gpr37, Grk4, Hemgn, Htr6, Ifi202b, Mak, Mhc Class Ii (Complex), Mir-24-3p (And Other Mirnas W/Seed Ggcucag), Msmo1, Myc, Ntf4, Parp8, Pmm2, Pomc, Sprr2g, Sprr2i, Tbx19, Tgm6, Transglutaminase, Zg16
9	– Cell Cycle – Cell Morphology – Cell-To-Cell Signaling and Interaction	19	13	Actl7b, App, Brms1, Ccnb2, Ccnb3, Clec2e/Clec2h, Crebbp, Crybb2, Endothelin, Gjb1, Gng2, Hmgb4, Hspa2, Iqcf5, Kcnn4, Kctd16, Lsmem1, Mac, Mastl, Ms4a15, Nanog, Prkar2a, Psg18 (Includes Others), Ptger2, Rnasel, Sik2, Slc25a13, Stfa2/Stfa2l1, Sycp2l, Tbx22, Tigd4, Ttk, Usp8, Utp, Zdhhc21
10	– Cell Cycle – Cell-To-Cell Signaling and Interaction – Cellular Growth and Proliferation	17	12	9830107b12rik/A530064d06rik, Abcb9, Aim2, Apol11b (Includes Others), Bc048679, Chil3/Chil4, Cntnap5, Crabp1, Ctsk, Cyp4f11, Dyrk2, Eln, Ern2, Esr1, Fmr1, Gchfr, Gvin1 (Includes Others), Hla Class I, Hla-G, Ifi202b, Ifng, Muc2, Nr1d1, Pcdhb14, Pcdhb4, Pla2g7, Rcvrn, Tgfbr2, Th2 Cytokine, Ticam2, Tlr3, Tnfsf9, Tretinoin, Ttc22, Uba6

D **E 7.25 6J Alcohol vs. Vehicle**

	Diseases and Functions	-log(Fisher's exact *p*-value)	Molecules in Network	Molecules
1	– Cancer – Gastrointestinal Disease – Hepatic System Disease	99	64	Aasdh, Abcb8, Aebp2, Aldh3b1, Amfr, Ammecr1, Anxa10, Apbb2, Arhgap23, Atp2a2, Atpase, Bag3, Banp, Bod1, Btbd1, Caap1, Cacybp, Carm1, Carnmt1, Crebrf, Dars1, Eed, Entpd2, Faf1, Fxr2, G3bp1, Glud1, H1-0, Hdac, Hemgn, Hsp70, Hspa5, Hspa8, Hspd1, Hsph1, Klhdc2, Lrrc47, Map1lc3, Mapre1, Mettl17, Mpp6, Mrps27, Noa1, Nr2e1, Ogt, Pcbp1, Pex6, Ppp1r10, Ptov1, Rabl3, Rbm26, Rbpms, Rif1, Rpa, Sfpq, Slc35e1, Slco2b1, Smc4, Spg7, Tmem165, Trim29, Trmt12, Trmt44, Tssk1b, Ube2m, Ubxn2b, Ugt2b17, Vegf, Ywhah, Znf746

2	– Cell Morphology – Drug Metabolism – Endocrine System Development and Function	89	60	Alkbh5, Asb13, B4galt4, Bbc3, Bbs4, Bmt2, Brd7, Brpf3, Cables2, Capns2, Ccnt1, Ccny, Cct3, Cct4, Cdc73, Cnppd1, Cofilin, Ctbp1, Ctdp1, Dazap2, Dnaja1, Eif4a2, Ercc8, Fam91a1, Fkbp5, Gcn5l, Gmcl1, Gtf2e2, Histone, Histone H3, Holo Rna Polymerase Ii, Inpp5k, Ipmk, Kdm1a, Kiaa2013, Mark3, Mbd3, Mcmbp, Mettl3, Mi2, Mlc1, Nars1, Nurd, Oma1, Orc3, P-Tefb, P38 Mapk, P4ha1, Pard3, Pard6b, Parp16, Paxbp1, Per1, Pmpcb, Ppp2r2d, Rhof, Rsrc2, Slc6a12, Snx5, Spata20, Spata3, Srsf2, Srsf9, Stip1, Strn3, Suv39h2, Tada3, Taf10, Taf5, Tip60
3	– Cancer – Cellular Development – Tissue Development	84	58	5730488b01rik, Ahcyl1, Alp, Alpg, Asb15, Bmp1, Cbx6, Chac1, Cirbp, Collagen Alpha1, Commd3-Bmi1, Coq2, Ctbp, Erk, Exog, Exosc6, Farnesyl Transferase, Fgf, Gata6, Get4, Hedgehog, Hes1, Hoxa9, Hoxd10, Leng8, Loxl1, Luc7l, Mafg, Mllt1, Mocs3, Mrps30, Napsa, Nog, Nop56, P3h2, Pip4k2a, Plcd3, Prc2, Prl2c2 (Includes Others), Prmt2, Psca, Ptch1, Rangap1, Riox1, Riox2, Rnr, Rrs1, Sdr39u1, Slfn12l, Smarca5, Sox, Sox17, Sox18, Sox2, Sox4, Spout1, Tcf, Tigd5, Tle1, Trmt10c, Trmt1l, Tsc22d1, Ugcg, Wars2, Wdr77, Wnt, Yars2, Ypel5, Zc3h14, Zmynd19
4	– Cancer – Connective Tissue Disorders – Organismal Injury and Abnormalities	73	53	26s Proteasome, Alyref, Ankrd13a, Apc/Apc2, Arrdc3, Arrdc4, Atp6v0d2, B3gnt5, Barx1, Bmp, Bok, Ccdc155, Cldn5, Clec4g, Cnpy3, Csnk1g3, Ctnna3, Eotaxin, Fam161a, Fgfbp1, Galnt1, Gas1, Gml, Got, Hoxd9, Hsd3b1, Igg, Igg2a, Igg2b, Igll1/Iglll5, Il25, Irak3, Lman2l, Lrig1, Lrrtm1, Mhc Class I (Family), Mhc Ii, Mir101, Mrm3, Msl2, Mto1, Nfkb (Complex), Noct, Otulin, P Glycoprotein, Rab6b, Rbm15b, Rnf11, Rnf149, Slc22a16, Srxn1, Tespa1, Tmem245, Tnfrsf17, Tnfsf15, Tpcn2, Trim10, Trim44, Trim8, Tspan33, Tysnd1, Ube2, Ube2q2, Ube2r2, Ubiquitin, Ubiquitin Ligase, Vacuolar H Atpase, Vash1, Wipi1, Zfand5
5	– Cardiac Necrosis/Cell Death – Cardiovascular Disease – Cell Death and Survival	60	47	Adrb, Alcohol Group Acceptor Phosphotransferase, Alpha Actin, Asb9, Becn1, Btg3, Cab39, Calcineurin A, Cdc25b, Cg, Chrna6, Chrnb3, Cited2, Creatine Kinase, Dapk3, Dll3, Dusp10, E2f1, Eno2, Ephb, Etfbkmt, Fjx1, Fsh, Gamma Tubulin, Gna11, Grk6, Hsd17b1, Klf11, Lh, Lmcd1, Mapk1, Mapk1ip1, Mapkapk2, Mcl1, Mef2, Mef2b, Mlc, Mlcp, Myh4, Mylk2, Myosin-Light-Chain Kinase, Neurod4, Ngf, Notch, Nrg (Family), Oxsr1, Pawr, Pi3k (Family), Pkn1, Plat, Ppp6r1, Ptpase, Ptpra, Pyy, Rasal2, Rnf130, Secreted Mmp, Slx1a/Slx1b, Smad6, Snx18, Sod, Spata5l1, Src (Family), Stk39, Tcaf2, Timp2, Tm4sf1, Tmem158, Tmsb4, Tsc22d2
6	– Energy Production – Lipid Metabolism – Small Molecule Biochemistry	49	41	Adh1c, Agfg1, Akirin2, Akr1c3, Ap5z1, Bag1, Brms1l, C/Ebp, Calc, Cbp/P300, Cd207, Coup-Tf, Crebzf, Cuzd1, Cyp11b2, Dgk, Dgkz, Emcn, Erk1/2, Estrogen Receptor, Gc-Gcr Dimer, Gm9573, Hdac7, Histone Deacetylase, Histone H4, Hnf3, Hnf4g, Iga, Jink1/2, Jun/Junb/Jund, Klf9, Mettl16, Mknk2, Mrrf, Muc5b, Mucin, N-Cor, Ncor1, Nr0b2, Nr1h, Nr2f6, Pepck, Phf23, Pki, Pnrc1, Polr2m, Ppp1r3a, Rar, Rdh, Reg3g, Rxr, Sbsn, Sdr16c5, Sema3f, Serpinf1, Slc44a1, Spink5, Suds3, Swi-Snf, T3-Tr-Rxr, Tbx1, Tfiia, Thymidine Kinase, Thyroid Hormone Receptor, Tlr7/8, Tph2, Ube2j2, Ucp3, Vitamind3-Vdr-Rxr, Wdr92
7	– Connective Tissue Disorders – Inflammatory Disease – Organismal Injury and Abnormalities	44	38	Abhd17b, Ago2, Ago2-Mirlet7, Ankrd10, Ap1ar, Arl5a, Atp1b4, Cnot6, Cpd, Ddx56, Eif2, Eif2s1, Elavl1, Fam135a, Fam83f, Fbxo27, Gpr180, Gtpase, Hdhd2, Hras, Hsp90, Ifi27, Iigp1, Interferon Alpha, Ints11, Lamp1, Lmf1, Mex3d, Mir-323-3p (And Other Mirnas W/Seed Acauuac), Mir-330, Mir-363, Mir-423, Mir-423-5p (And Other Mirnas W/Seed Gaggggc), Mob3b, Nadk2, Nfic, Oaf, Oas1b, Pank1, Pank3, Pdcd7, Pdia4, Pp1/Pp2a, Ppfia1, Ppfibp2, Ppp2ca, Ppp2r3d, Pptc7, Proinsulin, Prom2, Rasa4, Rbpj, Rna Polymerase Ii, Rnase A, Sfta2, Sh3d19, Smad2/3, Smco3, Spast, Tarbp2, Tbc1d20, Tbc1d30, Tmem14a, Tmem65, Tnf (Family), Txnip, Ubp1, Ulk2, Xxylt1, Zcchc7
8	– Cell Death and Survival – Cellular Compromise – DNA Replication, Recombination, and Repair	40	36	7s Ngf, Alpha 1 Antitrypsin, Alpha Tubulin, Beta Tubulin, Ces, Ces1b/Ces1c, Collagen Type Ii, Ctla2a/Ctla2b, Cytokine Receptor, Ecm, Enac, Fam171a2, Fbxo31, Fbxw8, Fc Gamma Receptor, Fcer1, Fgd1, Granzyme, Gzma, Gzmb, Gzmc, Gzmh, Hsp, Ifit1, Ifn, Ifn Alpha/Beta, Ifn Beta, Ifn Type 1, Ifnar, Il12 (Complex), Il1r1, Il20rb, Il6, Jak, Kallikrein, Klk3, Klk7, Klrb1, Lilrb3, Map6, Mapkapk2/3, Mbp, Mep1a, Mhc, Mhc Class I (Complex), Mhc Class Ii (Complex), Mir122a, B, Mir124, Mirlet7, Msln, Mus81, Pdk2, Polg2, Prss3, Rgmb, Rnasel, Scarb2, Serine Protease, Serpina1, Serpina9, Syk/Zap, Tap2, Tec/Btk/Itk/Txk/Bmx, Th2 Cytokine, Tlr, Tmem189, Tmprss7, Trypsin, Txk, Vbp1
9	– Nervous System Development and Function – Organ Morphology – Tissue Morphology	35	33	Adam19, Adamtsl3, Agfg2, App, Arl5c, Arl8a, Arnt2, Brwd1, Cd200r1l, Cpn2, Csnk1g1, Ddx43, Dnajb14, Dnajc30, Entpd2, Fbxl20, Fcho1, Filip1, Gjd4, Gucd1, Gypa, H2-K2/H2-Q9, H2-M2, Hspb7, Il20rb, Il4, Jtb, Kcnq1, Kctd16, Krt40, Laptm4a, Lnx1, Ly6a (Includes Others), Ly6d, Mobp, Mturn, Myot, Nat3, Nudt11, Pcyt1b, Pdxp, Pkib, Purg, Rnf144b, Rnf38, Rwdd2b, Serpinb6b, Slc25a38, St6galnac6, Stac2, Tcp10/Tcp10l2, Tmem176b, Tmem59, Tp73, Traf6, Tshz2, Ubc, Ubl3, Ulk2, Usp6, Wars2, Wfdc8, Zadh2, Zdhhc14, Zfand5, Znf202, Znf706, Znrf1, Zscan16, Zxdc

10	– Amino Acid Metabolism – Cardiovascular Disease – Organismal Injury and Abnormalities	34	32	Actin, Agpat5, Alpha Actinin, Alpha Catenin, Angel2, Angpt2, Calpain, Camp-Dependent Protein Kinase, Casein, Chordc1, Cnga2, Collagen, Collagen Type I (Complex), Collagen Type I (Family), Collagen Type Iv, Collagen(S), Creb, Eif4ebp2, Eif4g, Eva1c, Exoc3, Exoc8, Fam136a, Fgfr, Focal Adhesion Kinase, G Protein Alphai, Gaba-A Receptor, Gabrg2, Gclc, Gclm, Gp6, Gria2, Growth Hormone, Gαq, Histone H1, Hrg, Hsp27, Importin Beta, Integrin, Itpka, Jak1/2, Laminin (Complex), Lfa-1, Lrp, Lum, Mapk, Mmp, Nup35, Pi3k (Complex), Pkc(S), Plc Beta, Plc Gamma, Pom121/Pom121c, Pp2a, Prap1, Prkcg, Ptk, Rab5, Secretase Gamma, Si, Spp1, Tars2, Tgf Beta, Ubqln1, Uros, Vps50, Vps51, Ythdc1, Ythdf1, Znf804a

E **E 7.25 6N Alcohol vs. Vehicle**

	Diseases and Functions	-log(Fisher's exact *p*-value)	Molecules in Network	Molecules
1	– Cancer – Gastrointestinal Disease – Organismal Injury and Abnormalities	94	60	26s Proteasome, Ankrd13a, Apc (Complex), Arrdc1, Aven, Azin1, Bmt2, Btbd1, C1ql4, Caap1, Cab39, Cab39l, Carnmt1, Casein, Ccar1, Ccdc149, Cd200r1, Cdyl, Ctcfl, Cxxc1, Exog, Gmcl1, Haus4, Histone, Hivep3, Hoxc10, Kdm4b, Krt75, Leng8, Lypd3, Map4k2, Mark3, Mex3c, Mfhas1, Micu2, Mif4gd, Nfkb (Complex), Nr2e1, Parp, Parp16, Pdk2, Pip4k2a, Pip4k2b, Pkhd1, Plcd3, Prickle3, Prkaa, Pxk, Rbm26, Rcbtb2, Rnf25, Serpina12, Smurf1, Sult2b1, Tbrg4, Traf, Trib3, Trim13, Trim44, Trim69, Trmt1l, Ube2, Ube2g2, Ube2q2, Ubiquitin, Utp4, Znf263, Znf414, Znf761, Zranb1
2	– Cell Cycle – Cellular Assembly and Organization – DNA Replication, Recombination, and Repair	94	60	Actr5, Alpha Catenin, Anapc4, Atpase, Bbs4, Bcor, Cbp/P300, Ccdc117, Ccnl2, Cdc73, Cdipt, Ceacam, Ceacam20, Colec12, Dars1, Daxx, Fam161a, Fam91a1, Fbxo17, Fbxw21 (Includes Others), Figla, Fsd2, Histone H3, Hnrnph1, Hspa8, Igdcc3, Il1bos, Ilf2, Kdm1a, Klhl15, Lman2l, Mapk, Mapre1, Mettl3, Mi2, Myo19, Nlrp4b, Nsun4, Orc3, P-Tefb, Padi6, Pex6, Phkg2, Polr3h, Ppp2ca, Prkab1, Rbbp4, Rbpj, Rgs13, Rna Polymerase Ii, Rnr, Samd7, Smarca5, Sohlh1, Sp9, Spata19, Spice1, Spout1, Srsf2, Supt16h, Tcf19, Tmem25, Troap, Tssk1b, Tuba4a, Ythdc1, Ythdf1, Zbtb1, Znf639, Znf804a
3	– Gastrointestinal Disease – Neurological Disease – Organismal Injury and Abnormalities	59	44	Akr1c4, Amylase, Ankrd39, Anxa10, Arrb2, Bag3, Bdkrb1, Calmodulin, Card19, Cg, Chrm3, Ck2, Cpa3, Csnk1g3, Cyp4a11, Dazap2, Efcab5, Exoc3, Ffar2, Focal Adhesion Kinase, Fsh, Gbp6, Gnrh, Gpcr, Gpr160, Gpr4, Gpr50, Gpr88, Gtpase, Hemoglobin, Hsp90, Htr1d, Htr2b, Ice2, Ikk (Complex), Insulin, Klf1, Mtorc1, Ncbp2, Pka, Plc, Prmt3, Pstpip2, Ptprz1, Rab5c, Rac1, Ras Homolog, Rnf208, Rxfp1, Secretase Gamma, Sfk, Shc, Slc8b1, Slitrk1, Smarcal1, Src (Family), Sstr1, Stat, Stxbp4, Tas1r2, Tcf, Tcr, Tmem17, Tnk1, Tpcn2, Tsc22d1, Tsc22d2, Tubulin, Vamp2, Vegf
4	– Cell Morphology – Cellular Development – Cellular Movement	49	39	Acac, Actin, Afmid, Akirin2, Alp, Arp2/3, Arrdc4, Bcar1, Collagen, Collagen Alpha1, Collagen Type I (Complex), Collagen Type I (Family), Collagen Type Iv, Collagen(S), Commd3-Bmi1, Crebzf, Cuzd1, Cxcl13, Dynll2, Ecm, Erk1/2, Fam102a, Fap, Fcer1, Fermt1, Fgf, Fgf13, Fgf16, Fgf6, Fgf7, Fgfr, Gas1, Gp6, Gpiib-Iiia, Hcrt, Hedgehog, Hhat, Histone Deacetylase, Igsf3, Igsf8, Integrin, Itga3, Jink1/2, Laminin (Complex), Lfa-1, Loxl1, Lrig1, Mep1a, Myoc, Plc Gamma, Ppp1r15a, Rab5, Rap1, Rasgrp3, Rsk, Sh2d3c, Sharpin, Skap1, Slfn12l, Sox15, Srsf5, Talin, Tgf Beta, Tlr7/8, Ubiquitin Ligase, Ucn2, Wasf2, Wnt, Wnt8b, Zdhhc2
5	– Cell Cycle – Developmental Disorder – Endocrine System Disorders	47	38	Adaptor Protein, Adaptor Protein 2, Ap1s2, Ap2, Ap2 Alpha, Atn1, Beta Arrestin, Bmp15, Bok, Brms1l, Carboxylic Ester Hydrolase, Caspase, Caspase 3/7, Ccne2, Cdc2, Cdk, Cebpg, Ces, Ces1b/Ces1c, Ces1e, Ces4a, Cidec, Clathrin, Cpt1, Cyclin A, Cyclin D, Cyclin E, Dio1, Dynamin, Dzip3, E2f, E2f1, Hdac, Histone H4, Jnk, Kcnab3, Map1lc3, Mxd1, N-Cor, Ncor1, Nr1h, Pctp, Pepck, Polr2m, Ptgds, Rar, Rb, Rhobtb3, Rnf165, Rprd1a, Rxr, Shisa5, Siah2, Slc29a2, Smad1/5/9, Smad2/3, Ston2, Swi-Snf, Tars2, Tbx1, Tespa1, Tfap2b, Thymidine Kinase, Tnfrsf14, Uck2, Ulk2, Unc13d, Vps50, Wars2, Wdr62
6	– Hematological System Development and Function – Lymphoid Tissue Structure and Development – Tissue Morphology	45	37	Akt, Arfip2, C/Ebp, Cd180, Cd4, Chemokine, Chka, Cirbp, Cxcl16, Cytokine, Dsg1, Eif2ak2, Fcamr, Galnt1, Gm9573, Got, Grk6, Hk1, Ifn, Ifn Alpha/Beta, Ifn Beta, Ifnar, Iga, Ige, Igg, Igg1, Igg2a, Igg2b, Igg3, Igll1/Igll5, Igm, Ikb, Il1, Il12 (Complex), Il12 (Family), Il17d, Il36b, Immunoglobulin, Insrr, Interferon Alpha, Ly9, Mhc Class I (Complex), Mhc Class I (Family), Mhc Class Ii (Complex), Mhc Ii, Mlip, Mucin, Notch, Npas4, Pax5, Pdcd1lg2, Pro-Inflammatory Cytokine, Prr5, Rbm38, Reg3g, Saa3, Sema4b, Stat5a/B, Tlr, Tnf (Family), Tnfrsf17, Tnfsf12-Tnfsf13, Tnfsf13, Tnfsf15, Trem1, Trim59, Trpm4, Ugt2b17, Unc93b1, Vip
7	– Carbohydrate Metabolism – Cell-To-Cell Signaling and Interaction – Small Molecule Biochemistry	45	37	Abra, Adarb1, Adrb, Aldose Reductase, Alpha Tubulin, Ampa Receptor, Ampk, Ap1, Arf, Arhgap8/Prr5-Arhgap8, Bcr (Complex), C6, Calcineurin Protein(S), Camkii, Cd3, Clnk, Cofilin, Dock3, Epb41l1, Erk, Ern2, Flrt3, Gadd45a, Gcsam, Gk, Gria2, Histone H1, Ica1, Inpp5, Inpp5a, Inpp5k, Isl1, Kiaa1522, Lrrc10, Map2k1/2, Mgst2, Miip, Mlc, Mtch1, Mthfd2, Nck, Nck1, Nfat (Complex), P70 S6k, Pak, Pak6, Pde, Pdgf (Complex), Pdgf Bb, Pfkfb3, Pp1 Protein Complex Group, Pp2a, Proinsulin, Rac, Rhov, Rock, Sapk, Scarb2, Scd, Slc6a3, Sos, Srsf7, Ssbp4, Synj1, Tra2b, Trmt6, Tyrosine Kinase, Ubp1, Unc5b, Vav

8	– Energy Production – Lipid Metabolism – Small Molecule Biochemistry	42	35	14-3-3, Adcy, Adcy8, Alkbh3, Asb9, Atypical Protein Kinase C, Bbox1, Casp2, Creb, Cyct, Cyp2c8, Cytochrome C, Enac, Estrogen Receptor, F2rl1, G Protein, G Protein Alphai, G Protein Beta Gamma, Gnai1, Growth Hormone, Gsk3, Gαq, Hdl-Cholesterol, Helt, Hsp27, Hsp70, Irs1, Kcnj1, Klk3, Klra7 (Includes Others), Kndc1, Ldl, Ldl-Cholesterol, Lh, Mek, Muc5b, Neurog2, Nfat (Family), Nqo1, Nr0b2, Nr1d1, Nr2e3, Nr4a2, P38 Mapk, P85 (Pik3r), Paqr7, Pde3b, Pex14, Pi3k (Complex), Pi3k (Family), Pi3k P85, Pkc(S), Pnpla2, Prkd1, Prss29, Prss50, Ptpase, Rara, Ras, Serine Protease, Sod, T3-Tr-Rxr, Tmem54, Tmprss11b, Tmprss7, Trypsin, Tsh, Ucp2, Ucp3, Voltage-Gated Calcium Channel
9	– Cancer – Cell Cycle – Cellular Development	36	32	Acetyl-L-Carnitine, Acox, Acox1, Adss1, Ankar, Bco1, Bpifb6, C1orf159, Catsperg, Ces3, Cholesterol, Chtop, Dec1, Egr2, Fabp9, Fgf13, Fuca1, Fyn, Hcn2, Heparin, Hnrnpl, Hpd, Impg2, Inpp5a, Jpt2, Katnal1, Lrrc29, Lrtm1, Mir-100-5p (And Other Mirnas W/Seed Acccgua), Msl2, Mtmr11, Mup1 (Includes Others), Ncmap, Nfib, Nxph4, Obp2b, Ogdhl, Osbpl5, Pak6, Pctp, Pex2, Plekhg5, Pmm1, Pparg, Ppfia2, Ppp1ca, Ppp1r27, Ppp2r3d, Pstpip2, Ralgapa1, Rassf6, Rdh11, Rnf144b, Rorc, Shisa5, Shroom2, Slc16a14, Slc22a22, Slc22a25, Stard5, Tep1, Tex19.1, Tmem242, Tmem47, Tmem63a, Tmprss5, Tp53, Tpra1, Ubxn2b, Ywhaz
10	– Cell Cycle – Cellular Assembly and Organization – DNA Replication, Recombination, and Repair	35	31	Adal, Adamtsl3, Ammecr1, Amy2b, Arl5a, Asb15, Aspn, Aven, B4galnt3, C15orf39, Ccdc28a, Ccdc97, Cdc42se1, Cdh19, Cdr1, Ces2g, Cyp3a7, Ddx19a, Depdc7, Dmtn, Fam83g, Fermt1, Il10ra, Iws1, Kiaa0408, Klhdc3, Krtap10-3, Meikin, Meox2, Mex3d, Mobp, N4bp3, Npm1, Nr3c1, Nxf1, P3h2, Pax1, Paxbp1, Pnoc, Rad21, Rad21l1, Rdh11, Rec8, Reg4, Rgs18, Rnf144b, Rpp25, Rpp40, Sectm1, Selenop, Slc16a11, Slc22a16, Stag3, Sycp3, Tbccd1, Tcf3, Terb1, Tgfb1, Tlr7, Tmem104, Tomm34, Tomm40l, Tpst2, Tsen54, Ubl4b, Vgll2, Vim, Xpo1, Znf544, Znf780a

F **E 7.5 6J Alcohol vs. Vehicle**

	Diseases and Functions	-log(Fisher's exact *p*-value)	Molecules in Network	Molecules
1	– Dermatological Diseases and Conditions – Lipid Metabolism – Organismal Injury and Abnormalities	75	70	A4galt, Abhd17b, Agtrap, Arl14ep, Aunip, Carmil2, Casq1, Casq2, Ccdc184, Ccdc89, Ctnnbip1, Daglb, Dolpp1, Eaf1, Ensa, Epb41l5, Eri2, Extl1, Faf2, Fam114a1, Fam234a, Fbxo28, Gbx2, Gdf5, Gon7, Gpank1, Grb2, Grina, Hcn2, Hip1r, Ick, Inca1, Jsrp1, Kbtbd2, Klhdc3, Klhl36, Klk14, Lrrc8a, Lrrc8e, Lyg2, Map3k6, Ntf4, Pard6g, Pkp3, Plcd1, Plcd3, Plekho2, Pnma2, Pnma8a, Pop7, Ppp2r2d, Prap1, Prickle3, Rp1l1, Selenbp1, Snapc1, Snapc3, Spata2l, Stambpl1, Syt16, Tmem102, Ttyh2, Tulp1, Ubxn2a, Ubxn2b, Ubxn7, Ulk2, Vezt, Zfand2b, Zmym6
2	– Cell Death and Survival – Cell Morphology – Cellular Compromise	75	70	Adat1, Anln, Anxa6, Anxa7, Atxn7l3b, C18orf54, C19orf44, Canx, Casd1, Ccdc127, Cdv3, Cipc, Dctd, Def6, Dpep3, Dynll1, Eed, Elavl1, Eml2, Fam76a, Fam83f, Gipc1, Gk5, Gpm6b, Gsn, Gvin1 (Includes Others), Hm13, Hpdl, Inppl1, Kcng3, Lgals3bp, Lmf1, Lrrc1, Lrtomt, Mfsd13a, Mkrn2os, Mob3a, Myo1c, Osgin2, Pafah1b1, Pcmtd1, Pink1, Plekhg6, Proca1, Prrc1, Pskh1, Pwp2, Rbmxl1, Rbmxl2, Rdh13, Sfn, Slc50a1, Slc66a2, Smim14, Surf6, Thap3, Tmem189, Tmem53, Tmem68, Trim14, Trim25, Ttc7a, Uros, Vim, Wdr41, Ywhah, Zbtb41, Zfx, Znf354b, Znf91
3	– Cancer – Connective Tissue Disorders – Organismal Injury and Abnormalities	72	69	Arl8a, Arpc1b, Cd101, Cenpb, Clrn1, Cmbl, Cntn2, Col11a1, Col4a5, Col8a1, Collagen, Ctsf, Dhrs7b, Dnlz, Errfi1, Esyt1, Fam13b, Fbxl2, Foxl1, Hells, Hydin, Jagn1, Kiaa0930, Klhl21, Klhl26, Me1, Metap1, Mllt10, Mxd3, Mxi1, Naa16, Naa40, Nars1, Ndufaf4, Nfxl1, Nol9, Nrp1, Pdrg1, Pef1, Pogk, Polr2m, Ppp1r16a, Puf60, Pxn, Rabggtb, Rbm22, Rcbtb2, Rfwd3, Ripk4, Rmnd5b, Rnf146, Rnf19b, Rpusd1, Samhd1, Sema6c, Smarcad1, Tmpo, Topors, Tram2, Trim31, Tspan11, Ube2d4, Ubox5, Ubtd1, Vwa1, Wars2, Ypel5, Zfp42, Zg16, Zmynd19
4	– Cancer – Organismal Injury and Abnormalities – RNA Post-Transcriptional Modification	67	67	Abi2, Adal, Ai987944 (Includes Others), Atg16l1, Atp11b, Bricd5, Cbx1, Cbx5, Cebpa, Coil, Cxxc1, Dazap1, Dedd2, Dhx15, Efhd2, Fgf17, Grwd1, Hebp2, Histone H3, Hnrnpk, Hoxa9, Hp1bp3, Igsf8, Ilf2, Itga4, Kank3, Krt7, Lmna, Lsm2, Lsm6, Magea3 (Includes Others), Maged2, Mmd2, Pcid2, Pou2f3, Ppp4r2, Prpf38b, Ptgr1, Ptrhd1, Rbbp5, Rbm18, Riox2, Rnpc3, Rpl27a, Shmt2, Slc35a4, Smndc1, Snrnp, Snrpd1, Syngr1, Tada1, Tcp11l1, Thoc1, Tmem14a, Tmem203, Tmem267, Tmem42, Tmem54, Tmem86a, Trappc13, Tuba4a, U1 Snrnp, Ubn1, Wsb1, Yipf6, Zfp1, Znf22, Znf280d, Znf623, Znf688
5	– Cellular Assembly and Organization – Cellular Function and Maintenance – Infectious Diseases	65	66	Alg2, Ano10, Arfgap2, Arrdc1, Atf1, Bc048679, Cdc42ep2, Cenpn, Crim1, Dbr1, Escrt1, Esr1, Fam118a, Fam136a, Fdxacb1, Fibp, Fkbp1b, Gatb, Gc-Gcr Dimer, Gjd3, Hacd1, Hnf4g, Ica1, Kcnq4, Kctd17, Lor, Micu3, Mier1, Miip, Mkks, Mob3c, Ncoa7, Npw, Nsd1, Nup35, Paqr4, Pcdhb14, Pcdhb4, Peptidylprolyl Isomerase, Plscr3, Plxdc1, Pnrc1, Pnrc2, Ppwd1, Prr15l, Pus1, Qrsl1, Rar, Rarg, Rnf138, Rnf38, Sec22c, Shroom1, Slc44a2, Slco1c1, Stk16, Tfap2c, Them6, Tjp3, Trim47, Tsg101, Ttc9, Vps37a, Vps37b, Vps37d, Wdr4, Xpnpep1, Ypel3, Zdhhc21, Zfand4
6	– Embryonic Development – Organ Development – Organismal Development	65	66	Actc1, Actr1a, Aipl1, Ankrd34c, Atf7, Atpase, Borcs6, Borcs8, Ccdc8, Dctn2, Dtnbp1, Eif3j, Entpd1, Fbxo25, Fgfr1op, Foxc1, Gemin2, Gins1, Haus8, Hnrnph1, Jdp2, Kcnab3, Kiaa0753, Kiz, Krt16, Kti12, Mab21l3, Mb21d2, Med4, Mettl3, Mphosph9, Myh14, Myo18b, N4bp3, Ncbp2, Nlrp10, Nop2, Odf2l, P Glycoprotein, Panx1, Par, Patz1, Pfkp, Phax, Prickle2, Psmc5, Rhof, Sec31b, Shtn1, Snw1, Sorbs1, Spats2, Spdl1, Swsap1, Tcf15, Tcp1, Tcp11l2, Thg1l, Tnni3k, Tnnt2, Tor1aip1, Tor1b, Trap/Media, Txndc9, Usp9x, Vill, Wtap, Yap1, Znf326, Znf524

7	– Developmental Disorder – Hereditary Disorder – Post-Translational Modification	63	65	Amigo1, Asl, Atp8b2, Azin2, B3gnt3, B4galnt1, B4gat1, Btbd10, Btd, C1ql1, Ccdc106, Cd160, Cers4, Chodl, Cntnap3, Cryl1, Dtwd1, Ethe1, Evx1, Ext1, Fbxo2, Fev, Fktn, Fos, Galnt12, Gpha2, Gpt2, Has, Hus1, Interleukin, Kiaa1841, Klrg2, Lamb2, Lonrf2, Lrif1, Mad2l2, Metrn, Mob4, Mto1, Nagpa, Nkiras2, Ornithine Decarboxylase, Pcdh19, Pdf, Ppp2c, Prrx1, Ptcd2, Pxk, Rmnd1, Rtn2, Scf, Sgtb, Sike1, Slc10a6, Slc25a20, Smg7, Smg8, Snai3, Snx25, St6galnac4, St8sia3, St8sia5, Stk25, Strn3, Tbpl1, Tmem143, Tmem30b, Tpgs1, Xylt1, Znf146
8	– Cell Morphology – Post-Translational Modification – Small Molecule Biochemistry	63	65	Agfg2, Angel1, Aplp1, Atic, Atxn7l2, C1orf35, Ccdc122, Cdyl2, Chst13, Clock, Col9a2, Cspp1, Dennd2d, Dis3l, Epc1, Epc2, Eps15, Etv2, Exosc6, Exosc7, Exosome, Fez1, Fgf16, Foxn2, Foxo6, G2e3, Gcdh, Gnl1, Hap1, Hid1, Hmgcs2, Hoxb8, Hs3st3a1, Ing3, Ing5, Katnbl1, Meaf6, Med23, Mipol1, Mis12, Mphosph6, Nuf2, Papss2, Pdcd7, Pkdcc, Pkn3, Plvap, Pnp, Pxr Ligand-Pxr-Retinoic Acid-Rxrα, Rbm48, Rcn3, Reep3, Sec62, Sgf29, Slc25a41, Spc24, Specc1l, Srcap, Stx18, Sulfotransferase, Sult1d1, Sult1e1, Thap11, Tip60, Vegf, Vps51, Yeats4, Znf24, Znf324, Znf394
9	– Digestive System Development and Function – Embryonic Development – Post-Translational Modification	63	65	Abhd8, Ahcyl2, Ammecr1l, Anapc16, Arhgap45, Armc5, Banp, Bcap29, Bend3, Bmt2, Ccng1, Ccnl2, Cdx4, Cfap97, Chp1, Cog8, Dip2a, Fam117a, Fam124a, Fam161a, Fam214b, Farnesyl Transferase, Fnta, Gabp, Gabpb1, Gata, Gem, Ggtase I, Gmip, Hectd1, Hmbox1, Homer2, Iffo1, Irf2bp2, Irx5, Isl1, Itfg2, Lhx6, Lmo1, Lmo2, Lmo4, Loc728392, Lrfn4, Mbnl1, Meis2, Mnx1, Necap2, Nova1, Nudt22, Ooep, Pars2, Pggt1b, Pitx1, Proser2, Purg, Ras, Rundc3a, Ssbp4, Suox, Tal2, Tle6, Trim54, Uba6, Uck1, Vmac, Wdr33, Zbtb43, Zdhhc1, Znf513, Zzz3
10	– Cell Morphology – Cellular Assembly and Organization – Protein Synthesis	63	65	Adck5, Adss1, Appl2, Atm/Atr, Azin1, Chdh, Cpne7, Crlf3, Cxcl12, Dcaf15, Dtwd2, Eme2, Etaa1, Fa, Faap24, Fanc, Fancc, Fance, Gls, Grpel2, Grsf1, Gsap, Hoga1, Iba57, Id4, Lman2l, Mapre3, Mepce, Mfap3, Mgme1, Mmadhc, Mrm3, Mrn, Mrpl19, Mrpl21, Mrpl32, Mrpl39, Mrpl44, Mrpl45, Mrpl49, Mrpl9, Mrps25, Mrps27, Mrps30, Mrps7, Nit1, Oxld1, Pagr1, Psrc1, Rab31, Rmi2, Rpa, Rpusd3, Rpusd4, Sertad3, Slx1a/Slx1b, Slx4ip, Susd1, Tmc4, Tmco4, Tmem231, Tmem245, Top3a, Tra2a, Trmt1, Wfdc1, Xrcc2, Yars2, Ybey, Znf503

G **E 7.5 6N Alcohol vs. Vehicle**

	Diseases and Functions	-log(Fisher's exact *p*-value)	Molecules in Network	Molecules
1	– Cell Morphology – Embryonic Development – Hair and Skin Development and Function	70	49	26s Proteasome, Adgrg6, Azin2, Calmodulin, Col4a6, Complement, Cxcr6, Dmc1, Dnajc6, Etv1, Fam222a, Fbn2, Fbxo6, Fpr1, Hemgn, Hnrnpk, Hspd1, Igg1, Igm, Il12 (Complex), Il12 (Family), Il1bos, Iqcb1, Kcnn1, Kcnn2, Keratin, Klhl22, Kpnb1, Krt16, Krt26, Krt33a, Krt35, Krt37, Krt73, Krt75, Krt86, Kyat1, Lgals3bp, Mapk, Mkrn3, Ndufa4l2, Noa1, Notch2, Notch3, Ornithine Decarboxylase, P-Tefb, Pbx1, Proinsulin, Pspc1, Ras, Rbm14, Rbmx, Rna Polymerase Ii, Sdr39u1, Sfpq, Sil1, Six2, Slc25a20, Speg, Sstr4, Stat, Syt2, Tbx19, Tcea2, Trim28, Trim31, Tuba4a, Tubulin, Ubr1, Znf462
2	– Cardiovascular Disease – Cell Death and Survival – Cellular Assembly and Organization	70	49	Adss1, Ak1, Ankrd37, Aven, Ccdc155, Ccnjl, Cga, Cldn13, Coq8b, Dio2, Dnpep, Egln, Fcn1, Fhl2, Gata2, Gmppa, Gpr158, Gpr25, Gpr37l1, Hebp2, Hmx1, Hnrnpl, Hnrnpu, Htr3b, Igsf9, Krtcap3, Kyat3, Lhfpl5, Lrrc57, Lyg2, Maml2, Marchf2, Mkrn2os, Morn1, Mtnr1b, Nanos2, Nr3c1, Nsg1, Nudt13, Odf4, Pdzph1, Pitx2, Prss56, Ptgr1, Retnlg, Rhag, Rhce/Rhd, Rhox3a (Includes Others), Rnf122, Rtn4rl1, Scube1, Selenbp1, Serp2, Serpinb9f (Includes Others), Serpini2, Slc44a4, Smim14, Sox13, Spire2, Stag3, Stfa2/Stfa2l1, Syngr1, Terb1, Tgfb1, Trim25, Trim58, Ubc, Upk3b, Wdpcp, Wdr34
3	– Lipid Metabolism – Nucleic Acid Metabolism – Small Molecule Biochemistry	58	43	Acss2, Acvr2b, Alp, Alpl, Ampk, Bcl11a, Bmp15, Bspry, Calcineurin Protein(S), Caspase 3/7, Cbp/P300, Ccnd2, Collagen Alpha1, Ctbp, Cuedc2, Cyclin A, Cyp11a1, Cyp2c40 (Includes Others), Cyp2c8, Cyp2e1, Cyp4f11, Dkk1, Elovl6, Emid1, Etv6, Fasn, Frizzled, Fsh, Gzmh, Hdac, Histone H3, Histone H4, Hsp70, Jnk, Kat2b, Khk, Lmcd1, Mef2, Mef2c, Mgmt, Mlycd, N-Cor, Nadh2 Or Nadph2 1 Atom Incorporation:Oxygen Oxidoreductase, Ncs1, Nr1h, P70 S6k, Prc2, Prkag2, Proc, Qki, Rab29, Rb, Rbm15, Sat2, Scd2, Six3, Smad, Smad2/3, Sp7, Tcf, Tgf Beta, Tgm2, Tnfrsf14, Tnn, Tp63, Trerf1, Unspecific Monooxygenase, Vgll2, Vill, Wnt1
4	– Cellular Movement – Hematological System Development and Function – Post-Translational Modification	58	43	2210010c04rik, Abl1, Adam22, Alpha 1 Antitrypsin, Ap1, Arrdc1, Atp6v1g3, Blvrb, Calpain, Caspase, Cd44, Cilp, Ck2, Cog8, Crabp2, Cstf3, Ctla2a/Ctla2b, Cytochrome C, Cytokine, Dsg1, Ecm, Efna4, Entpd1, F9, Focal Adhesion Kinase, Gbe1, Gcdh, Gsk3, H2ax, Histone, Hnrnpa1, Hnrnpdl, Hsp90, Il1r2, Immunoglobulin, Interleukin, Klk12, Lancl2, Ldb1, Ldl, Macrod1, Mdn1, Metalloprotease, Micb, Mmp, Mmp2, Necap2, P Glycoprotein, P38 Mapk, Parp, Phosphatase, Pink1, Pkc(S), Plppr3, Prap1, Prickle3, Prkch, Prss50, Prss56, Serine Protease, Sgca, Shp, St3gal2, Stx4, Tet1, Trypsin, Ubiquitin, Usp17le (Includes Others), Utp20, Vegf

5	– Developmental Disorder – Organismal Injury and Abnormalities – Skeletal and Muscular Disorders	54	41	Alpha Actinin, Amylase, Anxa4, Bmp, C3, Camk1, Cd55, Cd68, Cdh11, Cer1, Chst3, Chymotrypsin, Col10a1, Collagen Type I (Complex), Collagen Type Ii, Collagen Type Iii, Collagen Type Iv, Collagen Type V, Collagen Type X, Collagen(S), Complement Component 1, Cpa1, Cr3, Elastase, Erk1/2, Etv2, Fbxl12, Fgf, Fgf13, Fibrin, Fibrinogen, Gli, Gli3, Glipr2, Hcrt, Hgh1, Hopx, Hs6st2, Inppl1, Integrin, Klf13, Klrc1, Laminin (Complex), Lrg1, Mmp8, Nkx2-5, Pdgf (Complex), Pla2, Pla2g5, Pld, Pld2, Prrx1, Pxr Ligand-Pxr-Retinoic Acid-Rxrα, Rab26, Rab3d, Rgs5, Rps6ka, Rsph6a, Serpinb7, Ski, Slco1b3, Smooth Muscle Actin, Sox17, St6galnac3, Sulfotransferase, Sult1e1, Tbx1, Ubash3a, Ucn3, Wnt
6	– Cellular Movement – Hematological System Development and Function – Immune Cell Trafficking	52	40	Ackr2, Acox, Acy1, Akt, Asb9, Atrial Natriuretic Peptide, Ccl1, Ccl22, Ccl24, Ccl7, Ccng1, Collagen Type I (Family), Cox6a2, Creatine Kinase, Creb3l3, Ctla4, Cxcl13, Cxcl3, Cyp7a1, Dbh, Dynamin, Fcer1, Fgd2, Foxp1, Gdf15, Guca1a, Hfe, Ige, Il-2r, Il17r, Il17rc, Il23, Il2rb, Jak, Jink1/2, Jun/Junb/Jund, Laminin1, Loc102724788/Prodh, Lpin1, Map2k1/2, Marco, Mcam, Mek, Mir122a, B, Nfatc4, Or51e2, Pi3k (Family), Pi3k P85, Pik3c2g, Plac8, Plk3, Ppp2c, Prcp, Raf, Rap1, Rar, Reg3a, Rsk, Rxr, Rxrg, S100, S100a4, S100a8, S100a9, Scgb3a1, Serpinb6b, Slc6a12, T3-Tr-Rxr, Thyroid Hormone Receptor, Vla-4
7	– Endocrine System Development and Function – Inflammatory Response – Organismal Injury and Abnormalities	52	40	2' 5' Oas, 9830107b12rik/A530064d06rik, Alb, Aldh, Apyrase, Aqp5, C/Ebp, Capg, Cd200r1, Cd209c, Cd276, Chemokine, Collagen, Cspg4, Cyp1a1, Cytokine Receptor, Elf3, Filamin, Fuca1, Gadd45b, Gngt1, Growth Hormone, Hat, Hdl, Hif1, Hp, Ifn, Ifn Beta, Ifna4, Ifnar, Il1, Il36g, Il36rn, Interferon Alpha, Krtap11-1, Lcn2, Ldl-Cholesterol, Mapk13, Mhc Class Ii (Complex), Mus81, Nap1l2, Nfkb (Complex), Nlr, Nlrp4, Nlrp6, Notch, Oas, Oas1, Oas1b, Oas1d (Includes Others), Pepck, Polr3gl, Pro-Inflammatory Cytokine, Prtn3, Rras, Sapk, Setbp1, Slc46a2, Ssbp4, Stap2, Tgfbr, Tlr, Tnf (Family), Tnfrsf17, Tnfsf8, Ugt, Ugt2a1, Ugt2b17, Unc93b1, Vcan
8	– Cancer – Organismal Injury and Abnormalities – Psychological Disorders	50	39	Adcy, Adrb, Akr1b7, Anxa9, Ap2, Bace1, Bcas1, Bco1, Beta Arrestin, Blk, Cadm4, Cg, Creb, Estrogen Receptor, Fam3d, Fhl5, Flot1, Foxo6, G Protein Alphai, Gabrg2, Gimap8, Gipc1, Gnao1, Gnat3, Got, Gpcr, Hnrnph1, Htr1a, Igf2bp3, Insulin, Kcnj1, Kdr, Kiss1r, Ldh (Complex), Lh, Mediator, Nefm, Neurod2, Ntrk3, P85 (Pik3r), Pcyt1b, Pdgfr, Pi3k (Complex), Pka, Pka Catalytic Subunit, Plc, Pp2a, Ppm1j, Ppy, Ptpase, Ptpn1, Ptpn18, Rassf2, Ros1, Sfk, Shc, Sod, Src (Family), Srxn1, Stat5a/B, Trh, Trk Receptor, Tro, Tsh, Tspo, Tubb4a, Tubulin (Family), Voltage-Gated Calcium Channel, Ypel3, Znf326
9	– Cellular Function and Maintenance – Cellular Growth and Proliferation – Hematological System Development and Function	43	35	Acr, Actin, Alpha Catenin, Alpha Tubulin, Arhgap9, Arhgef2, Bach2, Bcr (Complex), Camkii, Cap2, Cblc, Cd207, Cd3, Cofilin, Ctnna3, Eps8l2, Erk, Erm, F Actin, Frs3, Gcsam, Gm9573, Gmpr, Grik5, Gsn, H2-L, H2-M10.1 (Includes Others), Hla-A, Hla-G, Iga, Igg, Igg2a, Igg3, Iqub, Itgad, Jph4, Kcna5, Klra7 (Includes Others), Mapk15, Mhc, Mhc Class I (Complex), Mhc Class I (Family), Mlc, Mucin, Myosin, Nadph Oxidase, Nfat (Complex), Nfat (Family), Pak, Pdgf Bb, Plc Gamma, Ptk, Rab11, Rac, Rac3, Ras Homolog, Rhoc, Rnd2, Rock, Sec14l1, Serpinb10, Sos, Sptbn4, St8sia3, Tap, Tapbp, Tcr, Tesk1, Trio, Tyrosine Kinase
10	– Cell Death and Survival – DNA Replication, Recombination, and Repair – Nervous System Development and Function	41	34	Acss2, Acy3, Adra2b, Aoc1, Apoc3, Asl, Bmper, Bpifb2, C11orf71, Calcrl, Ccer1, Ccr5, Ces2e, Cst9l, Cxcr6, Cyp2a12/Cyp2a22, Depp1, Dhx29, Dmc1, Fgf13, Fxyd6, Fxyd7, Fzd3, Fzd6, Gchfr, Gdpd4, Gpr37, Gpr37l1, Hdl-Cholesterol, Hipk1, Hnf4a, Ikzf2, Il10ra, Impg1, Kcnk3, Krt8, Loc102724788/Prodh, Map3k8, Mutyh, Mycn, Ndrg4, Npffr2, Npm1, Npnt, Nrarp, Nynrin, Plscr1, Prkcz, Rhox6/Rhox9, Rnase4, Sdr42e1, Sh3bgrl2, Slc10a5, Slc39a2, Sox2, Speer4a (Includes Others), Sprr2h, Sprr2i, Sstr4, Sycn, Tada1, Tapbpl, Tet1, Tex15, Tm6sf1, Tp53, Unc5a, Urah, Yy2, Zic3

Down-regulated Genes

Gene Ontology: Biological Process

Term name	Term ID	# of genes	Log10 *p*-value
Cytolysis	GO:0019835	7	5.12
Granzyme-mediated apoptotic signaling	GO:0008626	5	4.85

Gene Ontology: Molecular Function

Term name	Term ID	# of genes	Log10 *p*-value
Serine-type endopeptidase activity	GO:0004252	11	4.30
Hydrolase activity, acting on acid phosphorus-nitrogen bonds	GO:0016825	11	3.80
Serine hydrolase activity	GO:0017171	11	3.80
Peptidase activity	GO:0008233	16	2.18
Peptidase activity, acting on L-amino acid peptides	GO:0070011	15	1.79

KEGG: Biological Process

Term name	Term ID	# of genes	Log10 *p*-value
Graft-versus-host disease	KEGG:05332	5	2.71
cAMP signaling	KEGG:04024	9	2.68
Neuroactive ligand-receptor interaction	KEGG:04080	10	1.84

Reactome

Term name	Term ID	# of genes	Log10 *p*-value
Activation, myristolyation of BID and translocation to mitochondria	REAC:R-MMU-75108	5	5.59
Intrinsic pathway for apoptosis	REAC:R-MMU-109606	5	2.63

Up-regulated Genes

KEGG: Biological Process

Term name	Term ID	# of genes	Log10 *p*-value
Caffeine metabolism	KEGG:00232	2	1.94

Down-regulated Genes

Gene Ontology: Molecular Function

Term name	Term ID	# of genes	Log10 *p*-value
Serine-type endopeptidase activity	GO:0004252	9	2.62
Serine-type peptidase activity	GO:0008236	9	2.30
Hydrolase activity, acting on acid phosphorus-nitrogen bonds	GO:0016825	9	2.22
Serine hydrolase activity	GO:0017171	9	2.22
Endopeptidase activity	GO:0004175	12	1.60

Up-regulated Genes

Reactome

Term name	Term ID	# of genes	Log10 *p*-value
Peptide ligand-binding receptors	R-MMU-375276	7	2.74
GPCR ligand binding	R-MMU-500792	9	2.58
Class A/1 (Rhodopsin-like receptors)	R-MMU-373076	8	2.42

Human Phenotype Ontology

Term name	Term ID	# of genes	Log10 *p*-value
Hyperprostaglandinuria	HP:0003527	2	1.93
Increased serum prostaglandin E2	HP:0003566	2	1.93
Renal juxtaglomerular cell hypertrophy/hyperplasia	HP:0000111	2	1.93
Abnormal circulating prostaglandin circulation	HP:0011023	2	1.93

Down-regulated Genes

Gene Ontology: Biological Process

Term name	Term ID	# of genes	Log10 *p*-value
Cellular metabolic process	GO:0044237	275	10.45
Gene expression	GO:0010467	162	6.44
Methylation	GO:0032259	27	5.47
Protein modification process	GO:0036211	119	4.32
Cell cycle	GO:0007049	66	3.91
Cellular biosynthetic process	GO:0044249	154	2.96
RNA modification	GO:0009451	14	2.69
Chromosome organization	GO:0051276	45	1.73
Programmed cell death	GO:0012501	65	1.43
Transcription by RNA polymerase II	GO:0006366	66	1.39

Gene Ontology: Molecular Function

Term name	Term ID	# of genes	Log10 *p*-value
Heterocyclic compound binding	GO:1901363	172	7.10
Methyltransferase activity	GO:0008168	19	4.81
Catalytic activity	GO:0003824	159	3.24
Nucleic acid binding	GO:0003676	110	3.05
Enzyme binding	GO:0019899	76	2.66
ATP binding	GO:0005524	55	2.57
Protein binding	GO:0005515	241	2.51
miRNA binding	GO:0035198	6	1.83
Ribonucleotide binding	GO:0032553	64	1.82
transcription regulator activity	GO:0140110	49	1.31

Human Phenotype Ontonology

Term name	Term ID	# of genes	Log10 *p*-value
Broad forehead	HP:0000337	13	2.57

Up-regulated Genes

Gene Ontology: Biological Process

Term name	Term ID	# of genes	Log10 *p*-value
Cytolysis	GO:0019835	9	5.53
Granzyme-mediated apoptotic signaling	GO:0008626	5	3.19
Primary alcohol metabolic process	GO:0034308	8	1.69

Gene Ontology: Molecular Function

Term name	Term ID	# of genes	Log10 *p*-value
Serine-type endopeptidase activity	GO:0004252	12	2.14
Endopeptidase activity	GO:0004175	19	1.93
Hydrolase activity, acting on acid phosphorus-nitrogen bonds	GO:0016825	12	1.66
Serine hydrolase activity	GO:0017171	12	1.66

KEGG: Biological Process

Term name	Term ID	# of genes	Log10 *p*-value
Graft-versus-host disease	KEGG:05332	5	1.38

Reactome

Term name	Term ID	# of genes	Log10 *p*-value
Activation, myristolyation of BID and translocation to mitochondria	REAC:R-MMU-75108	5	4.08

Down-regulated Genes

Gene Ontology: Biological Process

Term name	Term ID	# of genes	Log10 *p*-value
Organic substance metabolic process	GO:0071704	179	3.38
Macromolecule metabolic process	GO:0043170	159	3.01
Primary metabolic process	GO:0044238	171	2.98
Methylation	GO:0032259	18	2.71
Metabolic process	GO:0008152	182	2.27
Macromolecule methylation	GO:0043414	16	2.17
Regulation of metabolic process	GO:0019222	119	1.71
Nitrogen compound metabolic process	GO:0006807	159	1.68
RNA metabolic process	GO:0016070	87	1.67
Regulation of cellular metabolic process	GO:0031323	111	1.44

Gene Ontology: Molecular Function

Term name	Term ID	# of genes	Log10 *p*-value
rRNA (adenine) methyltransferase activity	GO:0016433	3	1.74
Catalytic activity	GO:0003824	107	1.62
Sterol esterase activity	GO:0004771	4	1.50
Methyltransferase activity	GO:0008168	11	1.35

Reactome

Term name	Term ID	# of genes	Log10 *p*-value
Gene expression (transcription)	R-MMU-74160	29	1.78
RNA polymerase II transcription	R-MMU-73857	27	1.73

Down-regulated Genes

Gene Ontology: Biological Process

Term name	Term ID	# of genes	Log10 *p*-value
Nucleic acid metabolic process	GO:0090304	552	69.99
Gene expression	GO:0010467	559	57.57
Primary metabolic process	GO:0044238	819	45.95
Embryo development	GO:0009790	136	13.2
Heart development	GO:0007507	77	7.33
Skeletal system development	GO:0001501	66	6.40
Cellular response to DNA damage stimulus	GO:0006974	82	4.75
Regulation of cell cycle	GO:0051726	100	4.02
Circulatory system development	GO:0072359	108	3.84
Brain development	GO:0007420	76	3.40

Gene Ontology: Molecular Function

Term name	Term ID	# of genes	Log10 *p*-value
Nucleic acid binding	GO:0003676	432	54.31
Organic cyclic compound binding	GO:0097159	550	40.57
DNA binding	GO:0003677	266	33.72
RNA binding	GO:0003723	156	18.46
Transcription factor binding	GO:0008134	88	9.27
Catalytic activity, acting on RNA	GO:0140098	55	7.99
Histone acetyltransferase activity	GO:0004402	14	2.62
Protein binding	GO:0005515	636	1.86
miRNA binding	GO:0035198	9	1.68
Histone binding	GO:0042393	30	1.50

KEGG: Biological Process

Term name	Term ID	# of genes	Log10 *p*-value
Spliceosome	KEGG:03040	22	3.67
Signaling pathways regulating pluripotency of stem cells	KEGG:04550	21	2.67
RNA transport	KEGG:03013	22	2.06
Ribosome biogenesis in eukaryotes	KEGG:03008	13	1.64

Reactome

Term name	Term ID	# of genes	Log10 *p*-value
Gene expression (transcription)	R-MMU-74160	112	6.92
Metabolism of RNA	R-MMU-8953854	72	6.67
Processing of capped intron-containing pre-mRNA	R-MMU-72203	38	4.93
RNA polymerase II transcription	R-MMU-73857	94	3.84
mRNA splicing	R-MMU-72172	29	3.04
mRNA splicing - major pathway	R-MMU-72163	28	2.86
RNA polymerase II transcribes snRNA genes	R-MMU-6807505	15	2.34

Human Phenotype Ontology

Term name	Term ID	# of genes	Log10 *p*-value
Abnormal lip morphology	HP:0000159	81	3.41
Abnormal palate morphology	HP:0000174	84	3.07
Abnormality of the outer ear	HP:0000356	89	2.93
Holoprosencephaly	HP:0001360	15	2.39
Abnormal facial shape	HP:0001999	80	1.73
Anal atresia	HP:0002023	21	1.65
Atrioventricular canal defect	HP:0006695	11	1.53
Oral cleft	HP:0000202	53	1.42

Up-regulated Genes

Gene Ontology: Biological Process

Term name	Term ID	# of genes	Log10 *p*-value
Localization	GO:0051179	529	9.04
Transport	GO:0006810	411	7.64
Transmembrane transport	GO:0055085	160	4.75
Protein phosphorylation	GO:0006468	189	4.25
Intracellular signal transduction	GO:0035556	236	4.11
Cellular response to chemical stimulus	GO:0070887	272	3.12
Anatomical structure development	GO:0048856	466	2.18
Response to stress	GO:0006950	316	1.71
Cell death	GO:0008219	191	1.48
Positive regulation of cell differentiation	GO:0045597	109	1.42

Gene Ontology: Molecular Function

Term name	Term ID	# of genes	Log10 *p*-value
Protein binding	GO:0005515	821	9.85
TAP binding	GO:0046977	8	4.52
GTP binding	GO:0005525	54	3.42
Nucleotide binding	GO:0000166	204	2.82
Enzyme binding	GO:0019899	207	1.79
Beta-2-microglobulin binding	GO:0030881	6	1.78
Cytoskeletal protein binding	GO:0008092	98	1.57
GTPase activity	GO:0003924	40	1.48
Protein kinase binding	GO:0019901	76	1.38

Reactome

Term name	Term ID	# of genes	Log10 *p*-value
Metabolism	R-MMU-1430728	158	1.78
Ion channel transport	R-MMU-983712	27	1.68
Stimuli-sensing channels	R-MMU-2672351	18	1.35
Formation of xylulose-5-phosphate	R-MMU-5661270	4	1.31

Down-regulated Genes

Gene Ontology: Biological Process

Term name	Term ID	# of genes	Log10 *p*-value
Positive regulation of transcription by RNA polymerase II	GO:0045944	37	5.02
Positive regulation of cellular metabolic process	GO:0031325	69	4.56
Transcription by RNA polymerase II	GO:0006366	47	3.27
Regulation of cell differentiation	GO:0045595	44	2.61
Cell fate commitment	GO:0045165	13	1.85
Skeletal system development	GO:0001501	18	1.72
Primary metabolic process	GO:0044238	140	1.53
Embryonic morphogenesis	GO:0048598	20	1.52
Generation of neurons	GO:0048699	36	1.47
Regulation of nervous system development	GO:0051960	27	1.46

Gene Ontology: Molecular Function

Term name	Term ID	# of genes	Log10 *p*-value
Sequence-specific DNA binding	GO:0043565	38	6.17
RNA polymerase II regulatory region sequence-specific DNA binding	GO:0000977	29	5.17
Transcription regulatory region DNA binding	GO:0044212	32	5.15
Cis-regulatory region binding	GO:0035326	25	4.87
Transcription regulator activity	GO:0140110	37	3.50
DNA-binding transcription activator activity	GO:0001216	17	2.77
DNA binding	GO:0003677	43	1.65

KEGG: Biological Process

Term name	Term ID	# of genes	Log10 *p*-value
Steroid hormone biosynthesis	KEGG:00140	6	1.77

Human Phenotype Ontology

Term name	Term ID	# of genes	Log10 *p*-value
Hypoplasia of the epiglottis	HP:0005349	3	1.31

Up-regulated Genes

Gene Ontology: Biological Process

Term name	Term ID	# of genes	Log10 *p*-value
Antigen processing and presentation of endogenous antigen	GO:0019883	10	6.37
Antigen processing and presentation via MHC class Ib	GO:0002475	9	5.31
Antigen processing and presentation of peptide antigen	GO:0048002	10	4.18
Defense response	GO:0006952	52	3.78
Response to stress	GO:0006950	91	3.16
Antigen processing and presentation of peptide antigen via MHC class I	GO:0002474	6	3.07
Antigen processing and presentation	GO:0019882	11	2.87
Inflammatory response	GO:0006954	27	1.90

Gene Ontology: Molecular Function

Term name	Term ID	# of genes	Log10 *p*-value
TAP binding	GO:0046977	6	5.78
Beta-2-microglobulin binding	GO:0030881	6	5.78
Peptide antigen binding	GO:0042605	6	4.06
Catalytic activity	GO:0003824	121	2.68
RAGE receptor binding	GO:0050786	4	2.64

KEGG: Biological Function

Term name	Term ID	# of genes	Log10 *p*-value
IL-17 signaling pathway	KEGG:04657	8	1.74

Reactome

Term name	Term ID	# of genes	Log10 *p*-value
ER-phagosome pathway	R-MMU-1236974	8	4.39
Neutrophil degranulation	R-MMU-6798695	25	3.47
Endosomal/vacuolar pathway	R-MMU-1236977	6	2.66
Antigen presentation: Folding, assembly and peptide loading of class I MHC	R-MMU-983170	7	2.57
Metal sequestration by antimicrobial proteins	R-MMU-6799990	3	2.23
Peptide ligand-binding receptors	R-MMU-375276	12	1.60

Human Phenotype Ontology

Term name	Term ID	# of genes	Log10 *p*-value
Crazy paving pattern on pulmonary HRCT	HP:0025391	5	3.27
Elevated carcinoembryonic antigen level	HP:0031029	5	3.05
Recurrent acute respiratory tract infection	HP:0011948	6	2.94
Acute infectious pneumonia	HP:0011949	5	2.48
Foam cells	HP:0003651	5	2.18
Respiratory failure requiring assisted ventilation	HP:0004887	5	1.92
Abnormal blood oxygen level	HP:0500165	5	1.80
Hypoxemia	HP:0012418	5	1.80
Abnormal blood gas level	HP:0012415	5	1.48
Abnormal pulmonary thoracic imaging finding	HP:0031983	5	1.48

GD7.0		GD7.25				GD7.5			
6J's vs. 6N's		6J's		6N's		6J's		6N's	
Baseline		PAE vs. Vehicle		PAE vs. Vehicle		PAE vs. Vehicle		PAE vs. Vehicle	
Gene	Log2 FC	Gene	Log2 FC	Gene	Log2 FC	Gene	Log2 FC	Gene	Log2 FC
Fam65b	0.30	*Fam161a*	*0.86*	*Fam161a*	*0.98*	*Mchr1*	1.28	*Iqub*	0.95
Efcab7	-0.89	*Tbc1d30*	*0.75*	*Tex40*	*0.94*	*Fam161a*	1.17	*Tekt1*	0.82
		Hydin	*0.65*	*Hk1*	*0.81*	*Hydin*	0.88	*Tulp1*	0.80
		Map6	*0.61*	*Ak1*	*0.80*	*Rab29*	0.85	*Rab29*	0.68
		Bbs4	*0.61*	*Tuba4a*	*0.61*	*Efcab7*	0.81	*Tuba4a*	0.67
		Ptch1	*0.46*	*Bbs4*	*0.52*	*Tmem231*	0.81	*Wdpcp*	0.62
		Arl2bp	*0.38*	*Tmem17*	*0.43*	*Mxi1*	0.80	*Cep72*	0.49
		Ttll1	*0.28*	*Haus4*	*0.35*	*Tuba4a*	0.78	*Wdr34*	0.48
		Cnga2	*0.041*	*Pkhd1*	*0.34*	*Rilpl2*	0.74	*Pkd2l1*	0.33
		Myoc	*0.02*	*Tekt3*	*0.03*	*Ccno*	0.72	*Ropn1*	-0.06
		Ccr6	*-0.03*	*Ttll8*	*0.01*	*Tulp1*	0.71	*Iqcb1*	-0.35
		Mapre1	*-0.17*	*Myoc*	*-0.06*	*Hspb11*	0.68	*Rsg1*	-0.80
		Cct3	*-0.21*	*Cngb3*	*-0.08*	*Rilpl1*	0.68	*Gli3*	-0.83
		Exoc3	*-0.23*	*Mapre1*	*-0.19*	*Mok*	0.60		
		Dnaja1	*-0.30*	*Exoc3*	*-0.24*	*Kiz*	0.56		
		Nup35	*-0.44*	*Hspa8*	*-0.36*	*Kif3b*	0.52		
		Hspa8	*-0.45*	*Ralgapa1*	*-0.51*	*Mdm1*	0.51		
		Gna11	*-0.48*	*Trim59*	*-0.56*	*Snx10*	0.44		
		Pard3	*-0.58*	*Katnal1*	*-0.58*	*Pde6d*	0.44		
		Tapt1	*-0.59*	*Pex6*	*-0.74*	*Usp9x*	0.44		
		Gnb1	*-0.71*	*Wdr78*	*-0.78*	*Prkar2a*	0.43		
		Dyx1c1	*-0.72*			*Ick*	0.40		
		Atp2a2	*-1.02*			*Tubb2a*	0.34		
		Prkaca	*-1.19*			*Unc119*	0.33		
		Pex6	*-1.38*			*Rp1l1*	0.07		
						Dpcd	-0.35		
						Plk4	-0.39		
						Aurka	-0.42		
						Fgfr1op	-0.48		
						Tmem80	-0.51		
						Topors	-0.56		
						Smo	-0.59		
						Gli3	-0.59		
						Pafah1b1	-0.59		
						Pifo	-0.61		
						Dnajb13	-0.65		
						Cspp1	-0.66		
						Rttn	-0.66		
						Flcn	-0.67		
						Noto	-0.68		
						Pkd2	-0.69		
						Rab11b	-0.69		
						Morn3	-0.72		
						Cfap161	-0.77		
						Ptch1	-0.79		
						Spef2	-0.83		
						Tapt1	-0.90		
						Mkks	-1.03		
						Osr1	-1.43		

Table S2.

Click here to download Table S2